

Strengthening reinforced concrete bridge T-beams with CFRP sheets plus bi-directional GFRP
U-wraps

by

Andrew S. Foerster

B.S., Kansas State University, 2017

A THESIS

submitted in partial fulfillment of the requirements for the degree

MASTER OF SCIENCE

Department of Civil Engineering
College of Engineering

KANSAS STATE UNIVERSITY
Manhattan, Kansas

2019

Approved by:

Major Professor
Dr. Hayder Rasheed

Copyright

© Andrew Foerster 2019.

Abstract

The use of externally bonded Fiber Reinforced Polymer (FRP) to strengthen concrete structures has become more common. As this continues to grow, research is needed to ensure that the best design practices are being used. In this study, externally bonded Carbon FRP is used to strengthen reinforced concrete T-beams. In addition to the flexural CFRP, $\pm 45^\circ$ bi-directional Glass FRP as well as Carbon FRP splay anchors are used as anchorage systems on some of the beams. The goal of adding anchorage systems is to prevent premature failure due to debonding and allow the CFRP to reach its full capacity with a rupture failure. An experimental program is conducted in which six T-beams are designed, built, and tested in three-point bending with a clear span of 15.5 ft. The first beam was tested as a control beam failing at around 64.58 kips. The second beam was strengthened with one layer of CFRP, spanning 15 feet and starting 3 inches from each support. This beam failed 60.13 kips. The third beam was strengthened the same way as the second beam, but in addition to the CFRP sheet Carbon FRP splay anchors were added to each shear span. This beam has five splay anchors per shear span and failed at 58.88 kips by a premature rupture of CFRP sheet in between the anchors. The fourth beam was strengthened with the same layout for the CFRP sheet and had one layer of a full-length $\pm 45^\circ$ bi-directional Glass FRP U-wrap. This beam failed at a load of 80.02 kips. The fifth beam used the same layout as the fourth beam, but instead of a full-length U-wrap, this beam had one layer of one-foot wide $\pm 45^\circ$ bi-directional Glass FRP U-wraps with one foot of space between them. For this configuration the first U-wrap was centered at the mid-span of the beam. The fifth beam failed at 79.76 kips. The sixth beam was strengthened the same way as beam five but had two layers of $\pm 45^\circ$ bi-directional Glass FRP U-wraps. This beam failed at a load of 72.17 kips. These test results show that using $\pm 45^\circ$ bidirectional U-wraps is more effective for reaching higher

ultimate loads. The results for beams five and six show that using one layer of bidirectional U-wraps instead of two still provides around the same amount of effective anchorage. However, the former configuration yields higher beam deflection at failure.

Table of Contents

List of Figures	vii
List of Tables	xii
Acknowledgements	xiii
Chapter 1 - Introduction.....	1
Background	1
Objectives	1
Scope	2
Chapter 2 - Literature Review.....	3
Externally Bonded FRP	3
Carbon FRP Splay Anchors	4
U-wrap Anchorage Systems	6
Chapter 3 - Design and Construction of Specimens	9
Design of T-Beams	9
T-Beam Geometry	10
Design of Strengthening for T-Beams	11
Carbon FRP Sheets	11
Anchorage Using Carbon FRP Splay Anchors	12
Anchorage Using Bidirectional Glass FRP U-wraps	14
Formwork and Steel Caging	16
Casting of Beams	20
Surface Preparation.....	23
Installation of FRP	27
Chapter 4 - Material Properties.....	36
Testing of Concrete Cylinders	36
Testing of Steel Rebar.....	38
FRP Properties	41
Chapter 5 - Experimental Setup and Testing	43
Experimental Setup.....	43
Test Results.....	47

Control Beam (T1).....	47
T-Beam with Carbon FRP Flexural Reinforcement (T2)	50
T-Beam with Carbon FRP Flexural Reinforcement and 5 Carbon FRP Splay Anchors per Shear Span (T3)	54
T-Beam with Carbon FRP Flexural Reinforcement and Full-Length Glass FRP U- wrap (T4)	62
T-Beam with Carbon FRP Flexural Reinforcement with One Layer of One Foot Wide Glass FRP U-wraps (T5).....	66
T-Beam with Carbon FRP Flexural Reinforcement with Two Layers of One Foot Wide Glass FRP U-wraps (T6).....	72
Comparison of Beam Results.....	79
Chapter 6 - Analysis of Results	81
Analysis Program.....	81
Specimen T1	82
Specimen T2	85
Specimen T3	88
Specimen T4	94
Specimen T5	97
Specimen T6	102
Improvement Strain Ratio of Strengthened Beams.....	107
Chapter 7 - Summary, Conclusions and Recommendations.....	108
Summary	108
Conclusions.....	108
Recommendations for Future Work	109
References.....	111

List of Figures

Figure 3-1: Excel Spreadsheet Used for T-Beam Design	10
Figure 3-2: Cross Section of Final Beam Design	11
Figure 3-3: Shear Reinforcement and Support Locations for Final Beam Design	11
Figure 3-4: Profile of Strengthened Beam with Carbon FRP Sheet Only	12
Figure 3-5: Carbon FRP Splay Anchor Design	13
Figure 3-6: Profile of Strengthened Beam with Carbon FRP Sheet and Carbon FRP Splay Anchors	14
Figure 3-7: View of Bottom of Beam with Carbon FRP Sheet and Splay Anchors.....	14
Figure 3-8: Profile of Beam Strengthened with Carbon FRP Sheet and Full Length $\pm 45^\circ$ Bi- Directional Glass FRP U-wrap	15
Figure 3-9: Diagram of Layout of Beams Strengthened with Carbon FRP Sheet and One Foot Wide $\pm 45^\circ$ Bi-Directional Glass FRP U-wraps	16
Figure 3-10: Two Sets of Assembled Formwork.....	17
Figure 3-11: Full Length Formwork	17
Figure 3-12: Section of Finished Rebar Caging	19
Figure 3-13: Finished Rebar Caging For All Beams	19
Figure 3-14: Rebar Caging Placed in Formwork before Casting	20
Figure 3-15: Casting of Beams	21
Figure 3-16: Placing and Vibrating the Concrete in the Formwork	22
Figure 3-17: Screeding the Tops of the Beams.....	22
Figure 3-18: Finished Beams with Outside of Formwork Removed.....	23
Figure 3-19: Flipping Beam for Surface Preparation	24
Figure 3-20: Preparing the Beam Surfaces with Masonry Wheel	25
Figure 3-21: Prepared Beam Surface (Left) vs. Unprepared Beam Surface (Right).....	25
Figure 3-22: Example of Drilled Hole in the Beam for Installation of Carbon FRP Splay Anchors	26
Figure 3-23: Unrounded Corner (Left) vs. Rounded Corner (Right).....	26
Figure 3-24: Mixing the Regular Resin	29
Figure 3-25: Applying Regular Resin to Beam Surface	29

Figure 3-26: Applying Carbon FRP Sheet to Beam	30
Figure 3-27: Carbon FRP Splay Anchors used for Beam T3	30
Figure 3-28: Inserting Thickened Resin into Anchor Holes for Beam T3	31
Figure 3-29: Carbon FRP Splay Anchors Installed in Anchor Holes.....	31
Figure 3-30: Regular Resin Applied to Beam Surface	32
Figure 3-31: Mixing Thickened Resin.....	32
Figure 3-32: Applying Thickened Resin to Beam Surface	33
Figure 3-33: Saturating FRP Sheets.....	33
Figure 3-34: Applying Carbon FRP Sheet to the Beam	34
Figure 3-35: Rolling out the Carbon FRP Sheet with Rib Roller	34
Figure 3-36: Applying $\pm 45^\circ$ Bi-Directional Glass FRP U-wrap to the Beam	35
Figure 3-37: Rolling Out U-wrap with Rib Roller.....	35
Figure 4-1: Testing Apparatus used to Test Concrete Cylinders.....	37
Figure 4-2: Example of Concrete Cylinder in Testing Apparatus	37
Figure 4-3: Example of Digital Readout of Concrete Cylinder Test Results	38
Figure 4-4: Testing Apparatus for Steel Rebar Testing.....	39
Figure 4-5: Example of Digital Readout of Steel Rebar Testing.....	40
Figure 4-6: Example of Test Results Print Out for Rebar Testing	40
Figure 4-7: Carbon FRP Manufacturer Properties.....	41
Figure 4-8: $\pm 45^\circ$ Bi-Directional Glass FRP Manufacturer Properties.....	42
Figure 5-1: Experimental Test Set Up	43
Figure 5-2: Concrete Strain Gauge Attached at the Top of the Flange at the Mid-span	46
Figure 5-3: FRP Strain Gauge Attached to the Bottom of the Web at the Mid-span	46
Figure 5-4: Beam T1 Setup before Testing.....	47
Figure 5-5: Beam T1 Shear Cracking at Mid-span after Testing.....	48
Figure 5-6: Beam T1 after Testing.....	48
Figure 5-7: Beam T1 Load vs. Deflection Response	49
Figure 5-8: Beam T1 Load vs. Concrete Top Strain Response	49
Figure 5-9: Beam T1 Load vs. Steel Bar Strain Response	50
Figure 5-10: Beam T2 Setup before Testing.....	51
Figure 5-11: Beam T2 after Failure with Debonded FRP Sheet Laying on the Floor.....	52

Figure 5-12: Beam T2 FRP Debonding and Rupture at Failure	52
Figure 5-13: Beam T2 Load vs. Deflection Response	53
Figure 5-14: Beam T2 Load vs. Concrete Top Strain Response	53
Figure 5-15: Beam T2 Load vs. Steel Bar Strain Response	54
Figure 5-16: Beam T2 Load vs. FRP Strain at the Beam Mid-span	54
Figure 5-17: Beam T3 Setup before Testing.....	56
Figure 5-18: Beam T3 after Testing.....	56
Figure 5-19: Beam T3 FRP Rupture at Mid-span.....	57
Figure 5-20: Beam T3 Load vs. Deflection Response	57
Figure 5-21: Beam T3 Load vs. Concrete Top Strain Response	58
Figure 5-22: Beam T3 Load vs. Steel Bar Strain Response	58
Figure 5-23: Beam T3 Load vs. FRP Strain at Mid-span Response	59
Figure 5-24: Beam T3 Load vs. FRP S7 Strain Response.....	59
Figure 5-25: Beam T3 Load vs. FRP S8 Strain Response.....	60
Figure 5-26: Beam T3 Load vs. FRP S9 Strain Response.....	60
Figure 5-27: Beam T3 Load vs. FRP S10 Strain Response.....	61
Figure 5-28: Beam T3 Load vs. FRP S11 Strain Response.....	61
Figure 5-29: Beam T3 Load vs. FRP S12 Strain Response.....	62
Figure 5-30: Beam T4 Setup before Testing.....	63
Figure 5-31: Beam T4 after Testing.....	63
Figure 5-32: Beam T4 Glass FRP U-wrap Debonding	64
Figure 5-33: Beam T3 Load vs. Deflection Response	64
Figure 5-34: Beam T4 Load vs. Concrete Top Strain Response	65
Figure 5-35: Beam T4 Load vs Steel Bar Strain Response	65
Figure 5-36: Beam T4 Load vs. FRP Strain at Mid-span Response	66
Figure 5-37: Beam T5 Setup before Testing.....	67
Figure 5-38: Beam T5 after Testing.....	68
Figure 5-39: Beam T5 Debonding of U-wrap with Exposed Rebar	68
Figure 5-40: Beam T5 Load vs. Deflection Response	69
Figure 5-41: Beam T5 Load vs. Concrete Top Strain Response	69
Figure 5-42: Beam T5 Load vs. Steel Bar Strain Response	70

Figure 5-43: Beam T5 Load vs. FRP Strain Response at Mid-span.....	70
Figure 5-44: Beam T5 Load vs. FRP S7 Strain Response.....	71
Figure 5-45: Beam T5 Load vs. FRP S8 Strain Response.....	71
Figure 5-46: Beam T5 Load vs. FRP S9 Strain Response.....	72
Figure 5-47: Beam T5 Load vs. FRP S10 Strain Response.....	72
Figure 5-48: Beam T6 Setup before Test.....	74
Figure 5-49: Beam T6 after Test.....	74
Figure 5-50: Beam T6 Debonding of Glass FRP U-wrap with Exposed Rebar	75
Figure 5-51: Beam T6 Load vs. Deflection Response.....	75
Figure 5-52: Beam T6 Load vs. Concrete Top Strain Response	76
Figure 5-53: Beam T6 Load vs. Steel Bar Strain Response	76
Figure 5-54: Beam T6 Load vs. FRP Strain Response at Mid-span.....	77
Figure 5-55: Beam T6 Load vs. FRP S7 Strain Response.....	77
Figure 5-56: Beam T6 Load vs. FRP S8 Strain Response.....	78
Figure 5-57: Beam T6 Load vs. FRP S9 Response	78
Figure 5-58: Beam T6 Load vs. FRP S10 Response	79
Figure 5-59: Comparison of Beams Load vs. Deflection Response.....	80
Figure 6-1: Beam T1 Experiment and Analytical Load vs. Deflection Response.....	83
Figure 6-2: Beam T1 Experiment and Analytical Load vs. Concrete Top Strain Response	84
Figure 6-3: Beam T1 Experiment and Analytical Load vs. Steel Bar Strain Response	84
Figure 6-4: Beam T2 Experiment and Analytical Load vs. Deflection Response.....	86
Figure 6-5: Beam T2 Experiment and Analytical Load vs. Concrete Top Strain Response	86
Figure 6-6: Beam T2 Experiment and Analytical Load vs. Steel Bar Strain Response	87
Figure 6-7: Beam T2 Experiment and Analytical Load vs. FRP Strain at Mid-span Response...	87
Figure 6-8: Beam T3 Experiment and Analytical Load vs. Deflection Response.....	89
Figure 6-9: Beam T3 Experiment and Analytical Load vs. Concrete Top Strain Response	89
Figure 6-10: Beam T3 Experiment and Analytical Load vs. Steel Bar Strain Response	90
Figure 6-11: Beam T3 Experiment and Analytical Load vs. FRP Strain at Mid-span Response.	90
Figure 6-12: Beam T3 Experiment and Analytical Load vs. FRP S7 Strain Response.....	91
Figure 6-13: Beam T3 Experiment and Analytical Load vs. FRP S8 Strain Response.....	91
Figure 6-14: Beam T3 Experiment and Analytical Load vs. FRP S9 Strain Response.....	92

Figure 6-15: Beam T3 Experiment and Analytical Load vs. FRP S10 Strain Response.....	92
Figure 6-16: Beam T3 Experiment and Analytical Load vs. FRP S11 Strain Response.....	93
Figure 6-17: Beam T3 Experiment and Analytical Load vs. FRP S12 Strain Response.....	93
Figure 6-18: Beam T4 Experiment and Analytical Load vs. Deflection Response.....	95
Figure 6-19: Beam T4 Experiment and Analytical Load vs. Concrete Top Strain Response	95
Figure 6-20: Beam T4 Experiment and Analytical Load vs. Steel Bar Strain Response	96
Figure 6-21: Beam T4 Experiment and Analytical Load vs. FRP Strain Response at Mid-span.	96
Figure 6-22: Beam T5 Experiment and Analytical Load vs. Deflection Response.....	98
Figure 6-23: Beam T5 Experiment and Analytical Load vs. Concrete Top Strain Response	98
Figure 6-24: Beam T5 Experiment and Analytical Load vs. Steel Bar Strain Response	99
Figure 6-25: Beam T5 Experiment and Analytical Load vs. FRP Strain Response at Mid-span.	99
Figure 6-26: Beam T5 Experiment and Analytical Load vs. FRP S7 Strain Response.....	100
Figure 6-27: Beam T5 Experiment and Analytical Load vs. FRP Strain S8 Response.....	100
Figure 6-28: Beam T5 Experiment and Analytical Load vs. FRP S9 Strain Response.....	101
Figure 6-29: Beam T5 Experiment and Analytical Load vs. FRP S10 Strain Response.....	101
Figure 6-30: Beam T6 Experiment and Analytical Load vs. Deflection Response.....	103
Figure 6-31: Beam T6 Experiment and Analytical Load vs. Concrete Top Strain Response	103
Figure 6-32: Beam T6 Experiment and Analytical Load vs. Steel Bar Strain Response	104
Figure 6-33: Beam T6 Experiment and Analytical Load vs. FRP Strain Response at Mid-span	104
Figure 6-34: Beam T6 Experiment and Analytical Load vs. FRP S7 Strain Response.....	105
Figure 6-35: Beam T6 Experiment and Analytical Load vs. FRP S8 Strain Response.....	105
Figure 6-36: Beam T6 Experiment and Analytical Load vs. FRP S9 Strain Response.....	106
Figure 6-37: Beam T6 Experiment and Analytical Load vs. FRP S10 Strain Response.....	106

List of Tables

Table 4-1: Results from Concrete Cylinder Testing	36
Table 4-2: Results from Steel Rebar Tests	39
Table 5-1: FRP Strain Gauge Locations for Beams T3, T5, and T6	45
Table 6-1: Improvement Strain Ratio of Strengthened Beams	107

Acknowledgements

I would like to thank my advisor, Dr. Hayder Rasheed, for all of his support throughout my time at Kansas State University and for giving me the opportunity to work on this project. I would also like to thank Dr. Hani Melhem and Dr. Christopher Jones for serving on my advisory committee.

I would also like to thank my fellow students, Mohammed Zaki and David Gudino, for all of their help with construction and strengthening of the beams. Finally I would like to thank our Civil Engineering Research Technician Cody Delaney and Research Technologist Ben Thurlow for all of their help in the lab with construction and testing of the beams.

Chapter 1 - Introduction

Background

As infrastructure continues to age and deteriorate, new creative solutions have surfaced with ways to repair and strengthen structures rather than tear them down. One particular technique that is becoming more common is the use of externally bonded fiber reinforced polymers (FRP) to strengthen concrete structures. The appeal of using FRP to strengthen a structure is that it is an economical and environmentally friendly option for strengthening a structure. As this strengthening technique becomes more common, it is important to continue research to address problems that arise from its behavior and application. The main problem that occurs when using FRP strengthening systems is that of debonding, where the bond between the epoxy and the concrete, or within the concrete substrate, fails prior to the full capacity of the FRP being reached. This results in FRP not being as economical because the full strength of the FRP is not being used. One solution to this problem is to use an anchorage system. The goal of using an anchorage system is to keep the FRP attached to the beam so that the full strength of the FRP can be reached, resulting in a rupture failure of the FRP rather than debonding. Different types of anchorage systems have been the focus of many different research projects in order to better understand how to best anchor FRP sheets to concrete beams. New research projects are necessary to help better understand and improve on current anchorage systems that are being used.

Objectives

This study has three main objectives. The first objective is to evaluate U-wrap anchorage systems using $\pm 45^\circ$ bi-directional Glass FRP for beams strengthened with Carbon FRP in flexure. To accomplish this objective the behavior of three beams with different U-wrap

anchorage systems were compared to a strengthened beam with no anchorage and a control beam. The second objective is to optimize the cost vs. gain in strength for the U-wrap anchorage. In order to complete this objective three different U-wrap configurations were used to be able to correlate the amount of fiber used for U-wraps with the increased strength of the beam over the control and strengthened beam with no anchorage. The third main objective is to qualify strain improvement due to U-wraps. This was accomplished by calculating different strain improvement ratios for each strengthened beam. The complete design, construction, and testing of the beam specimens will be discussed in this thesis. The results of each of the objective outcomes will be addressed in the conclusions.

Scope

This thesis is broken up into seven chapters. The first chapter is an introduction. After the introduction is a literature review. This literature review covers three topics: externally bonded FRP, Carbon FRP splay anchors, and finally U-wrap anchorage systems. Following the literature review is a discussion on the design, construction, and strengthening of the beam specimens. Next will be a chapter covering the material testing done for the concrete and steel rebar's actual strength. After the material testing is a chapter covering the experimental set up and test results from each beam specimen. The next chapter covers the analysis of each beam specimen and a comparison between the analytical and experimental results. Finally, the last chapter covers the conclusions from this study and the recommendations suggested for future work.

Chapter 2 - Literature Review

This literature review covers previous research on externally bonded FRP, Carbon splay anchors, and U-wrap anchorage systems. The goal of this chapter is to present research that correlates to the work of this study. The purpose of the externally bonded FRP section is to show research on debonding of FRP which is the main reason that anchorage systems like the ones examined in this study are needed.

Externally Bonded FRP

Ali-Ahmad et al (2006) performed experimental research to investigate debonding between concrete and FRP sheets. Concrete blocks with a length of 330 mm, width of 125 mm, and a height of 125 mm were cast to use in the tests. An FRP composite was applied to one side of the block for testing. A testing apparatus was developed for this study that loaded the specimens in direct shear. This was accomplished by a load fixture that applied a load directly to the FRP attached to the concrete and had supports to hold the concrete block in place. A quasi-static monotonic and a quasi-static cyclic direct shear test were run on different samples. During the testing of each specimen the surface strains in the FRP and the concrete were obtained using the digital image correlation technique. This is a technique that uses the mathematical correlation method and analyzes digital images of a specimen undergoing deformation and outputs strain values. The results from all the specimens resulted in a debonding failure. The conclusions that were drawn from the results include that debonding of FRP from a concrete surface is produced by an interfacial crack. Once this crack is started it continues to grow as the load continues to increase. Once the crack reaches a critical length, it continues to propagate but the load on the specimen remains constant. This causes an increase of the slippage of the FRP sheet. This study also tested the debonded FRP sheets in direct tensile tests to compare it with the control FRP

coupons. The results showed that the two had the same load response, so the debonded sheet had not reached any level of failure in the FRP itself.

Carbon FRP Splay Anchors

Orton et al (2008) conducted research on the effect of CFRP anchors on the overall tensile strength reached in an externally bonded CFRP sheet. The research consisted of 40 total specimens. Each specimen was constructed of two 20 cm wide by 81 cm long concrete blocks that were attached with an externally bonded sheet of CFRP. The goal of this set up was to simulate a concrete beam with a crack already at the mid-span. The blocks were simply supported and loaded at the mid-span in order to subject the CFRP to tension forces. The design parameters examined as a part of this study were the size, number, and spacing of CFRP anchors, offset height and angle between the two blocks, the type of CFRP material used, and the surface preparation technique. All these design parameters were changed throughout the 40 samples so that correlations between them could be found. First, seven beams were tested to examine the number, size, and spacing of anchors. From the results of these beams, the authors concluded that the total cross-sectional area of the anchor should be at least two times greater than the area of the CFRP sheet. It was also determined that a larger number of smaller anchors was more effective than less of a larger anchor size. The next set of beams tested looked at how the offset height of the two blocks and the transition slope between them effected the capacity of the CFRP sheet. The results showed that when a 1:4 transition slope was used, and the CFRP sheet was properly anchored, the beams reach loads resulting in the CFRP sheets attaining full capacity. Next the type of CFRP material was changed. One material had a lower ultimate strength which resulted in lower strength of the beam. This required a larger number of anchors to reach full strength. Finally, the surface preparation was studied by creating two specimens that had plastic

wrap between the concrete and the CFRP sheet so that the only thing holding the sheet onto the beam would be the anchors. The results showed that if the sheet was properly anchored to the beam and the anchors had enough capacity then the CFRP would still reach its full capacity. The authors concluded from this result that if adequate anchorage is applied then the surface preparation does not matter because the anchors can hold the CFRP sheet in place.

Ali et al (2014) conducted an experimental study to look at the behavior of concrete beams strengthened with CFRP sheets and plates and anchored with CFRP anchors. The total experiment consisted of sixteen beam specimens, but the study that was examined only contained information regarding five of the specimens. The beams had a cross section of 120 mm wide by 240 mm tall and were 1840 mm long with a 1690 mm clear span. The beams were loaded in four point bending for all the tests. The first beam was a control beam that failed at a load of 67.98 kN. The second beam was strengthened with a CFRP sheet that was 1000 mm long and failed at a load of 73.01 kips. The third beam was strengthened with the same CFRP sheet layout as the second beam, but it also contained one CFRP anchor on each end of the sheet. The holes for the anchors were 10 mm in diameter and 40 mm deep. This beam failed at a load of 80.15 kN. The fourth beam was strengthened with a 1000 mm long CFRP plate and failed at a load of 65.02 kN. The final beam was strengthened with a 1000 mm long CFRP plate and two CFRP anchors, one at each end of the plate. The holes for these anchors were 10 mm in diameter and 80 mm deep. This beam failed at a load of 78.28 kN. The results from this experiment showed an increase in the ultimate load for the beams that had CFRP anchors. The authors concluded that the control beam had the most ductility while the strengthened beams had lower ductility. They also concluded that for this study the anchors did not significantly contribute to the flexural stiffness of the beams.

U-wrap Anchorage Systems

Pham and Al-Mahaidi (2006) evaluated beams retrofitted with FRP and the debonding failure loads associated with it. The part of this research that related to U-wrap anchorage systems was the experimental program number two. This program consisted of testing eight rectangular concrete beams. The beams had a width of 140 mm and a height of 260 mm. The steel consisted of three 12 mm diameter bars for the tension steel and two 12 mm diameter bars for the compression steel. All the beams were strengthened with CFRP, but the first beam had no anchorage. Two of the beams had one non-prestressed U-strap at the end of the CFRP sheet and two beams had one prestressed U-strap at the end of the CFRP sheet. The final three beams had three U-straps spaced at 180 mm with two of the beams have prestressed U-straps and the third having non prestressed U-straps. The beams were tested in three point bending with a clear span of 1600 mm. The improvement in beam strength for the four beams with one U-strap ranged from 15 to 44%. The beams with multiple U-straps per shear span showed an increase in the ultimate capacity up to 79% above the beams with just one U-strap. The authors concluded that using U-wraps is an effective way to limit the debonding of externally bonded FRP. They found that placing multiple U-straps within the shear span limits the debonding because the opening of flexure-shear cracks is restricted. This study found that the prestressed U-straps used performed better than the non-prestressed, but the performance was only slightly better.

Yalim et al (2008) performed an experimental study that examined the performance of FRP strengthened reinforced concrete beams in flexure based on the amount of surface preparation and U-wrap anchorage. The overall study consisted of 26 specimens with two different Carbon FRP systems, wet layup and precured, as well as three different levels of surface preparation. The surface preparation was classified based on the roughness. These beams

also had different U-wrap layouts such as no U-wraps, 4 U-wraps, 7 U-wraps, 11 U-wraps, and a full length U-wrap. The flexural beams were T-beams with a web width of 152 mm and a web depth of 305 mm. The flange was 305 mm wide and 76 mm thick. The reinforcement was two No. 16M bars for the tension steel and two No. 10M bars for the compression steel. The beams were 2.1 meters long with a 2 meter clear span. All the beams were tested in three-point bending. From the results of this study the authors concluded that the amount of surface roughness did not significantly affect the performance of the beam regardless of the FRP system used, whether U-wrap anchorage was used or not, or if the failure load of the beam was debonding or FRP rupture.. The ultimate load of the beam is increased as the amount of anchorage is increased but the most significant difference between the beams is the ductility is greatly affected as the anchorage increases. The results of this study also showed that lower amounts of anchorage still resulted in FRP debonding as the failure mode. For the beams with four and seven straps, FRP debonding was still the failure mode that occurred after the straps themselves ruptured. For the beams with 11 straps and a full length continuous strap FRP rupture was reached as the failure mode,

Rasheed et al (2015) conducted research on the impact of CFRP U-wraps on the flexural capacity of concrete beams. Six total beams were constructed for this experiment, with the beams being split into two series. The first series consisted of three beams having a rectangular cross section while the second series contained the remaining three beams that had a T shaped cross section. All the beams had a total length of 4877 mm and a clear span of 4724 mm. The rectangular beams had a cross section of 152 mm by 305 mm. The tension steel consisted of two No. 5 bars and the compression steel was two No. 3 bars. The T-beams had the same dimensions as the rectangular beams for the web and then had flange dimensions of 406 mm wide by 102

mm thick. The rebar was also the same as the rectangular beams, but instead of two compression bars there were four. For each series of beams the first beam was a control beam, the second was strengthened with five layers of CFRP, and the third beam was strengthened with five layers of CFRP and additional transverse CFRP U-wraps. All the beams were tested in four point bending with load control at the beginning and then switching to displacement control partway through the test. The T-beam with U-wraps showed an increase in strength of around 130% from the strengthened T-beam with no U-wraps. This beam also showed an increase of around 210% when compared to the control beam. For the rectangular beams, the beam with U-wraps showed around a 110% increase in strength compared to the strengthened beam with no U-wraps, and an increase in strength of around 220% when compared to the control beam. This study concluded that using U-wraps as an anchorage system is an effective way to increase the flexural strengthening of a beam. In addition to this conclusion, this study proposed a design method to be used to determine the amount of U-wrap anchorage needed based on a shear friction model.

Chapter 3 - Design and Construction of Specimens

Design of T-Beams

The design of the T-beams was performed based on the requirements of ACI 318-14 and ACI 440.2R-17. These manuals are both based on the principles of strain compatibility and force/moment equilibrium. A set of design criteria was used to evaluate each different beam design. The first criterion used was that the beams needed to have a minimum web depth of 18 in. and a minimum web width of 10 in. The second criterion was that the strengthened beams, if the FRP reaches rupture strain, reached a failure load smaller than the capacity of the actuator used for the testing. The actuator used in this testing was a 150-kip capacity actuator. The third criterion for design was that the control beam needed to have a failure load lower than the FRP debonding and FRP rupture load. The fourth criterion required that concrete crushing failure occurred after FRP rupture failure for the strengthened beams. The final criterion used in evaluating the different designs was that all the beams must fail in flexure.

In order to make assessing multiple different designs easier and quicker, Excel was used to develop a worksheet that could quickly be changed for different design inputs and recalculated to show the failure loads for the different failure modes. To simplify the calculations in the spreadsheet, the compression steel was not included in the calculation of the flexural strength of the beam because the contribution from this steel would be typically negligible. Figure 3-1 below shows a picture of the Excel spreadsheet used for design.

Fiber Properties			Steel Properties			Concrete Properties			Section Properties			Reinforcement											
ffu	462	ksi	Es	29000	ksi	f'c	5	ksi	Flange Width	20	in		Diameter		Number	Area	Inputs=						
efu	0.014		fy	70	ksi				Flange Depth	4	in	Steel	#6	0.75	4	0.44							
Ef	33000	ksi							Web Width	10	in	Stirrups	#3	0.375		0.11							
tf	0.013	in							Web Depth	14	in	Cover	1	in									
									Total Depth	18	in	Fiber Layers	1										
												Fiber Wrapping	0	Wrapped (Y=2, N=0)	2								
d	16.25	in	<div>Shear Stirrup Design</div>																				
As	1.76	in ²																					
df1	18	in																					
df2	18	in																					
Ar1	0.13	in ²																					
			Vu=	46	kips	4phisqrt(f'c)b/d	34.47145558																
			phiVc	17.236	kips																		
			Sreq'd	6.525	in	Use 32 stirrups @ 6" C-C																	
Goal seek for c by setting the equilibrium cell to 0 by changing the cell with c																							
Rupture Calculation						Concrete Crushing Calculation						Debonding Calculation						Control Beam Calculation					
c=	2.6112			c=	2.6586			c=	2.8027			c=	1.8118										
Beta1	0.7653			Beta1	0.8217			Beta1	0.7251			Beta1	0.8										
ebi	0			ebi	0			ebi	0			ebi	0										
efe1	0.014	ecf	0.002376	efe1	0.0177	ecf	0.003067278	efe1	0.009	ecf	0.001653	efe1	0										
		e/c	0.002121			e/c	0.00212132			e/c	0.002121	efe2	0										
ffe1	462	alpha	0.701826	ffe1	584.1	alpha	0.743025434	ffe1	235.7	alpha	0.576726	ffe1	0										
												ffe2	0										
Force Equilibrium						Force Equilibrium						Force Equilibrium						Force Equilibrium					
a/cbc	183.26			a/cbc	199.13			a/cbc	161.64			a/cbc	0.85B1f'c	123.2									
Asfy	123.2			Asfy	123.2			Asfy	123.2			Asfy	123.2										
Alfe1	60.06			Alfe1	75.933			Alfe1	38.441			Alfe1	0										
								Alfe2	0			Alfe2	0										
Equilibrium	1E-05			Equilibrium	-3E-04			Equilibrium	-1E-06			Equilibrium	1E-14										
es	0.0124			es	0.0157			es	0.0079			es	0.0239										
Mn	2699.8	kip'in		Mn	3151.3	kip'in		Mn	2523.7	kip'in		Mn	1912.7	kip'in									
Mn	241.65	kip'ft		Mn	262.61	kip'ft		Mn	210.81	kip'ft		Mn	153.39	kip'ft									
Pn	60.41	kips		Pn	65.65	kips		Pn	52.7	kips		Pn	39.85	kips									

Figure 3-1: Excel Spreadsheet Used for T-Beam Design

T-Beam Geometry

After trying different design combinations, a final beam design was chosen. The final beam design consisted of a 16 ft. long T-beam with a 15.5 ft. clear span. The beams have a web depth of 18 in. with a web width of 10 in. The flanges of the beams have a width of 20 in. and are 4 in. thick. The rebar for each beam consisted of 4 No. 6 bars for the tension reinforcement and 4 No. 3 bars for the compression reinforcement. In order to insure that the beam failed in flexure and not shear, stirrups were placed throughout the beam. The minimum spacing required between the stirrups was determined to be 6.5 in. for a No. 3 stirrup. For the final design of shear stirrups No. 3 bars were used at a spacing distance of 6 in. on center. Figure 3-2 below shows a cross section view of the final beam design and Figure 3-3 shows a side view of the beam with the stirrups and support locations.

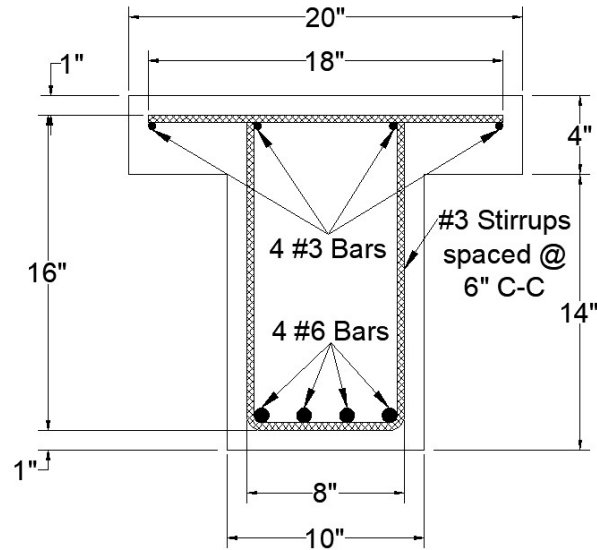


Figure 3-2: Cross Section of Final Beam Design

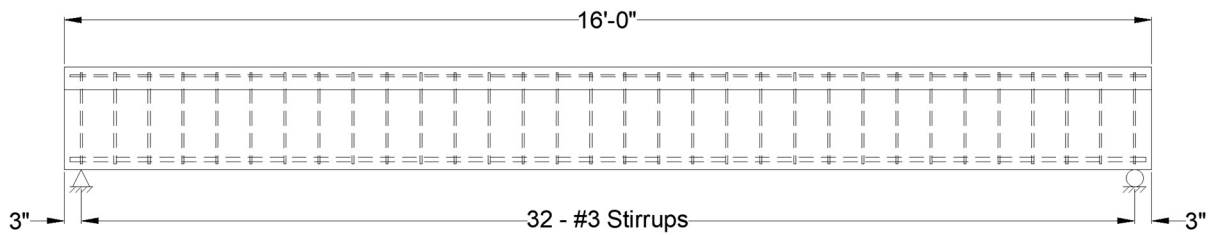


Figure 3-3: Shear Reinforcement and Support Locations for Final Beam Design

Design of Strengthening for T-Beams

Carbon FRP Sheets

For strengthening the designed T-beams, unidirectional carbon FRP sheets were used. Based on the final design of the beam, the finalized strengthening design was chosen to use one layer of carbon FRP with a 10in. width placed along the bottom face of the beam. This strengthening was applied to every strengthened beam in this study. The sheet was chosen to be 15 ft. long with each end of the sheet placed 3 in. from the support location. Figure 3-4 below

shows beam T2 from this study, which was the strengthened beam without any anchorage system.

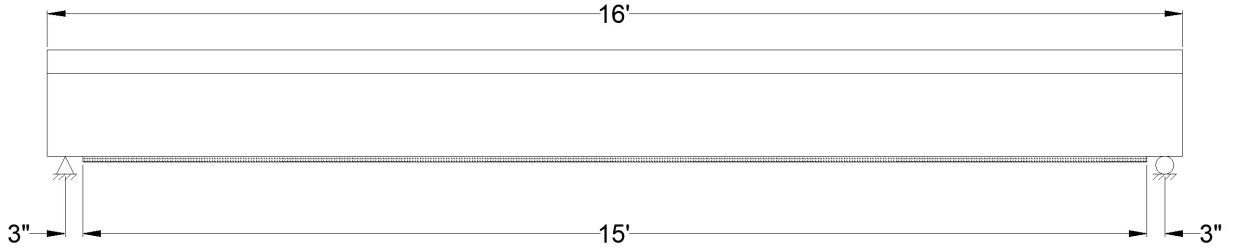


Figure 3-4: Profile of Strengthened Beam with Carbon FRP Sheet Only

Anchorage Using Carbon FRP Splay Anchors

The carbon FRP splay anchors used for this beam were predetermined to be 5/8 in. diameter carbon FRP splay anchors. The process used to obtain a preliminary design for the amount of anchors needed per shear span was outlined by Mohammed Zaki in his dissertation (Zaki 2018). The process involves calculating the maximum tension force in the externally bonded FRP sheet and then determining a maximum shear capacity of each anchor. The number of anchors is then determined by dividing the total tension force in the FRP by the shear capacity of each anchor. Below are the equations that were used to complete this design.

$$V_{anchor} = \frac{T_{max}}{\# \text{ of anchors per shear span}} \quad (3-1)$$

$$\gamma_{anchor} = (3.5^\circ) \times \left(\frac{\pi}{180}\right) \quad (3-2)$$

$$\tau_{anchor} = G_{12} \times \gamma_{anchor} \quad (3-3)$$

$$V_{anchor} = \tau_{anchor} \times A_{anchor} \quad (3-4)$$

In addition to the preliminary number of anchors required, the length of each anchor was calculated. The anchors had an embedment depth of 4 in. and the splay length was calculated to be two thirds of the length of the space between anchors. Figure 3-5 below shows the preliminary design calculations.

Number of Anchors Required Calculation		
$E_f =$	14240	ksi
$t_f =$	0.08	in
$e_{fu} =$	0.0127	
$b_f =$	10	in
$T_{max} = E_f * t_f * b_f * e_{fu} =$	144.6784	kips
$\gamma_{\text{anchor}} = (3.5 \text{ degrees}) * (\pi/180) =$	0.061087	radians
$G_{12} =$	700	kips/in ²
$\tau_{\text{anchor}} = G_{12} * \gamma_{\text{anchor}} =$	42.76057	kips/in ²
$\phi =$	0.85	
$A_{\text{anchor}} = (\pi/4) * ((5/8)^2) =$	0.306796	in ²
$V_{\text{anchor}} = \phi * \tau_{\text{anchor}} * A_{\text{anchor}} =$	11.15096	kips
Minimum Anchors per Shear Span	12.97452	anchors
Use 5 anchors per shear span		
Spacing from Support to Midspan =	93	in
Spacing from Support to First Anchor =	5	in
Spacing from Midspan to Anchor =	18	in
Spacing Between Anchors =	14	in
Length of Each Anchor =	13.38	in
Use anchors that are 14.00" long		

Figure 3-5: Carbon FRP Splay Anchor Design

After performing the initial design calculations it was determined that the 13 anchors required per shear span was excessive and instead a starting point of five anchors per shear span was selected for beam T3. The goal was to adjust the number of anchors per shear span for the remaining beams after testing beam T3 depending on if FRP rupture was reached. Figure 3-6 and 3-7 below show the layout of the anchors for beam T3.

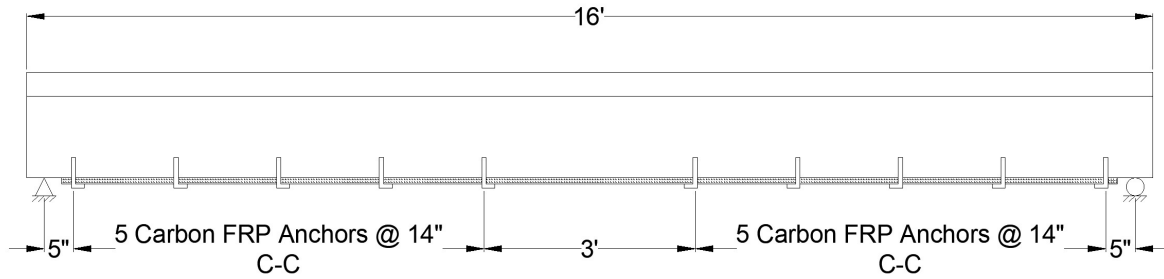


Figure 3-6: Profile of Strengthened Beam with Carbon FRP Sheet and Carbon FRP Splay Anchors

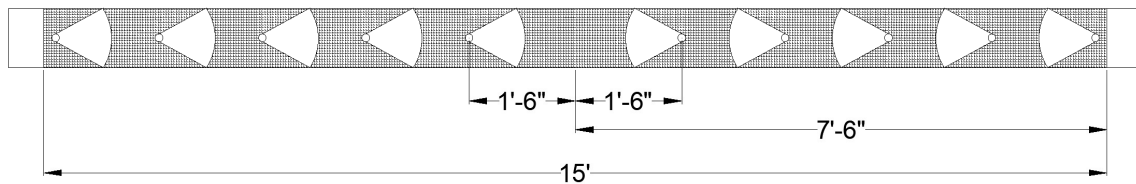


Figure 3-7: View of Bottom of Beam with Carbon FRP Sheet and Splay Anchors

Anchorage Using Bidirectional Glass FRP U-wraps

Following the test of beam T3 it was determined that changing the anchorage system to U-wraps would help ensure that useful results would be obtained from the experiments because due to the increased beam strength over the expected strength the beam experiences debonding before the beam failure load is reached. From previous work it is known that U-wraps are representative of a good anchorage system. To ensure that the strengthened beams would reach higher failure loads, U-wraps were used. The U-wraps used to anchor the carbon FRP sheet to the beams were selected to be $\pm 45^\circ$ bi-directional Glass FRP sheets. The $\pm 45^\circ$ bi-directional Glass FRP width was 25 in. and the entire width of the sheet was used in the U-wraps so the wrap went around 7.5 in. up each side of the web. In total three out of the six beams were anchored with these U-wraps. The layout of the U-wraps for the first beam was selected to be

one U-wrap sheet the entire length of the carbon FRP sheet. The second beam was chosen to have one layer of one foot wide U-wrap with a one foot space between U-wraps starting with the first wrap centered on the centerline of the beam. At each end of this beam a 6 in. space and 6 in. wide U-wrap was used to finish off the wrapping. This alignment was selected because this configuration used exactly half of the amount of $\pm 45^\circ$ bi-directional Glass FRP that the single layer of full length U-wrap used for the first beam. This allowed for the ultimate loads to be compared to see how the amount of fiber impacted the beam strength. The third beam that had U-wraps was selected to have the same configuration as the second beam but instead of one layer of Glass U-wraps it had two layers of Glass U-wraps. This configuration was selected because it had exactly the same amount of $\pm 45^\circ$ bi-directional Glass FRP as the full length U-wrap just in a different configuration so the results could be compared to see which technique was more effective. Figure 3-8 below shows a profile of the full length U-wrap configuration and Figure 3-9 shows a profile of the layout of the one foot wide U-wraps that were used with one layer for the second beam and two layers for the third specimen.

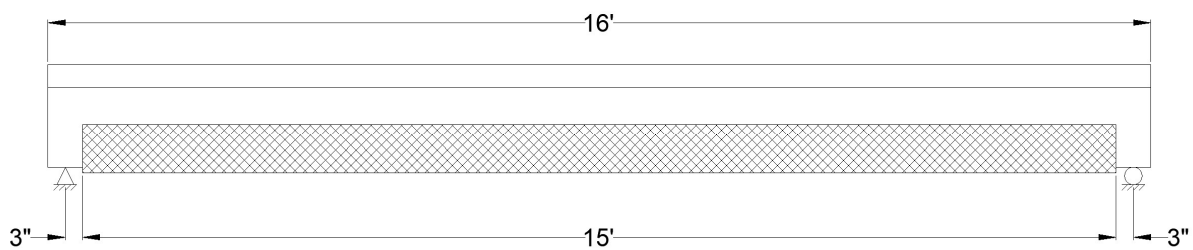


Figure 3-8: Profile of Beam Strengthened with Carbon FRP Sheet and Full Length $\pm 45^\circ$ Bi-Directional Glass FRP U-wrap

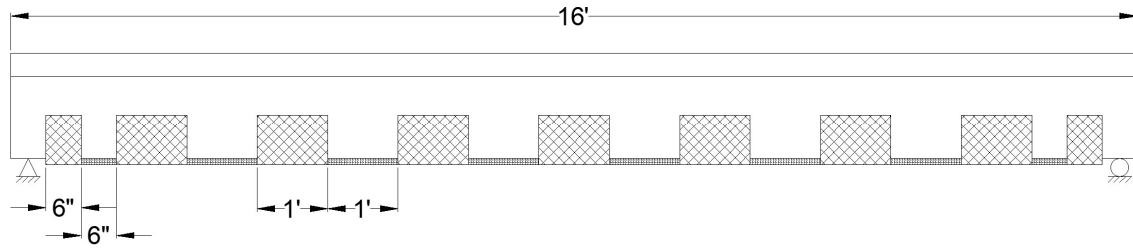


Figure 3-9: Diagram of Layout of Beams Strengthened with Carbon FRP Sheet and One Foot Wide $\pm 45^\circ$ Bi-Directional Glass FRP U-wraps

Formwork and Steel Caging

The formwork used for casting the beams was constructed from plywood sheets and 2 in. x 6 in. lumber planks. The plywood used for the formwork was 0.75 in. thick and 4 ft. x 8 ft. in width and length. Due to the size of the plywood sheets, the formwork was constructed in two 8 ft. long sections and then two 8 ft. sections were attached together to create the 16 ft. length needed for the beams. The 8 ft. sections of formwork were constructed in the Civil Engineering woodshop and then transported to the Civil Infrastructure Systems Laboratory (CISL) to be assembled into 16 ft. long sections. Each set of formwork consisted of two beams, so three total sets of formwork were constructed to cast the six total beams. In the endcap of each set of formwork a hole was predrilled at the centroid of the beam section so a piece of rebar could be held in place during casting. This rebar was used to flip the beams after casting and curing. Figures 3-10 and 3-11 below show pictures of the assembled formwork at CISL.



Figure 3-10: Two Sets of Assembled Formwork



Figure 3-11: Full Length Formwork

The rebars used for the longitudinal steel were delivered in 20 ft. long sections and were cut down to length using a steel cut off wheel. The stirrups used for the caging were ordered and delivered as prebent stirrups. The stirrups were attached to the longitudinal steel using rebar ties. In addition to the longitudinal bars and stirrups transverse bars were placed at each stirrup location to tie in the compression bars outside of the stirrups in the flange. These bars were also cut down using a steel cut off wheel and tied to the stirrups and longitudinal bars using rebar ties. Figure 3-12 below shows a section of finished rebar caging and Figure 3-13 below shows the finished rebar cages. Two strain gauges were attached to each rebar cage. They were placed at the mid-span of the cage with one on each of the outside tension reinforcement bars. In order to protect the strain gauges during casting the strain gauge was taped over and the wires were run out of the beam along the tension reinforcement and then up a stirrup with various points along both taped to the rebar. One inch steel chairs were used to raise the cage off of the bottom of the formwork to create the desired clear cover. After the cages were placed in the formwork, a No. 6 bar was placed through a predrilled hole in the end caps of the formwork so that the beams could be flipped after casting. Figure 3-14 below shows the rebar caging placed in the finished formwork before casting. Rebar hooks were cut, bent, and placed in the rebar caging to make the beams easier to move after curing. Each rebar hook consisted of two No. 3 bars tied together. Four total hooks were used for each beam with two of the hooks being approximately 10 in. from the mid-span of the beam and the other two hooks being placed at the end of the rebar caging.



Figure 3-12: Section of Finished Rebar Caging



Figure 3-13: Finished Rebar Caging For All Beams



Figure 3-14: Rebar Caging Placed in Formwork before Casting

Casting of Beams

The beams were cast using 4500 psi ready mix concrete. The concrete was provided by Midwest Concrete Materials, a local provider. Based on the amount of concrete needed to cast all six beams, the concrete was delivered in two batches so that it would be easier to work with the concrete and place it before it started to set. A super plasticizer was added to the mix on site so it would be easier for the concrete to flow down the chute and into the formwork. Several graduate students helped in casting the beams by vibrating the concrete, directing the truck, and screeding the top of the beams. In addition to the beams, cylinders were poured for each batch. The beams were covered with tarps since the temperature around the time of casting was mild. One week after casting the outside of all of the formwork was removed. Figures 3-15 through 3-17 below

show pictures of the casting. Figure 3-18 shows a picture of the beams with the outside of the formwork removed.



Figure 3-15: Casting of Beams



Figure 3-16: Placing and Vibrating the Concrete in the Formwork



Figure 3-17: Screeding the Tops of the Beams



Figure 3-18: Finished Beams with Outside of Formwork Removed

Surface Preparation

Prior to the installation of any FRP, the surfaces of each beam needed to undergo surface preparation. Before any surface preparation could be done the beams were moved inside CISL and flipped using the rebar extending from each end. Figure 3-18 below shows a picture of a beam being flipped. The surface preparation varied slightly for each beam depending on the strengthening that was used. For all strengthened beams, the bottom surface of the beam web was slightly roughened using a masonry grinding wheel in order to expose small air pockets and aggregate in the concrete so that the epoxy could fill these gaps and grip the surface. In addition to the surface grinding, for the beam with carbon FRP splay anchors, 4 in. deep holes that were 0.75 in. diameter were drilled into the bottom of the beam at the location of each anchor. For the beams with Glass FRP U-wraps the sides of the web were prepared using a masonry grinding wheel just like the bottom of the beams. In addition, for the beams with U-wraps the bottom

corners of the web were rounded off to a radius of approximately 0.5 in. in accordance with ACI 440.2R-17. Figures 3-19 and 3-20 below show a picture of preparing the surfaces as well as the difference between the prepared and unprepared surface. Figure 3-21 below shows a picture of the holes that were drilled in the beam for the anchors. Figure 3-22 below shows the difference between the rounded and unrounded corners.



Figure 3-19: Flipping Beam for Surface Preparation



Figure 3-20: Preparing the Beam Surfaces with Masonry Wheel



Figure 3-21: Prepared Beam Surface (Left) vs. Unprepared Beam Surface (Right)



Figure 3-22: Example of Drilled Hole in the Beam for Installation of Carbon FRP Splay Anchors



Figure 3-23: Unrounded Corner (Left) vs. Rounded Corner (Right)

Installation of FRP

After the surface preparation was complete the next step was installing the FRP onto the strengthened beams. The FRP installation was performed inside of CISL so that the resin and FRP was not affected by moisture or temperature. The installation process used for beams T2 and T3 was slightly different than the process used for beams T4, T5, and T6. The two different processes are both outlined in this section.

For beams T2 and T3 the first step in the installation process was to mix the resin according to the manufacturer specifications. Two different batches of resin were mixed, the first was the regular resin and the second was a thickened resin that consisted of silica fume added to the regular resin according to the manufacturer specifications. Second, a layer of regular resin was applied to the surface of each beam. Third, the carbon FRP sheet was placed on the beam and resin was rolled onto the sheet to saturate it. Finally, the carbon FRP sheet was rolled so all the air pockets were removed. After the carbon FRP was placed and saturated the next step was to install the carbon FRP splay anchors on beam T3. The first step for installing the splay anchors was to fill about half of each anchor hole with the thickened resin. Next the end of each anchor was inserted into the holes using a metal rod to make sure that each anchor reached the bottom of the hole. Finally, the ends of the splay anchors outside of the beam were splayed along the bottom of the beam towards the centerline of the beam and rolled with resin to saturate each end. Once the beams were strengthened, they were left to cure for around seven days to ensure that the resin had adequate time to cure before testing.

After testing beams T2 and T3 and discussing the results with the FRP manufacturer it was determined that the FRP installation process that was used may not have fully saturated the fibers which resulted in lower than expected ultimate strengths. The installation process was

slightly adjusted, with help from the manufacturer, to ensure that the FRP sheets used for strengthening of beams T4, T5, and T6 would be fully saturated. The first step in this updated installation process was to mix two batches of resin based on the manufacturer's instructions. The first batch of resin mixed was regular resin and the second batch was the thickened resin. The second step was applying a layer of regular resin to the surfaces of the beam where FRP would be applied. The third step was to apply a layer of thickened resin to the beam surfaces. Fourth, the carbon FRP sheets and $\pm 45^\circ$ bi-directional Glass FRP U-wraps were rolled out onto plastic sheets and rolled with regular resin to ensure that all of the sheets were fully saturated prior to being applied to the beams. Fifth, the carbon FRP sheet was applied to the beam and rolled out so that all the air bubbles were removed. Sixth, a layer of thickened resin was applied on top of the carbon FRP sheet so that the $\pm 45^\circ$ bi-directional Glass FRP U-wraps would hold in place better. Finally, the $\pm 45^\circ$ bi-directional Glass U-wraps were applied to the beam and rolled out to remove all the air pockets. These beams were left to cure for around seven days to ensure adequate curing time prior to testing.

Figures 3-24 through 3-29 show pictures of different steps of the FRP installation process used for beams T2 and T3. Figures 3-30 through 3-37 show pictures of the FRP installation process used for beams T4, T5, and T6.

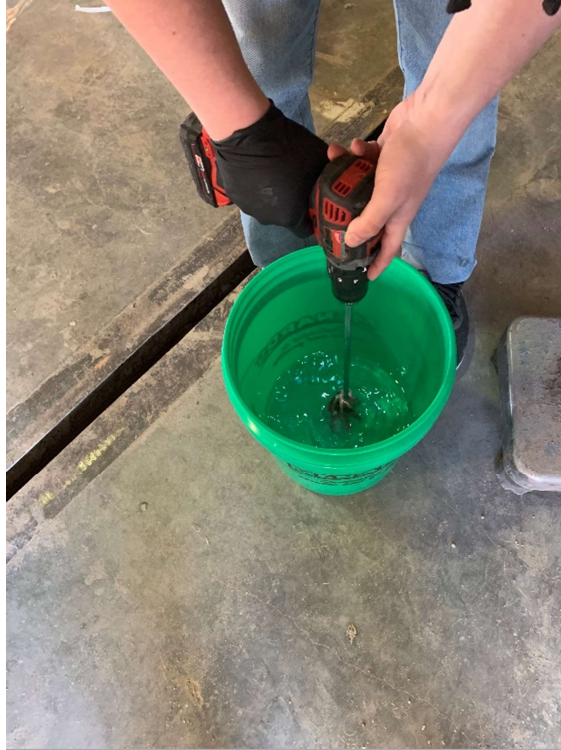


Figure 3-24: Mixing the Regular Resin



Figure 3-25: Applying Regular Resin to Beam Surface



Figure 3-26: Applying Carbon FRP Sheet to Beam



Figure 3-27: Carbon FRP Splay Anchors used for Beam T3



Figure 3-28: Inserting Thickened Resin into Anchor Holes for Beam T3

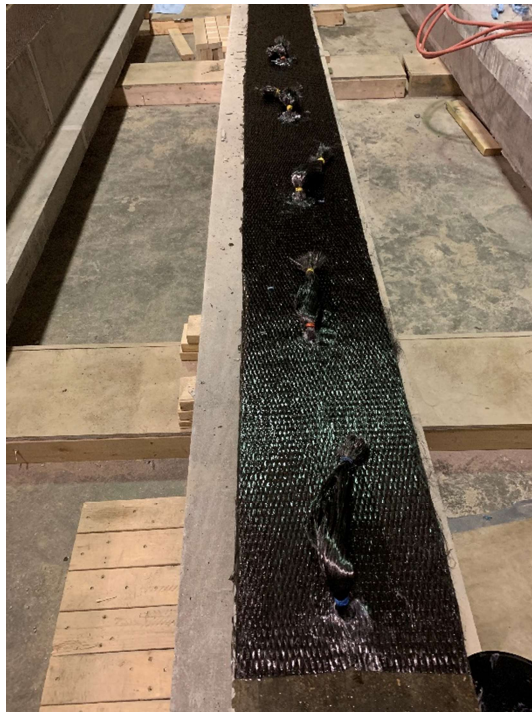


Figure 3-29: Carbon FRP Splay Anchors Installed in Anchor Holes



Figure 3-30: Regular Resin Applied to Beam Surface



Figure 3-31: Mixing Thickened Resin



Figure 3-32: Applying Thickened Resin to Beam Surface



Figure 3-33: Saturating FRP Sheets



Figure 3-34: Applying Carbon FRP Sheet to the Beam

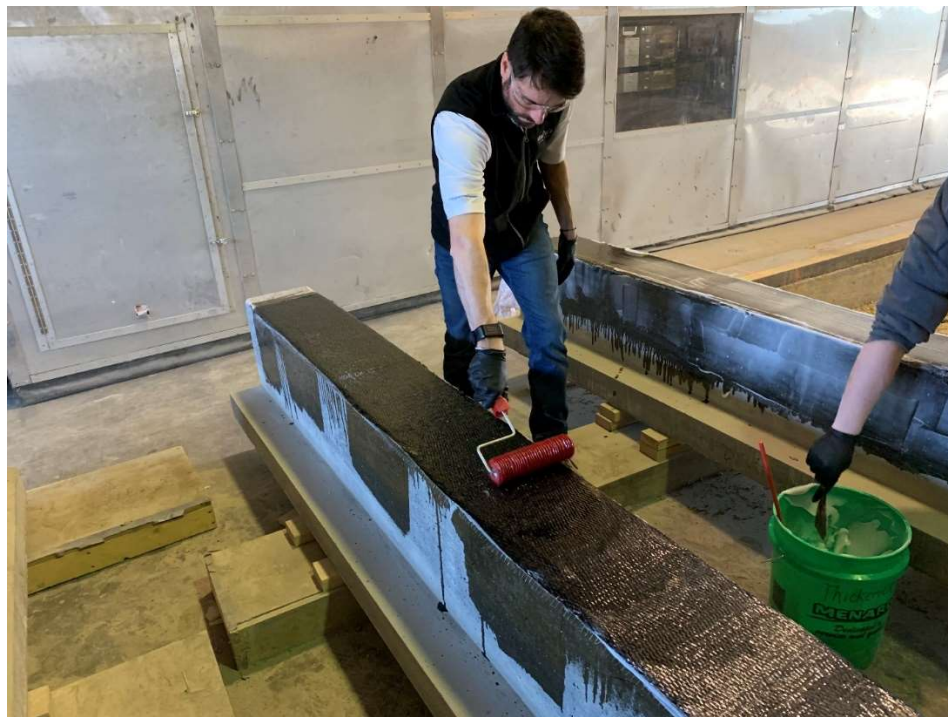


Figure 3-35: Rolling out the Carbon FRP Sheet with Rib Roller



Figure 3-36: Applying $\pm 45^\circ$ Bi-Directional Glass FRP U-wrap to the Beam

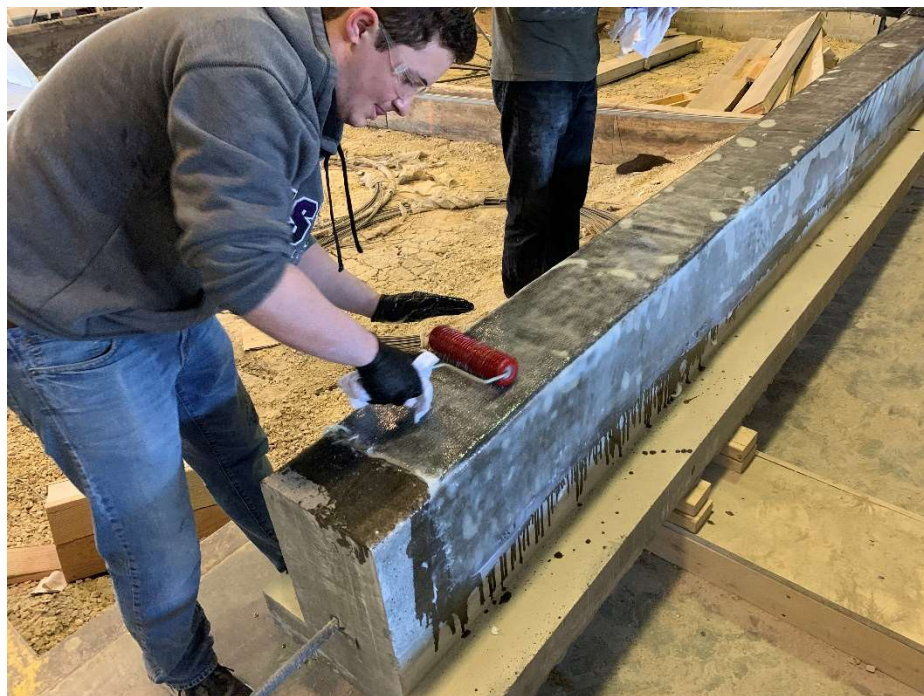


Figure 3-37: Rolling Out U-wrap with Rib Roller

Chapter 4 - Material Properties

Testing of Concrete Cylinders

For casting the beams, a ready-mix concrete was used with a requested nominal compressive strength of 4500 psi. The concrete was delivered in two different batches to make pouring and working with the concrete easier. During casting of the beams on 11/2/18, nine 4 in. x 8 in. cylinders were poured to test the experimental compressive strength of the concrete. Six of the cylinders were poured from batch one while the remaining three cylinders were poured from batch two. For the six cylinders poured from batch one, three of them were cured in a moisture room for twenty-eight days while the other three were cured outside sitting next to the beams for the same twenty-eight days. The three cylinders poured from batch two were cured for twenty-eight days in a moisture room. All nine of the cylinders were tested on 11/30/18, exactly twenty-eight days from the pour. The average compressive strength of the batch one cylinders cured in the moisture room was 7340 psi. The average compressive strength of the batch one cylinders cured outside next to the beams was 7276 psi. The average compressive strength of the batch two cylinders cured in the moisture room was 7899 psi. Table 4-1 below shows the results of the cylinder tests. Figures 4-1 through 4-3 below show pictures of the concrete cylinder testing.

Table 4-1: Results from Concrete Cylinder Testing

Batch and Cylinder #	Curing Location	Load (lbs)	Compressive Strength (f'c) (psi)	Date Tested
Batch 1 Cylinder 1	Moisture Room	90156	7174	11/30/2018
Batch 1 Cylinder 2	Moisture Room	92459	7358	
Batch 1 Cylinder 3	Moisture Room	94098	7488	
Batch 1 Cylinder 4	Outside with Beams	96024	7641	11/30/2018
Batch 1 Cylinder 5	Outside with Beams	86587	6890	
Batch 1 Cylinder 6	Outside with Beams	91704	7298	
Batch 2 Cylinder 1	Moisture Room	97486	7758	11/30/2018
Batch 2 Cylinder 2	Moisture Room	102292	8140	
Batch 2 Cylinder 3	Moisture Room	98021	7800	



Figure 4-1: Testing Apparatus used to Test Concrete Cylinders



Figure 4-2: Example of Concrete Cylinder in Testing Apparatus

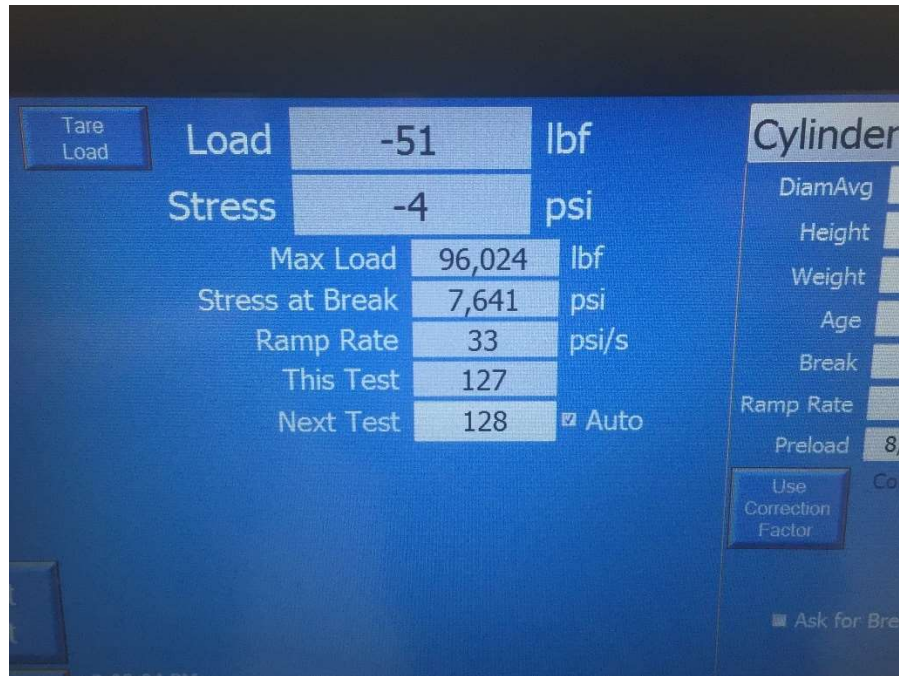


Figure 4-3: Example of Digital Readout of Concrete Cylinder Test Results

Testing of Steel Rebar

The steel rebar used in the construction of the beams consisted of No. 6 bars for the tension reinforcement and No. 3 bars for the compression reinforcement and stirrups. The rebar used had given manufacturers properties of 60 ksi for the minimum yield strength and 29000 ksi for the modulus. In order to verify the average yield strength of the rebar, samples were tested at the Kansas Department of Transportation Materials-Research Center. In order to get an average yield strength for each size of bar, three samples of each bar were tested. The average experimental yield strength of the No. 6 bars was 69.65 ksi. The average experimental yield strength of the No. 3 bars was 66.99 ksi. Table 4-2 below shows the results from the steel rebar testing. Figures 4-4 through 4-6 show pictures of the steel rebar testing set up and output information.

Table 4-2: Results from Steel Rebar Tests

Sample #	Bar Size No.	Yield Strength (fy) (ksi)	Ultimate Tensile Strength (ksi)
1	6	70.77	111.33
2	6	69.39	110.54
3	6	68.66	109.34
4	3	65.97	100.98
5	3	66.47	100.9
6	3	68.26	103.01

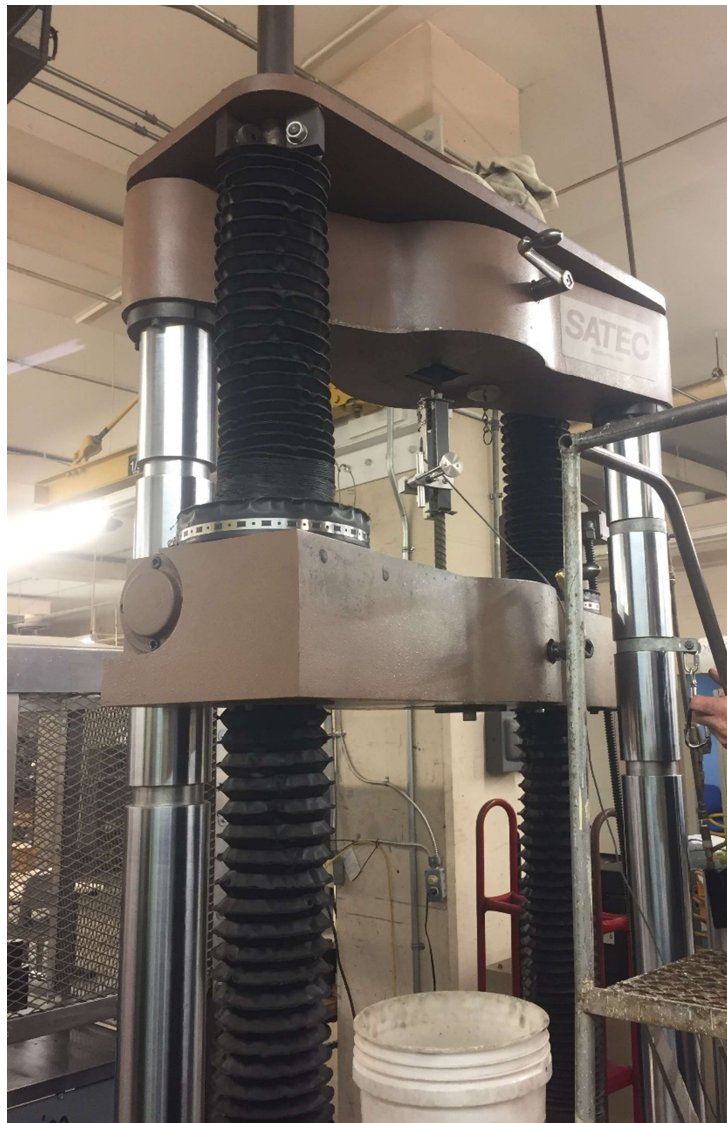


Figure 4-4: Testing Apparatus for Steel Rebar Testing

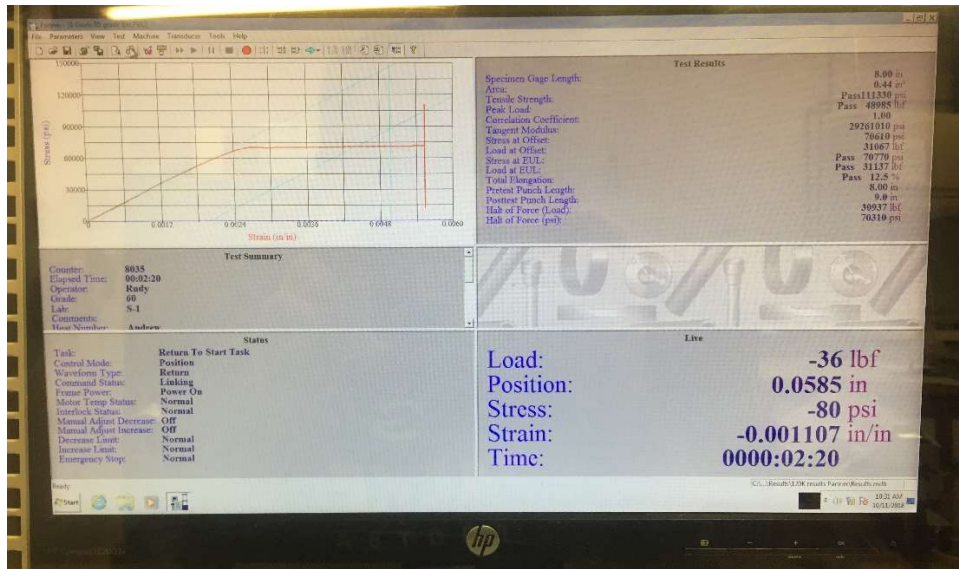


Figure 4-5: Example of Digital Readout of Steel Rebar Testing

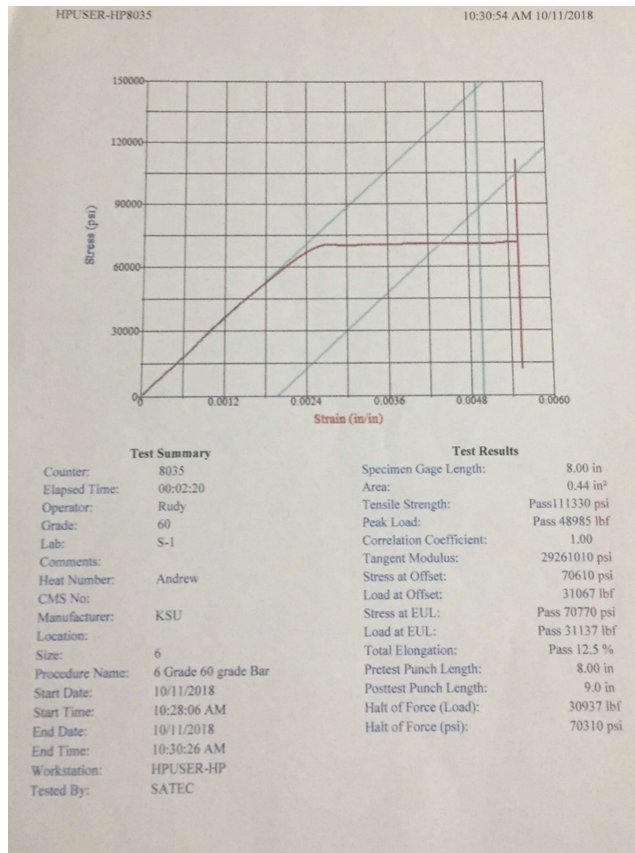


Figure 4-6: Example of Test Results Print Out for Rebar Testing

FRP Properties

This study used two different types of FRP, both of which were developed by Structural Technologies. The first type of FRP used was V-Wrap C200HM, which is a high modulus Carbon FRP that was used as the flexural strengthening for the beams. The second type of FRP used was V-Wrap EG50-B. This is the $\pm 45^\circ$ bi-directional Glass FRP that was used for the U-wraps. Figure 4-7 below shows the manufacturers given properties for the Carbon FRP and Figure 4-8 shows the manufacturers given properties for the $\pm 45^\circ$ bi-directional Glass FRP.

Strengthening Solutions

V-Wrap™ C200HM

High Modulus Carbon Fiber Fabric

structural
TECHNOLOGIES

structuraltechnologies.com

+1-410-859-6539

Typical Data for V-Wrap C200HM

Storage Conditions:

Color:

Primary Fiber Direction:

Weight:

Shelf life:

Store dry at 40°F – 90°F (4°C – 32°C)

Black

0° (unidirectional)

17.7 oz/yd² (600 g/m²)

10 years

Fiber Properties (Dry)

Tensile Strength:

Tensile Modulus:

Elongation:

790,000 psi (5,440 MPa)

42 x 10⁶ psi (289,550 MPa)

1.9 %

Cured Laminate Properties

Tensile Strength:

Modulus of Elasticity:

Elongation at Break:

Thickness:

Strength per Unit Width:

180,000 psi (1,241 MPa)

14.24 x 10⁶ psi (98,181 MPa)

1.27%

0.04 in. (1.02 mm)

7,200 lbs/in. (1.26 kN/mm)

Design Values*


155,000 psi (1,068 MPa)

14.0 x 10⁶ psi (96,527 MPa)

1.1%

0.04 in. (1.02 mm)

6,200 lbs/in. (1.09 kN/mm)



*Design properties are based on ACI 440.2R using average minus three standard deviations.

Figure 4-7: Carbon FRP Manufacturer Properties

Strengthening Solutions

V-Wrap™ EG50-B

High Strength Glass Fiber Fabric

structural
TECHNOLOGIES

structuraltechnologies.com

+1-410-859-6539

Typical Data for V-Wrap EG50-B

Storage Conditions:

Color:

Primary Fiber Direction:

Weight:

Shelf life:

Store dry at 40°F – 90°F (4°C – 32°C)

White

±45° (bi-directional)

24.6 oz/yd² (835 g/m²)

10 years

Fiber Properties (Dry)

Tensile Strength:

Tensile Modulus:

Elongation:

Density:

475,000 psi (3,275 MPa)

11.6 x 10⁶ psi (79,970 MPa)

4.1 %

0.095 lb/in³ (2.62 g/cm³)

Cured Laminate Properties

(In fiber direction)

Tensile Strength:

Modulus of Elasticity:

Elongation at Break:

Laminate Thickness:

Design Thickness:

Strength per Unit Width:

Average Values⁽¹⁾

89,800 psi (620 MPa)

4.6 x 10⁶ psi (31,700 MPa)

1.94%

0.034 in. (0.864 mm)

0.017 in. (0.432 mm)

1,527 lbs/in. (0.27 kN/mm)

Design Values⁽²⁾

74,500 psi (514 MPa)

4.6 x 10⁶ psi (31,700 MPa)

1.6%

0.034 in. (0.864 mm)

0.017 in. (0.432 mm)

1,267 lbs/in. (0.22 kN/mm)

(1) Typical average test values per ASTM 3039

(2) Design properties are based on ACI 440 guidelines will vary slightly. Contact STRUCTURAL TECHNOLOGIES to confirm project specific values.

Figure 4-8: ±45° Bi-Directional Glass FRP Manufacturer Properties

Chapter 5 - Experimental Setup and Testing

Experimental Setup

The flexural tests on the beams were performed at Kansas State University in the structural engineering testing laboratory. The beams were loaded in three-point bending using a steel plate to help distribute the load on the beam and a 150-kip capacity hydraulic actuator. The steel plate that was used measured 12 in. in the direction of the span by 22 in. transverse to the span and 2 in. thick. The actuator is run by a servo-hydraulic system produced by MTS. The system includes an accurate data acquisition program and requires MTS certification to operate.

The beams were simply supported for the loading applied. This set up was accomplished using plates and rollers at each support location with one support allowing movement in the direction of the beam span while the other support only allowed for rotation. The supports are each placed 3 inches from the ends of the beam on center, resulting in a clear span for each beam equal to 15 ft. 6 in. Figure 5-1 below shows a schematic of the experimental set up.

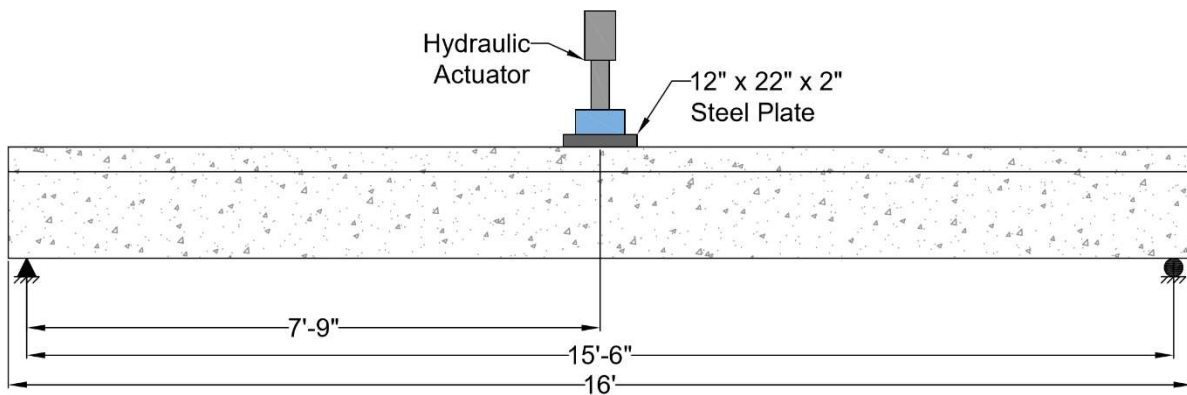


Figure 5-1: Experimental Test Set Up

The data that was collected for each beam was the load applied, the deflection at mid-span, the strain in the concrete at the top of the beam on either side of the flange, and the strain in the tension steel. For the five strengthened beams in addition to the data listed above the strain in

the FRP at mid-span and other various locations in the FRP along the shear span were recorded. For determining the deflection at the mid-span of the beam, two linear variable differential transducer (LVDT) sensors were used. The concrete strains were determined using two 120 Ω strain gauges. The steel strains were measured using two 120 Ω strain gauges installed on the tension rebar at the mid-span of the two outside tension reinforcement bars. The FRP strains were measured using 350 Ω strain gauges. For the beam with just Carbon FRP and the beam with a full length Glass FRP U-wrap, two strain gauges were placed at the mid-span of the beam on both sides of the bottom of the web. The beams that had anchors and one-foot wide U-wraps had two strain gauges installed at the mid-span just like the other two strengthened beams. In addition, the beam with anchors had six additional strain gauges, three in each shear span, along the length of the shear span that were installed at locations between the splay anchors and at the center of the bottom of the web. The beams with one-foot wide U-wraps had four additional strain gauges installed in addition to the two at mid-span. These strain gauges were installed with two per shear span and were attached to the center of the Carbon FRP in the spaces between U-wraps. Table 5-1 lists the location of each additional strain gauge from the centerline of the beam towards each support for the beams with anchors and with one-foot U-wraps.

Table 5-1: FRP Strain Gauge Locations for Beams T3, T5, and T6

Beam	Strain Gauge Label	Distance From Support Location to Strain Gauge (in.)
T3	FRP S7	70.75
	FRP S8	77.75
	FRP S9	52.75
	FRP S10	55
	FRP S11	35.37
	FRP S12	37.375
T5	FRP S7	83
	FRP S8	79.75
	FRP S9	58.5
	FRP S10	57.75
T6	FRP S7	80.25
	FRP S8	81.25
	FRP S9	55.75
	FRP S10	55.75

The data from the instrumentation was collected using a data acquisition system called series 7000, which is a system developed by Vishay. The data was recorded every 1.5 seconds during the test. The beams were loaded using displacement control at a rate of 0.1 inch per minute. Once the test had been completed, all of the data points for the load, displacement, and strains were imported into a Microsoft Excel file to perform analysis. Figures 5-2 and 5-3 below show examples of the concrete and FRP strain gauges installed on a beam.

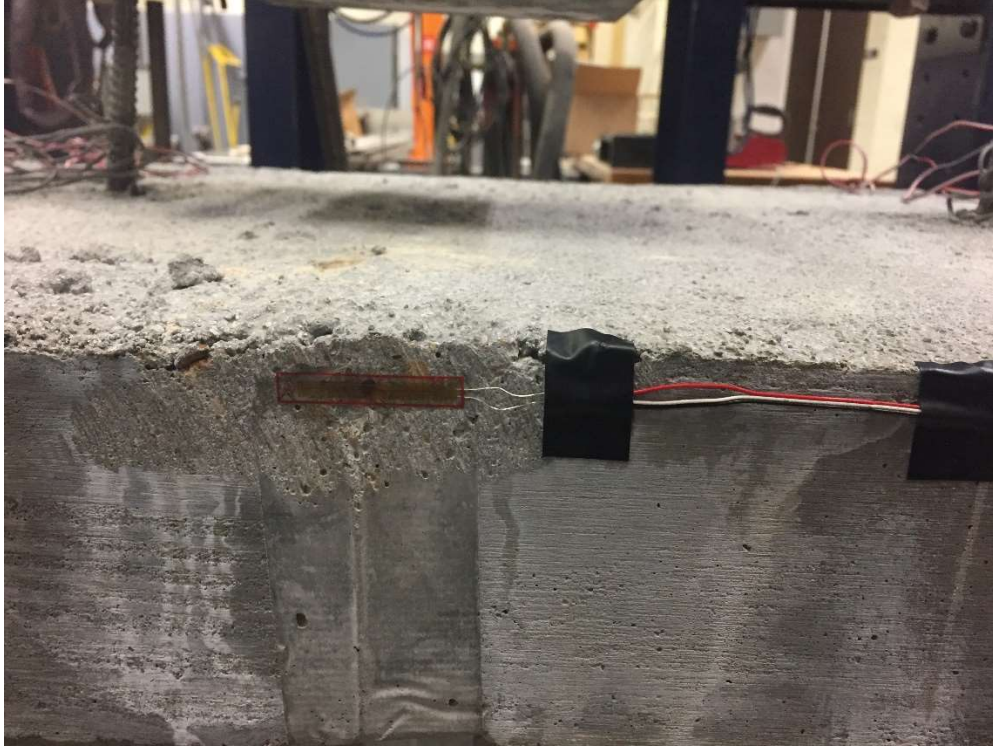


Figure 5-2: Concrete Strain Gauge Attached at the Top of the Flange at the Mid-span

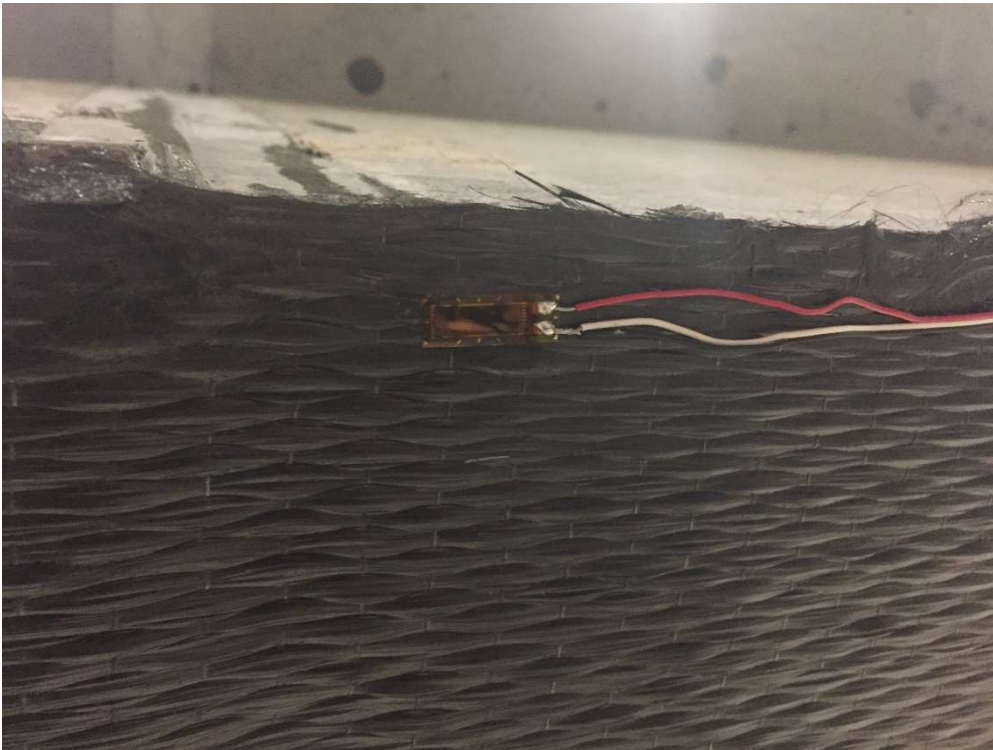


Figure 5-3: FRP Strain Gauge Attached to the Bottom of the Web at the Mid-span

Test Results

Control Beam (T1)

The first beam tested for this experiment was the control beam, named beam T1. This test has the load drop later on in the strain hardening range due to one of the supports getting out of the supporting plate. Even though the beam was not loaded all the way until failure the data recorded from this test was still valuable. From the experimental results the maximum load was 64.58 kips at a deflection of 4.13 in. at the mid-span, the maximum concrete strain was 0.0018, and the maximum steel strain was 0.028. Figure 5-4 below shows the control beam set up before beginning the test. Figures 5-5 and 5-6 show the control beam after testing. Figure 5-7 shows the load vs. deflection response of the beam and Figures 5-8 and 5-9 show the load vs. concrete strain and load vs. steel strain response respectively.

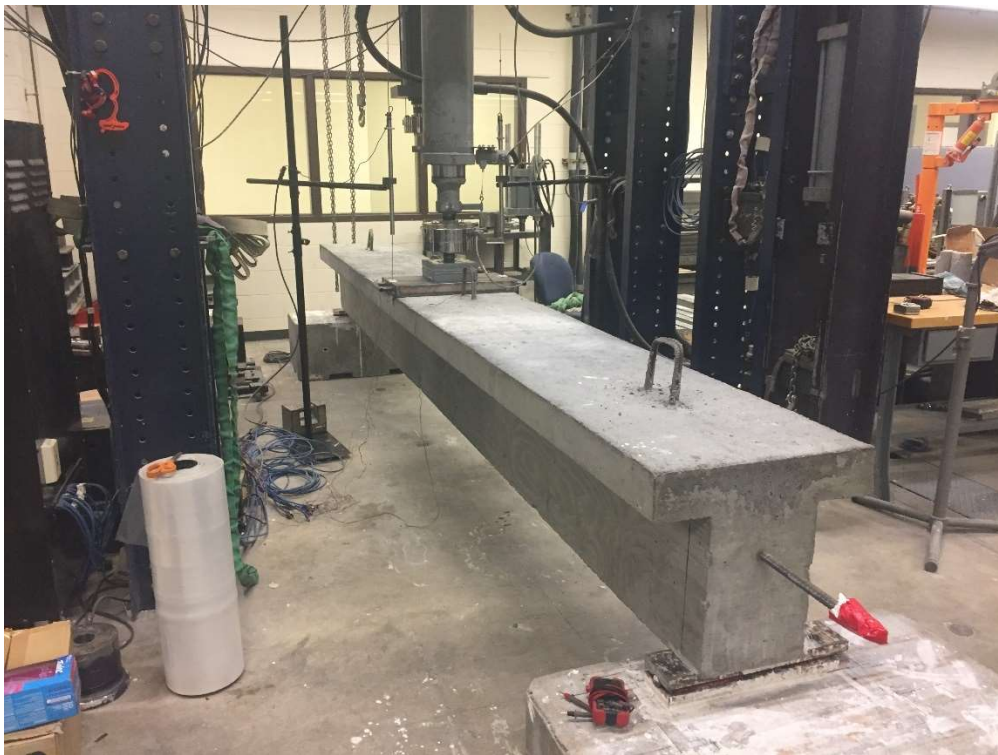


Figure 5-4: Beam T1 Setup before Testing



Figure 5-5: Beam T1 Shear Cracking at Mid-span after Testing

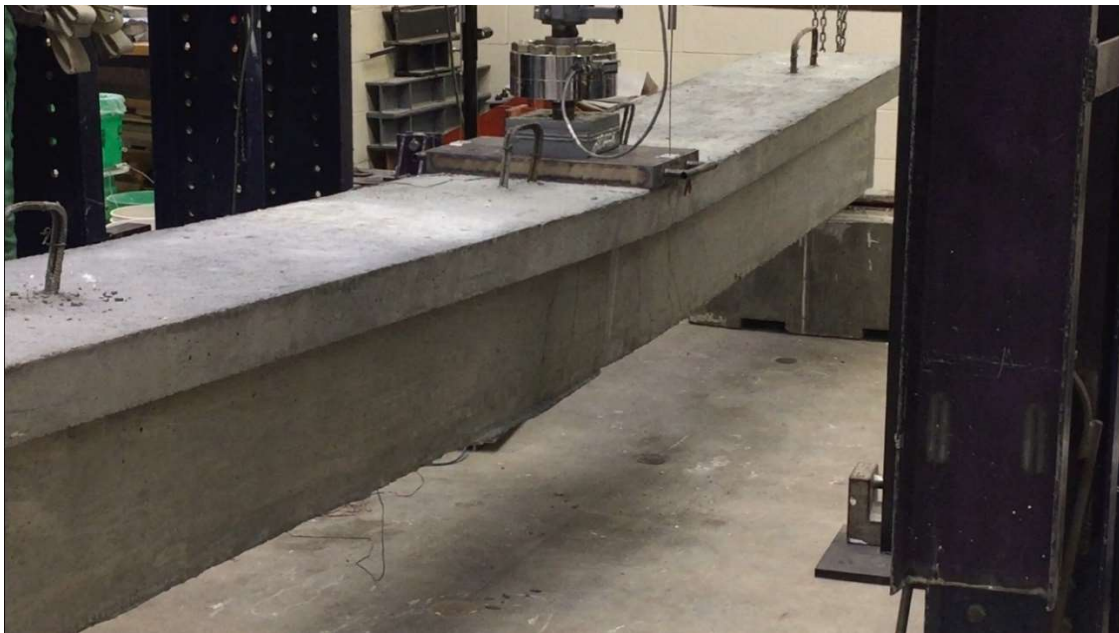


Figure 5-6: Beam T1 after Testing

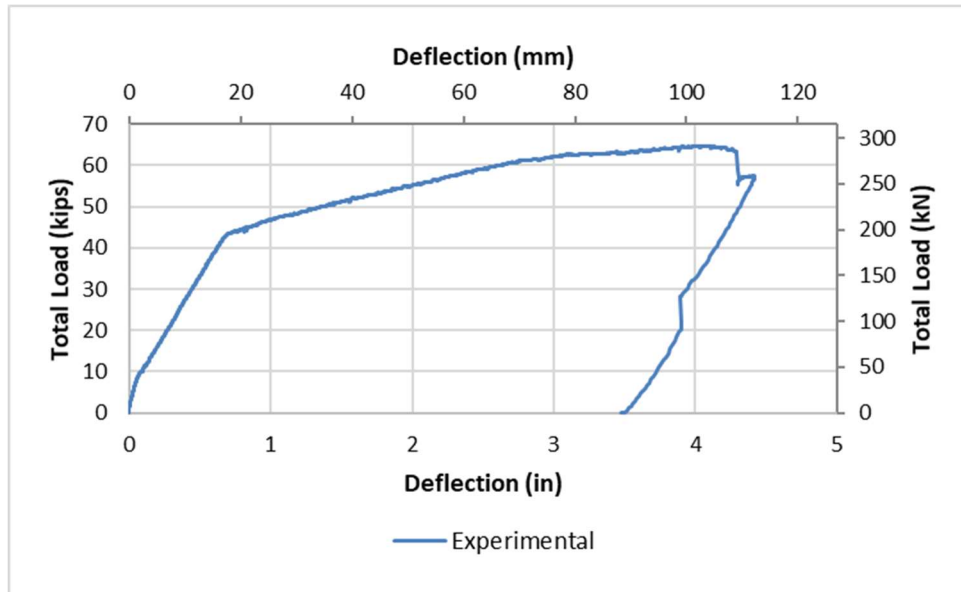


Figure 5-7: Beam T1 Load vs. Deflection Response

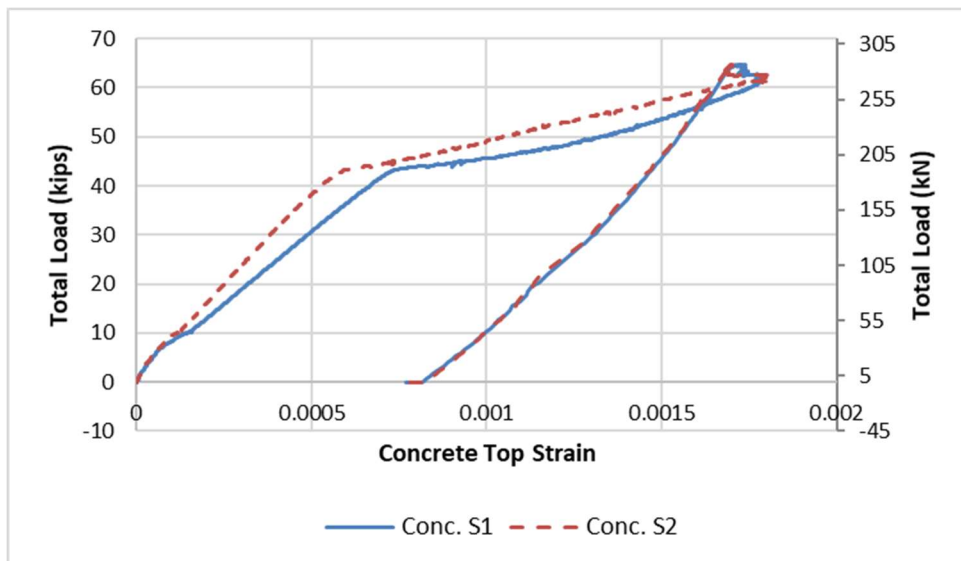


Figure 5-8: Beam T1 Load vs. Concrete Top Strain Response

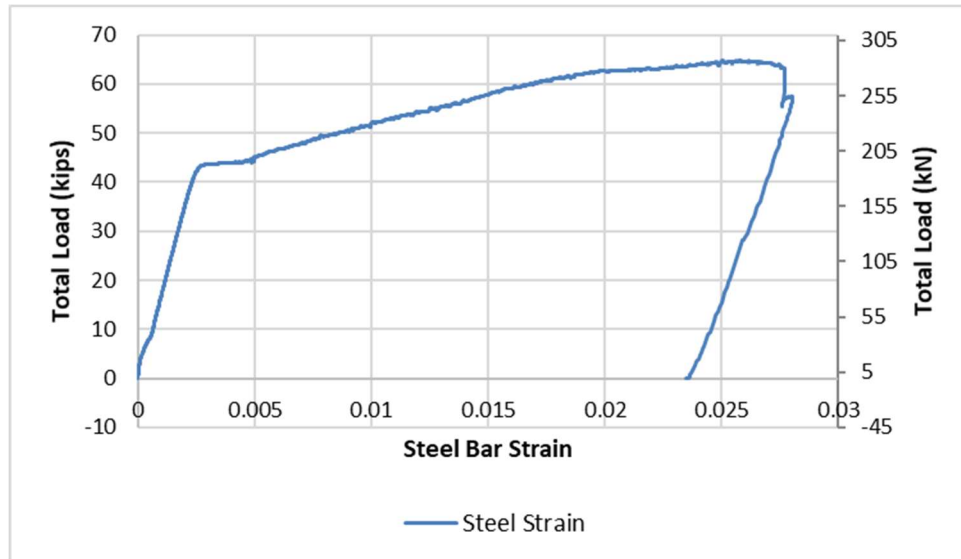


Figure 5-9: Beam T1 Load vs. Steel Bar Strain Response

T-Beam with Carbon FRP Flexural Reinforcement (T2)

The second beam tested was the beam strengthened with one layer of Carbon FRP on the bottom of the web, named T2 in this experiment. This beam reached a failure load due to a combination of FRP debonding and FRP rupture. The Carbon FRP sheet at failure had completely debonded from one half of the beam and at failure the FRP sheet ruptured at the mid-span. From the experimental data, the ultimate load at failure was 60.13 kips at a deflection of 1.442 in. at the mid-span. The maximum strain in the concrete was 0.00172 and the maximum strain in the steel was 0.0109. For the FRP strain gauges at the mid-span of the beam, one strain gauge reached a maximum strain of 0.0061. The second strain gauge followed a similar trend and had similar values until the failure was reached when the strain reached 0.0153 because this strain gauge was at a location where fiber ruptured.

Figure 5-10 below shows the strengthened beam without any anchorage set up before beginning the test. Figures 5-11 and 5-12 show the beam after testing. Figure 5-13 shows the load vs. deflection response of the beam and Figures 5-14 and 5-15 show the load vs. concrete

strain and load vs. steel strain response respectively. Finally Figure 5-16 shows the load vs. FRP strain response at the mid-span of the beam.



Figure 5-10: Beam T2 Setup before Testing



Figure 5-11: Beam T2 after Failure with Debonded FRP Sheet Laying on the Floor



Figure 5-12: Beam T2 FRP Debonding and Rupture at Failure

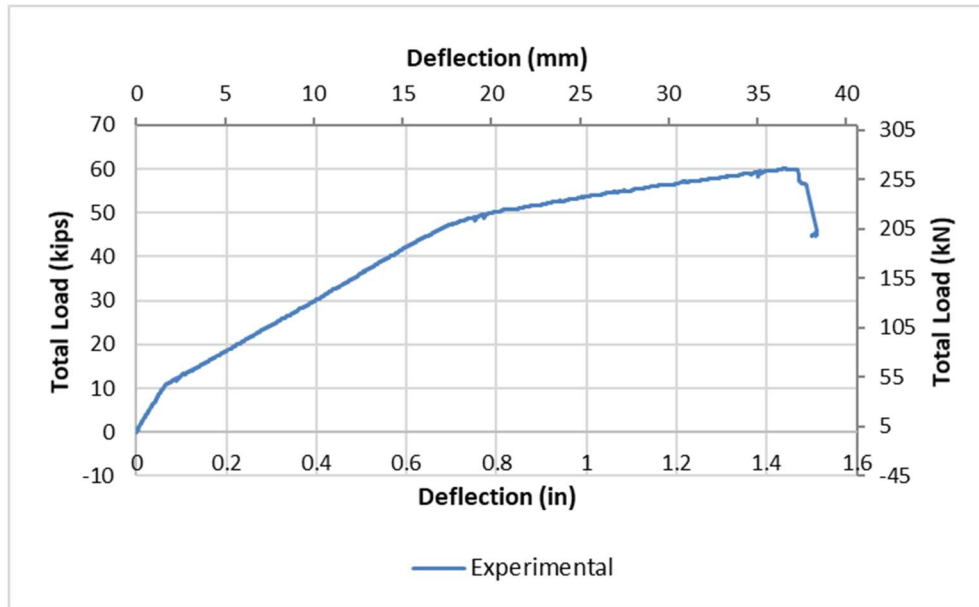


Figure 5-13: Beam T2 Load vs. Deflection Response

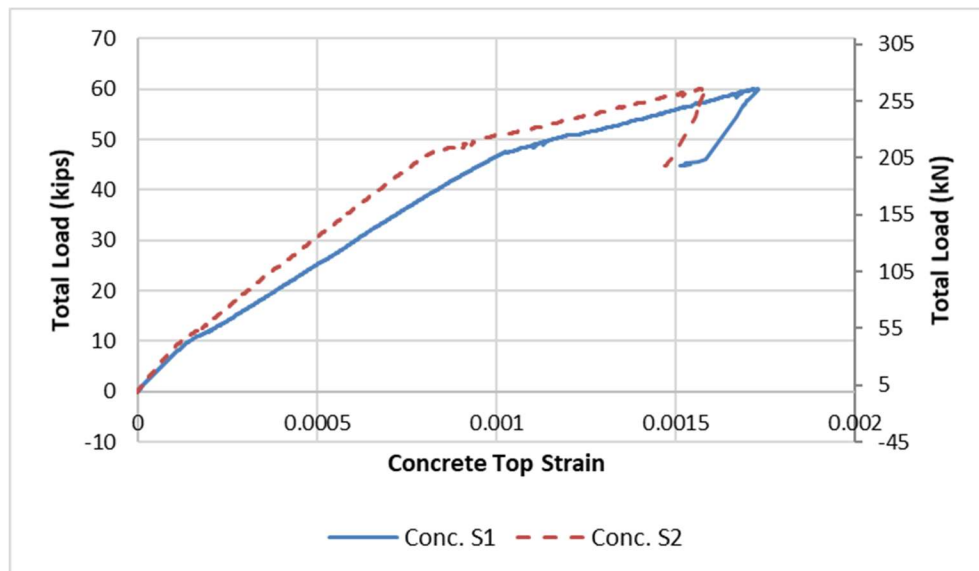


Figure 5-14: Beam T2 Load vs. Concrete Top Strain Response

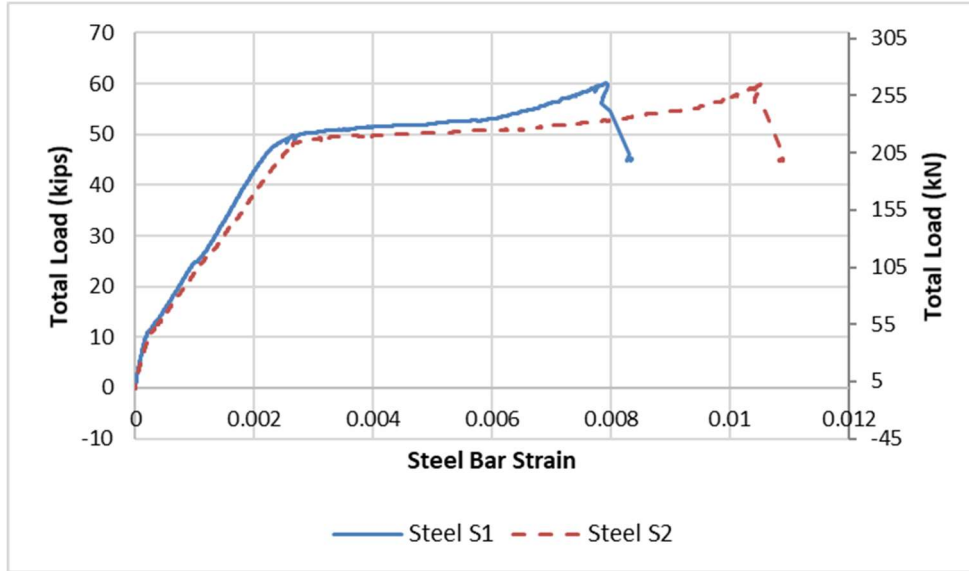


Figure 5-15: Beam T2 Load vs. Steel Bar Strain Response

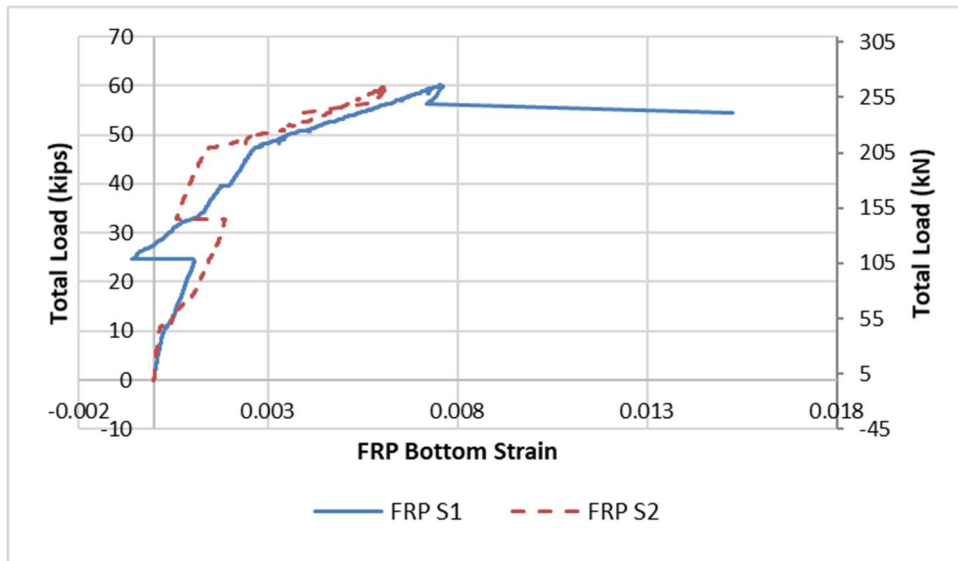


Figure 5-16: Beam T2 Load vs. FRP Strain at the Beam Mid-span

T-Beam with Carbon FRP Flexural Reinforcement and 5 Carbon FRP Splay

Anchors per Shear Span (T3)

The third beam tested was the beam strengthened with one layer of Carbon FRP on the bottom of the web and anchored with five Carbon FRP splay anchors per shear span, named T3

in this experiment. This beam reached a failure load due FRP rupture. From the experimental data, the load at failure was 58.88 kips at a deflection of 2.823 in. at the mid-span, the maximum strain in the concrete was 0.001204 and the maximum strain in the steel was 0.016933. For the FRP strain gauges at the mid-span of the beam, one strain gauge reached a maximum strain of 0.01355 while the second reached a maximum strain of 0.005044.

In addition to these two mid-span FRP strain gauges, additional FRP strain gauges were used at a measured distance from the supports, see Table 5-1. The strain gauges were labeled so that FRP S7 and FRP S8 are in similar locations along each shear span on either side of the mid-span. This pattern holds true for the pairs of FRP S9 and S10 as well as for FRP S11 and S12. The strain gauge labeled FRP S7 was 70.75 in. from the support and reached a maximum strain of 0.007273. Strain gauge FRP S8 was 77.75 in. from the support and reached a maximum strain of 0.008024. Strain gauge FRP S9 was 52.75 in. from the support and reached a maximum strain of 0.00356. FRP S10 was 55 in. from the support and reached a maximum strain of 0.00367. Strain gauge FRP S11 was 35.75 in. from the support and reached a maximum strain of 0.00156. FRP S12 was 37.375 in. from the support and reached a maximum strain of 0.001456. FRP S12 was closer to the load than FRP S11 but experienced lower strain. This could have been caused by the location of FRP S12 experiencing localized debonding or from the strain gauge not reading correct values.

Figure 5-17 below shows the beam set up before beginning the test. Figures 5-18 and 5-19 show the beam after testing. Figure 5-20 shows the load vs. deflection response of the beam and Figures 5-21 and 5-22 show the load vs. concrete strain and load vs. steel strain response respectively. Finally Figures 5-23 through 5-29 show the load vs. FRP strain response for the various strain gauges discussed above.



Figure 5-17: Beam T3 Setup before Testing



Figure 5-18: Beam T3 after Testing



Figure 5-19: Beam T3 FRP Rupture at Mid-span

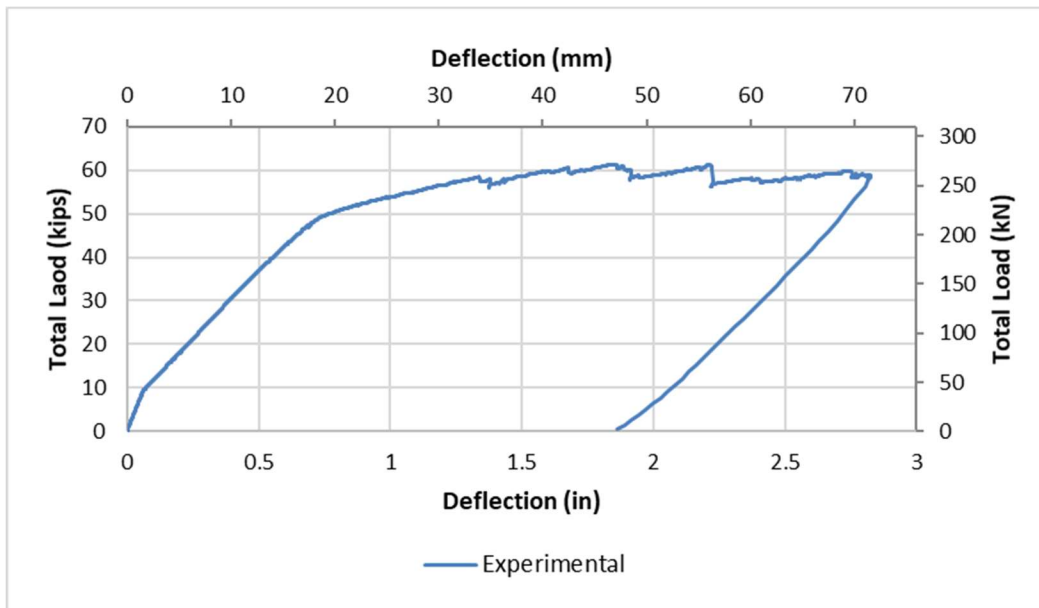


Figure 5-20: Beam T3 Load vs. Deflection Response

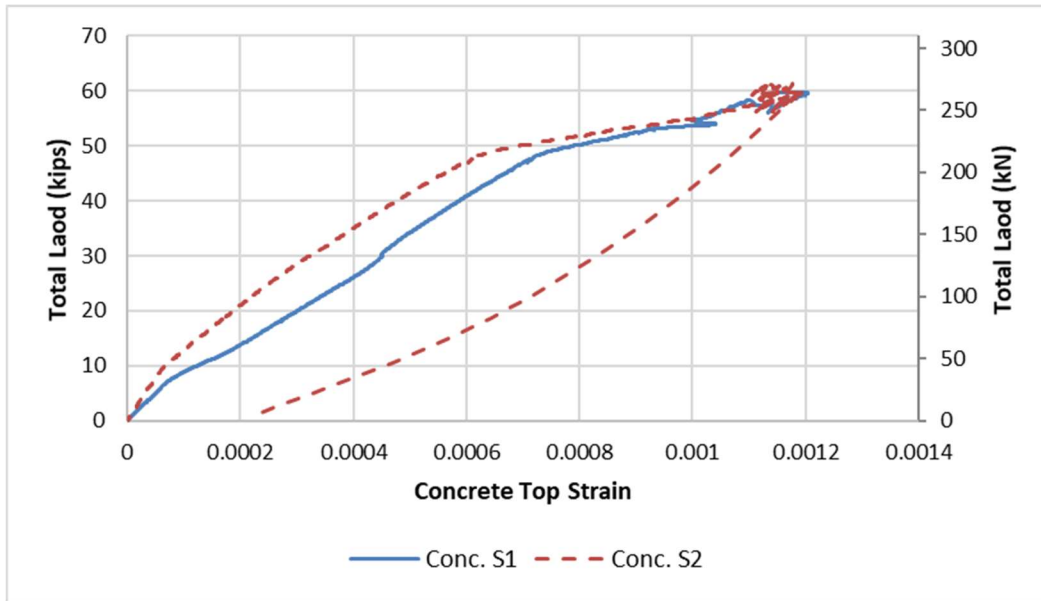


Figure 5-21: Beam T3 Load vs. Concrete Top Strain Response

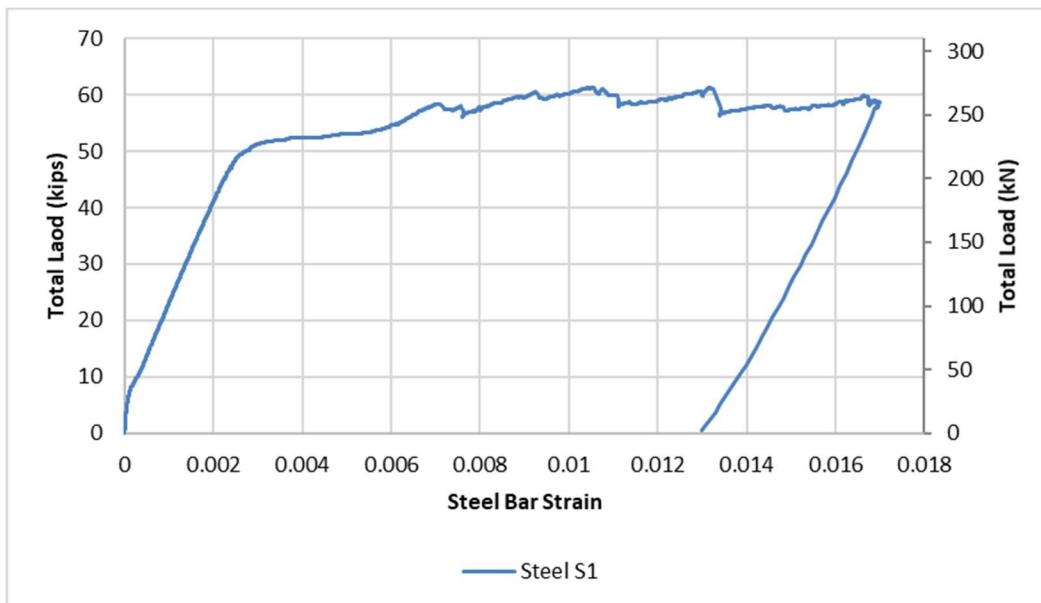


Figure 5-22: Beam T3 Load vs. Steel Bar Strain Response

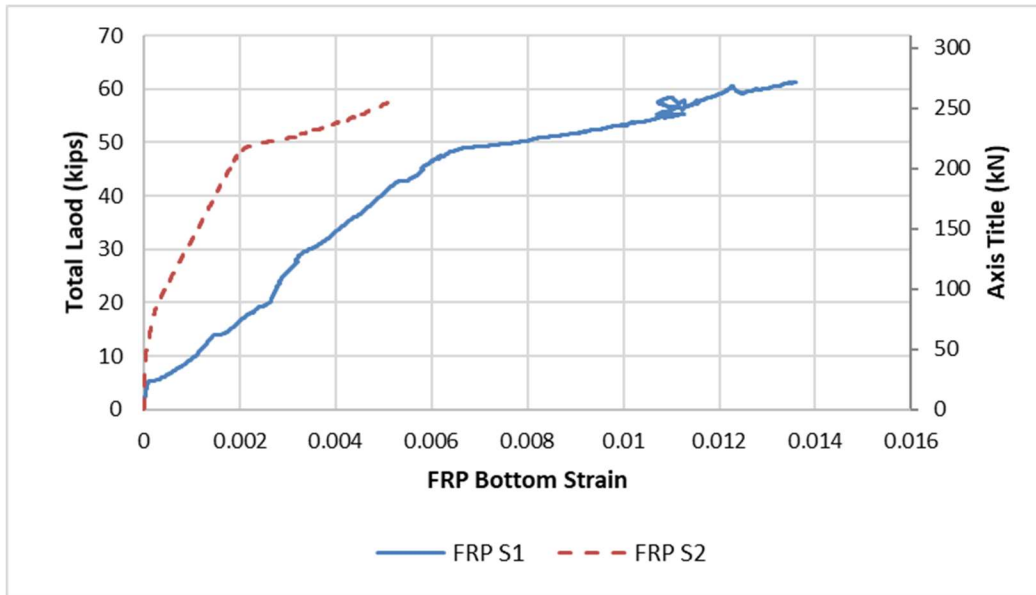


Figure 5-23: Beam T3 Load vs. FRP Strain at Mid-span Response

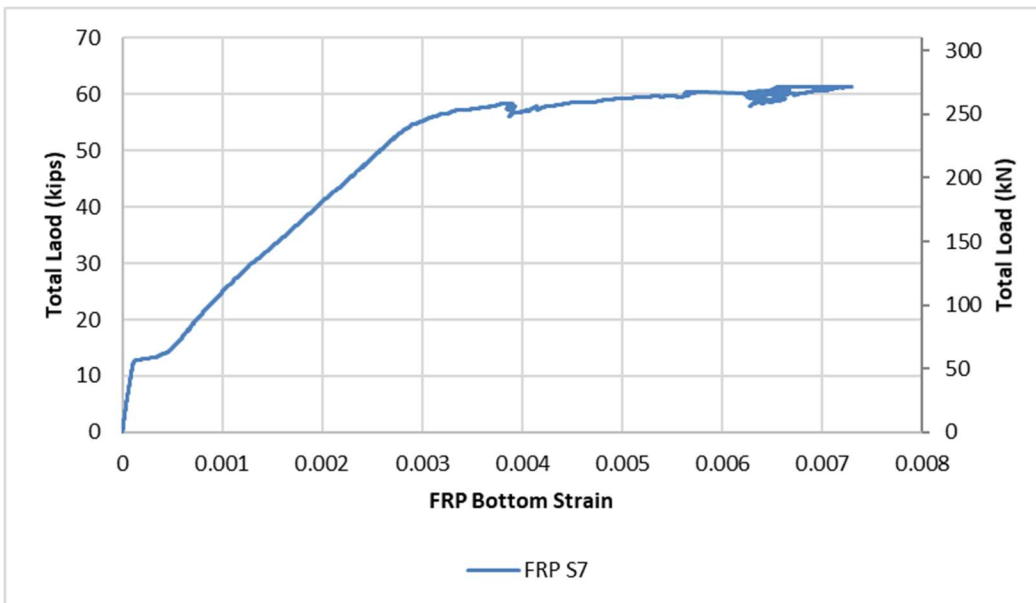


Figure 5-24: Beam T3 Load vs. FRP S7 Strain Response

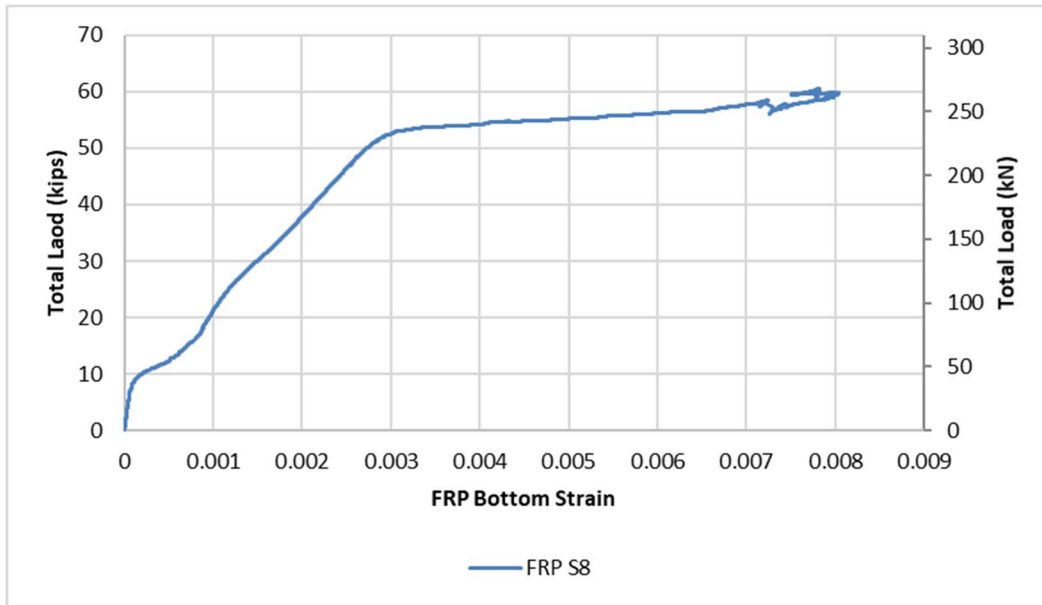


Figure 5-25: Beam T3 Load vs. FRP S8 Strain Response

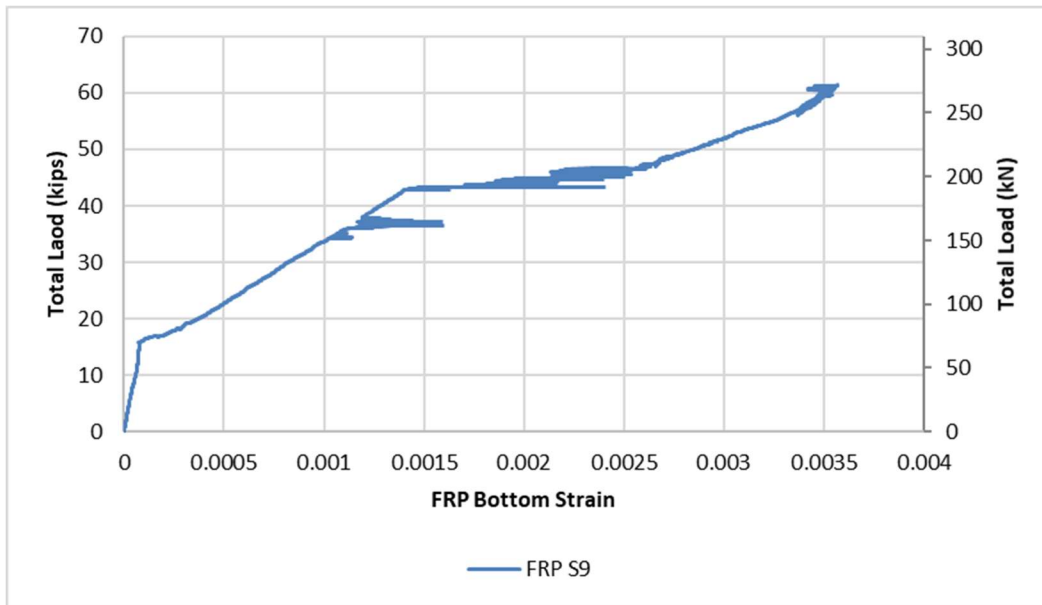


Figure 5-26: Beam T3 Load vs. FRP S9 Strain Response

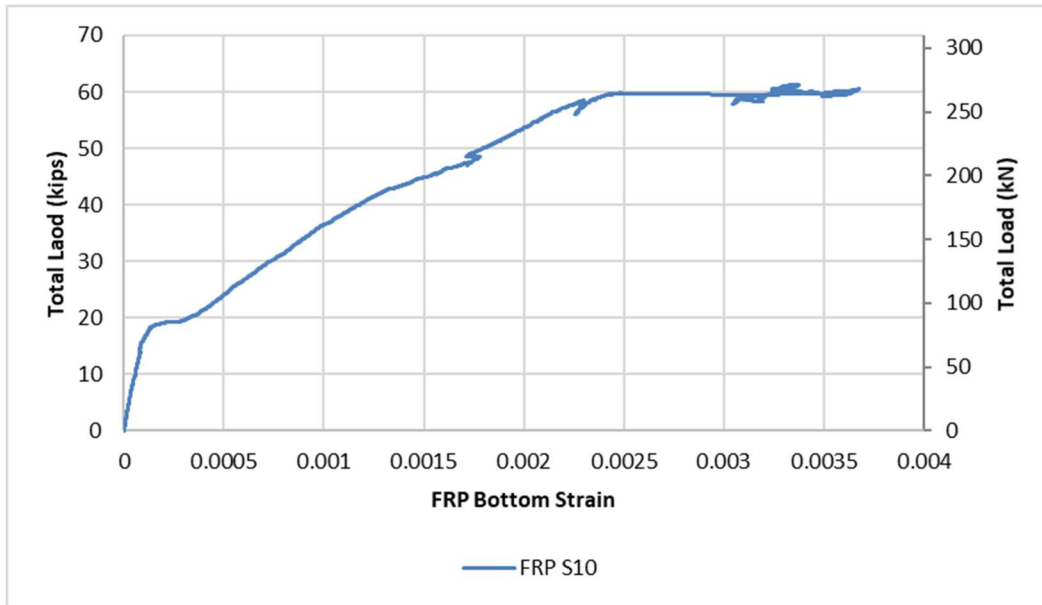


Figure 5-27: Beam T3 Load vs. FRP S10 Strain Response

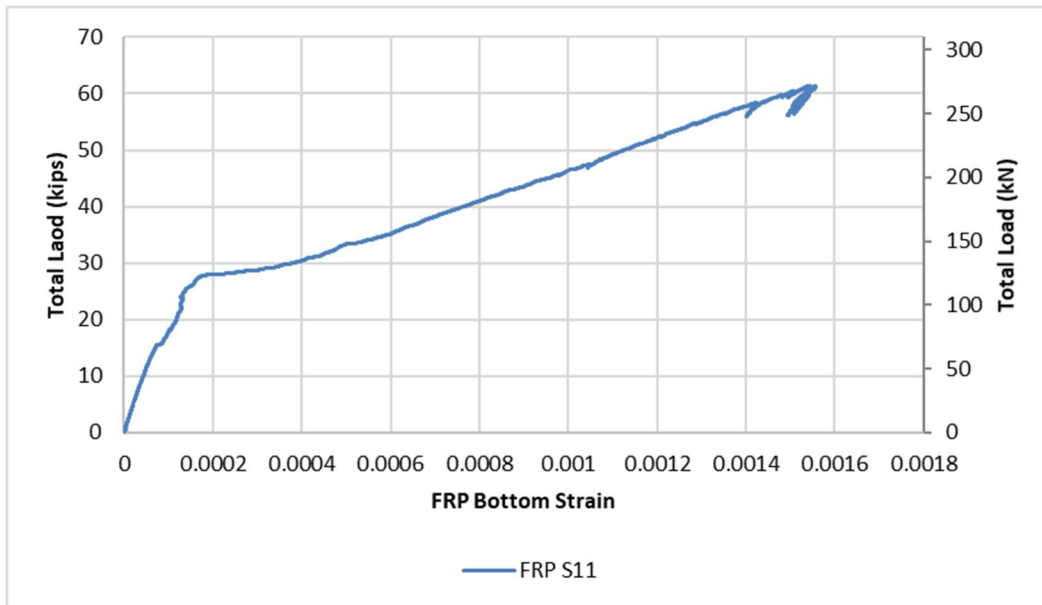


Figure 5-28: Beam T3 Load vs. FRP S11 Strain Response

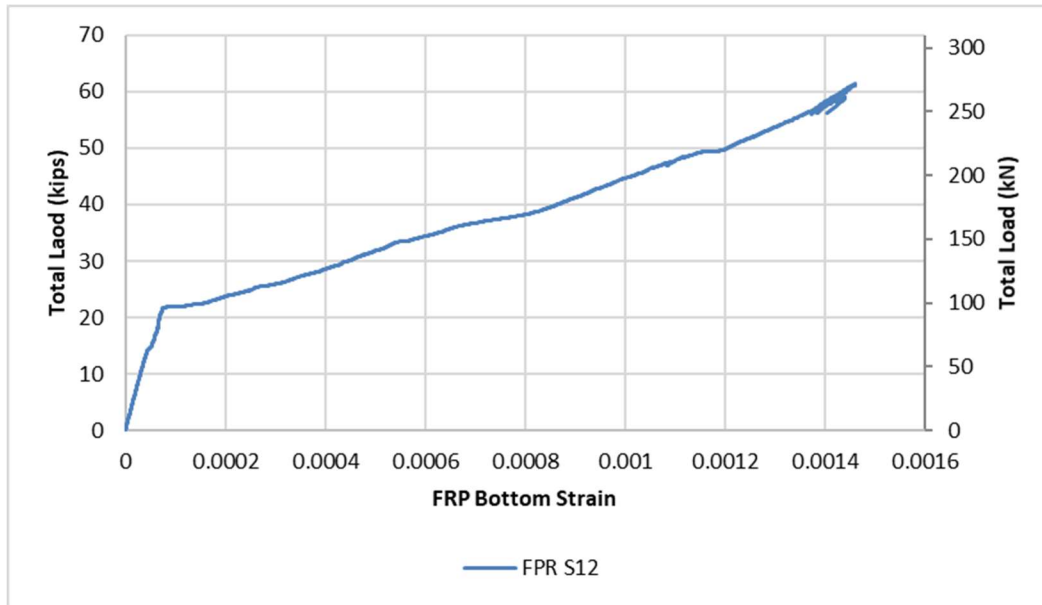


Figure 5-29: Beam T3 Load vs. FRP S12 Strain Response

T-Beam with Carbon FRP Flexural Reinforcement and Full-Length Glass FRP U-wrap (T4)

The fourth beam tested was the beam strengthened with one layer of Carbon FRP on the bottom of the web and anchored with a $\pm 45^\circ$ bi-directional Glass FRP U-wrap that was the entire length of the carbon sheet, named T4 in this experiment. This beam reached a failure load due FRP debonding of the GFRP U-wrap. From the experimental data, the load at failure was 80.02 kips at a deflection of 2.52 in. at the mid-span. The maximum strain in the concrete was 0.00396, and the maximum strain in the steel was 0.0132. For the FRP strain gauges at the mid-span of the beam, one strain gauge reached a maximum strain of 0.0175 while the second reached a maximum strain of 0.0121.

Figure 5-30 below shows the strengthened beam set up before beginning the test. Figures 5-31 and 5-32 show the beam after testing. Figure 5-33 shows the load vs. deflection response of the beam and Figures 5-34 and 5-35 show the load vs. concrete strain and load vs. steel strain

response respectively. Finally Figure 5-36 shows the load vs. FRP strain response at the mid-span of the beam.



Figure 5-30: Beam T4 Setup before Testing



Figure 5-31: Beam T4 after Testing



Figure 5-32: Beam T4 Glass FRP U-wrap Debonding

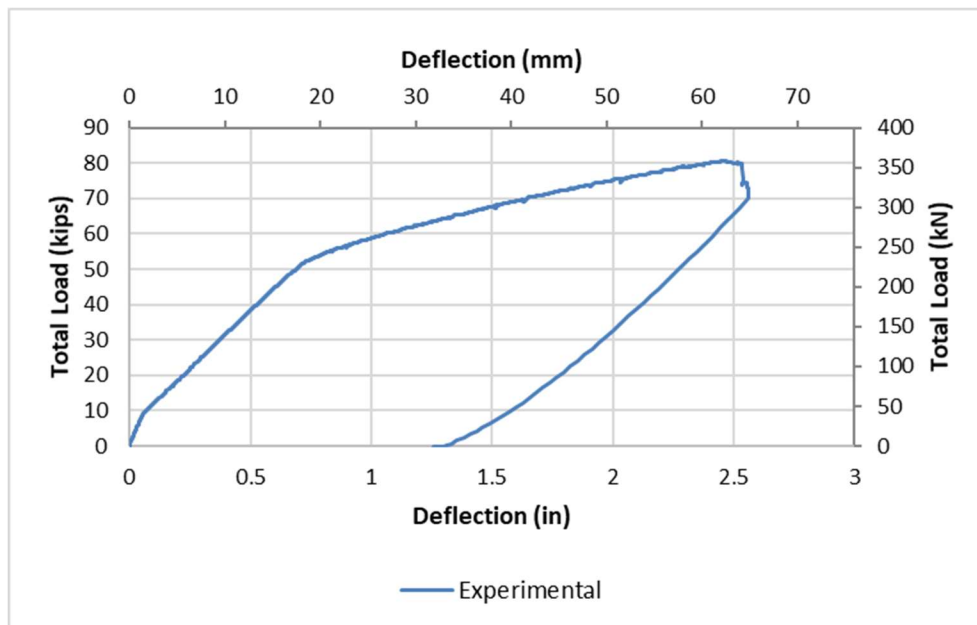


Figure 5-33: Beam T3 Load vs. Deflection Response

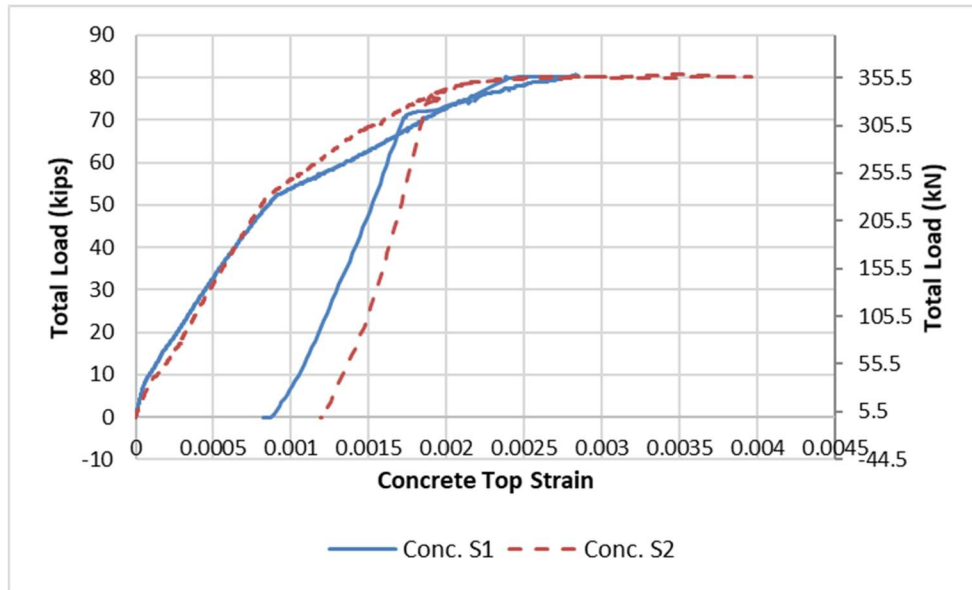


Figure 5-34: Beam T4 Load vs. Concrete Top Strain Response

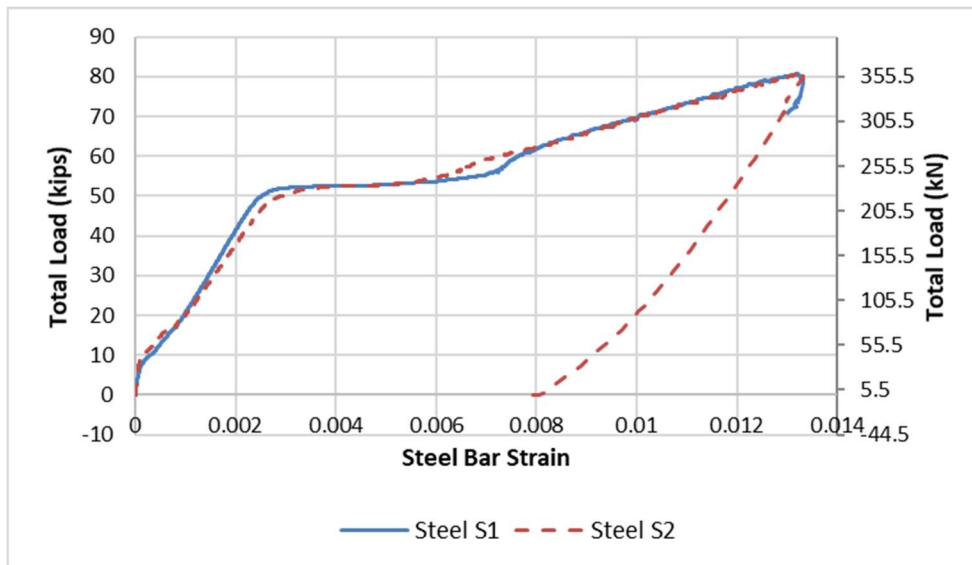


Figure 5-35: Beam T4 Load vs. Steel Bar Strain Response

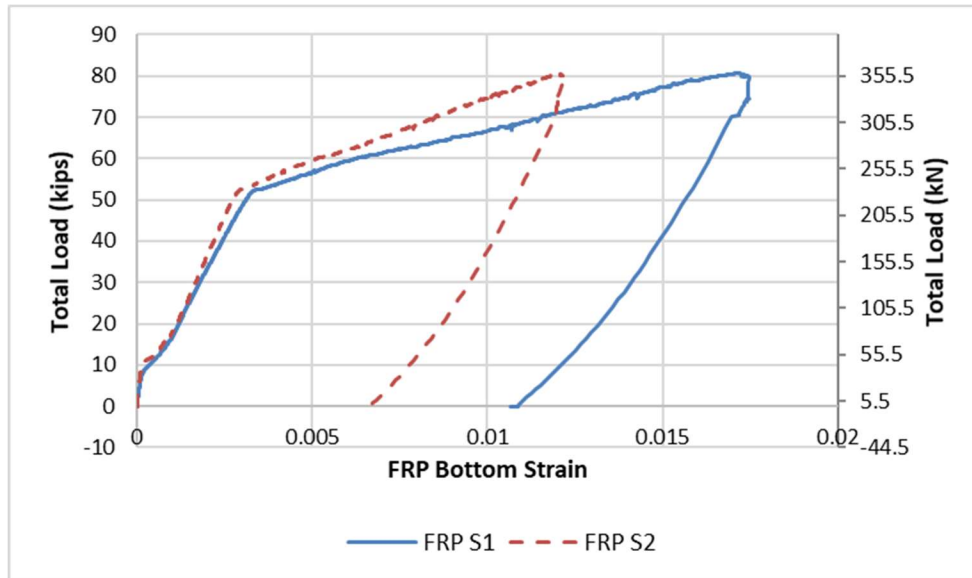


Figure 5-36: Beam T4 Load vs. FRP Strain at Mid-span Response

T-Beam with Carbon FRP Flexural Reinforcement with One Layer of One Foot

Wide Glass FRP U-wraps (T5)

The fifth beam tested was the beam strengthened with one layer of carbon FRP on the bottom of the web and anchored with one layer of one-foot wide $\pm 45^\circ$ bi-directional Glass FRP U-wraps with one foot of space between U-wraps. This beam was called T5 for this experiment. This beam reached a failure load due to FRP debonding of the U-wraps. From the experimental data, the load at failure was 79.76 kips at a deflection of 3.428 in. at the mid-span. The maximum strain in the concrete was 0.002565 and the maximum strain in the steel at failure load was 0.01266. For the FRP strain gauges at the mid-span of the beam, one strain gauge reached a maximum strain of 0.01258 while the second reached a maximum strain of 0.008967.

In addition to these two mid-span FRP strain gauges, additional FRP strain gauges were used at a measured distance from the supports, see Table 5-1. The strain gauges were labeled so that FRP S7 and FRP S8 are in similar locations along each shear span on either side of the mid-span. This pattern holds true for the pair of FRP S9 and S10. The strain gauge labeled FRP S7

was 83 in. from the support and reached a maximum strain of 0.01326. Strain gauge FRP S8 was 79.75 in. from the support and reached a maximum strain of 0.01288. Strain gauge FRP S9 was 58.5 in. from the support and reached a maximum strain of 0.008136. FRP S10 was 57.75 in. from the support and reached a maximum strain of 0.008171.

Figure 5-37 below shows the strengthened beam set up before beginning the test. Figures 5-38 and 5-39 show the beam after testing. Figure 5-40 shows the load vs. deflection response of the beam and Figures 5-41 and 5-42 show the load vs. concrete strain and load vs. steel strain response respectively. Finally Figures 5-43 through 5-47 show the load vs. FRP strain response for the various strain gauges discussed above.



Figure 5-37: Beam T5 Setup before Testing



Figure 5-38: Beam T5 after Testing



Figure 5-39: Beam T5 Debonding of U-wrap with Exposed Rebar

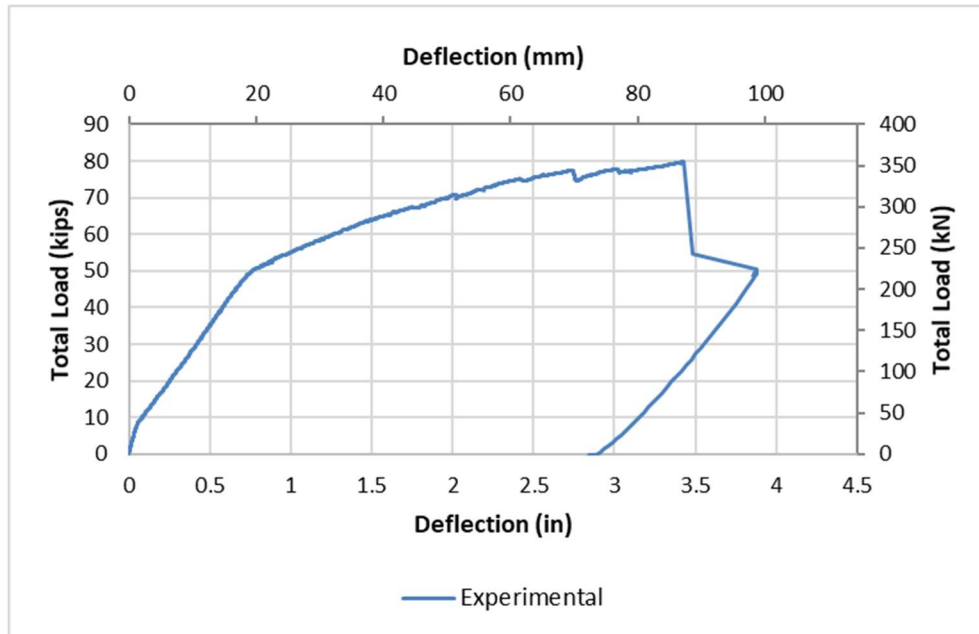


Figure 5-40: Beam T5 Load vs. Deflection Response

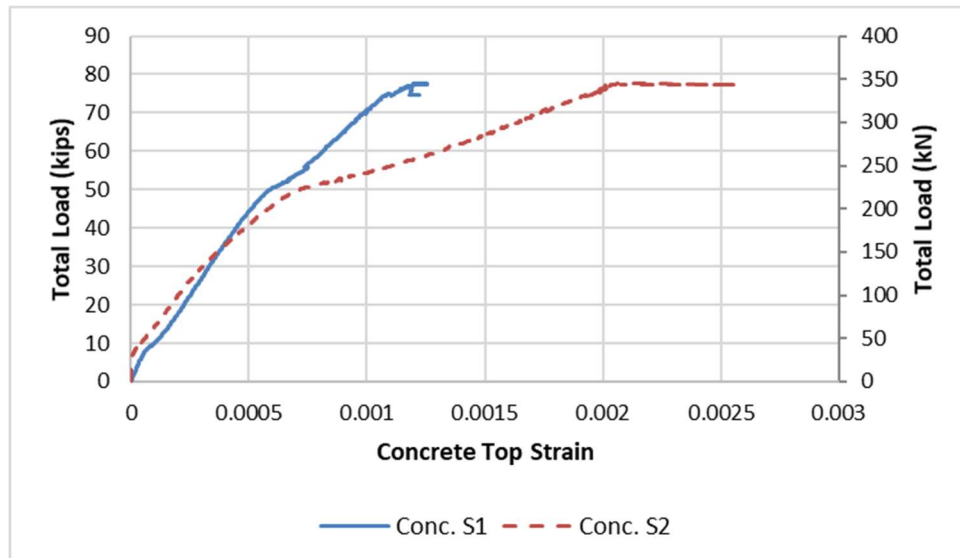


Figure 5-41: Beam T5 Load vs. Concrete Top Strain Response

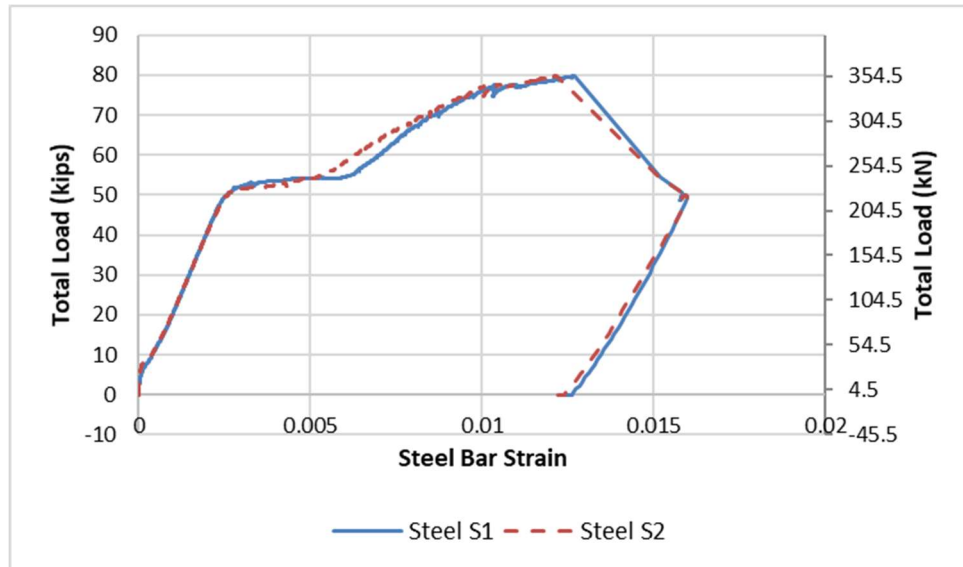


Figure 5-42: Beam T5 Load vs. Steel Bar Strain Response

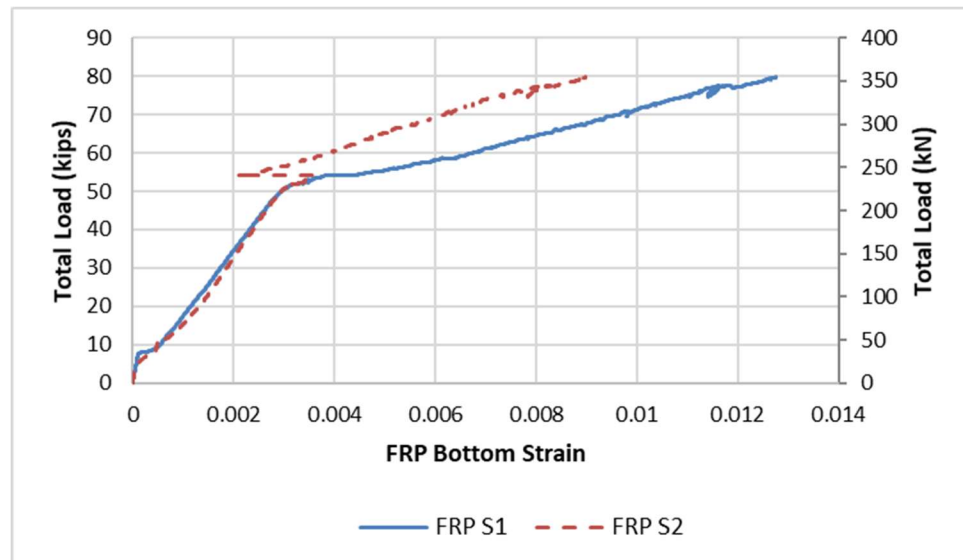


Figure 5-43: Beam T5 Load vs. FRP Strain Response at Mid-span

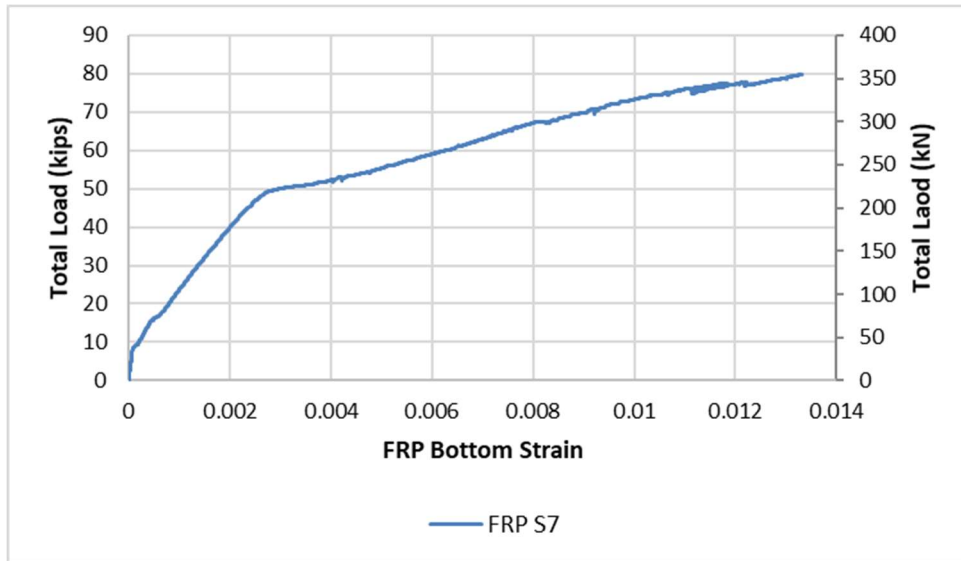


Figure 5-44: Beam T5 Load vs. FRP S7 Strain Response

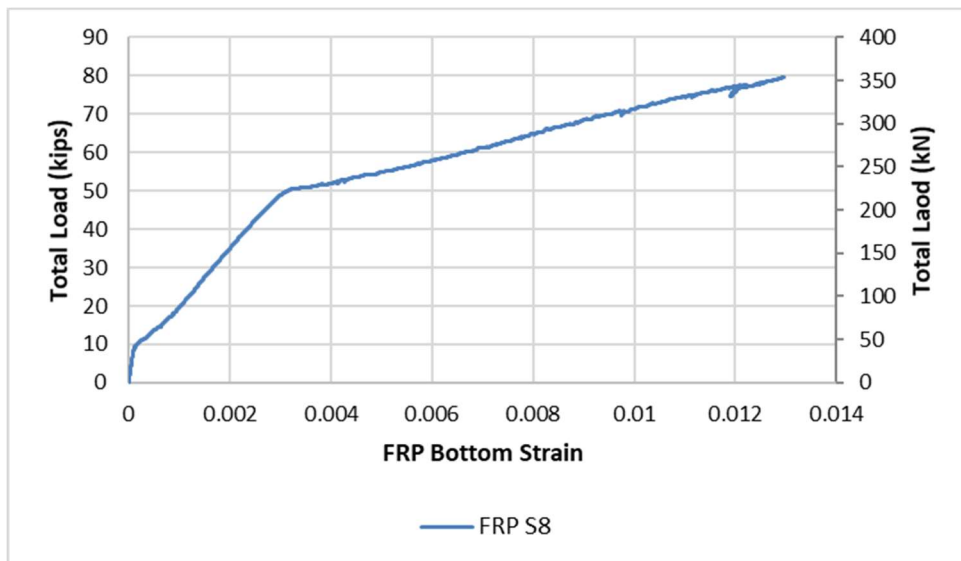


Figure 5-45: Beam T5 Load vs. FRP S8 Strain Response

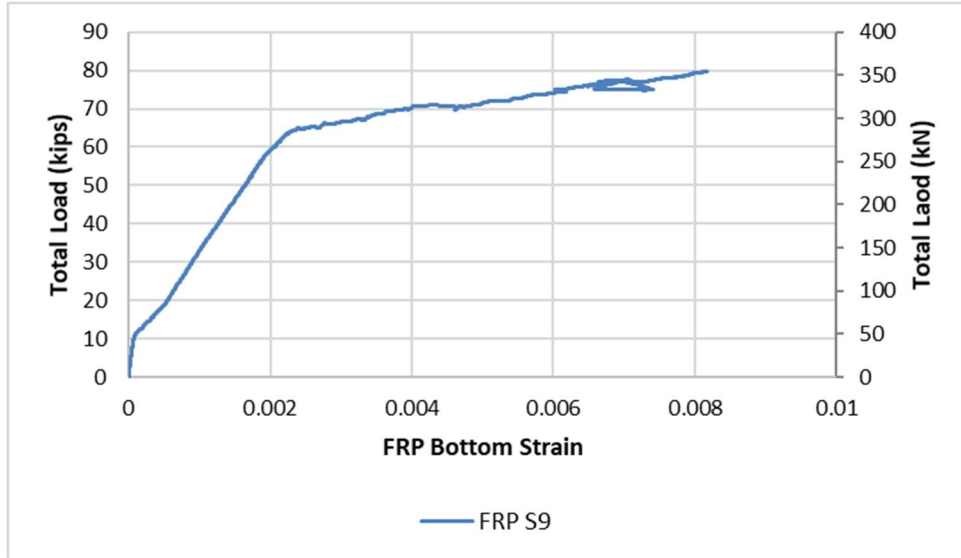


Figure 5-46: Beam T5 Load vs. FRP S9 Strain Response

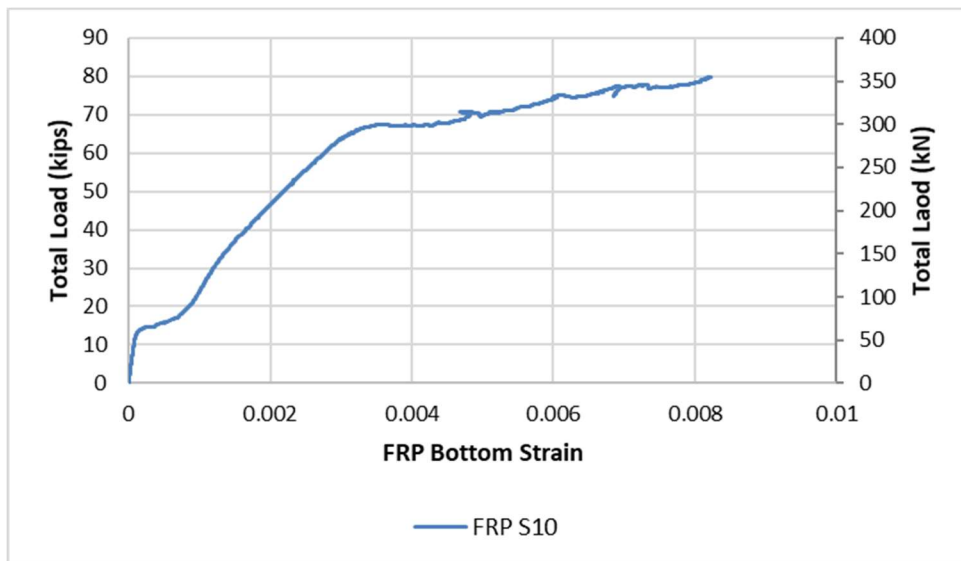


Figure 5-47: Beam T5 Load vs. FRP S10 Strain Response

T-Beam with Carbon FRP Flexural Reinforcement with Two Layers of One Foot

Wide Glass FRP U-wraps (T6)

The final beam tested was the beam strengthened with one layer of carbon FRP on the bottom of the web and anchored with two layers of one-foot wide $\pm 45^\circ$ bi-directional Glass FRP

U-wraps with one foot of space between U-wraps. This beam was called T6 for this experiment. This beam reached a failure load due to FRP debonding of the GFRP U-wraps. From the experimental data, the load at failure was 72.17 kips at a deflection of 3.025 in. at the mid-span. the maximum strain in the concrete was 0.002536 and the maximum strain in the steel at failure load was 0.014457. For the FRP strain gauges at the mid-span of the beam, one strain gauge reached a maximum strain of 0.01261 while the second one reached a maximum strain of 0.016415.

In addition to these two mid-span FRP strain gauges, additional FRP strain gauges were used at a measured distance from the supports, see Table 5-1. The strain gauges were labeled so that FRP S7 and FRP S8 are in similar locations along each shear span on either side of the mid-span. This pattern holds true for the pair of FRP S9 and S10. The strain gauge labeled FRP S7 was 80.25 in. from the support and reached a maximum strain of 0.01056. Strain gauge FRP S8 was 81.25 in. from the support and reached a maximum strain of 0.009757. Strain gauge FRP S9 was 55.75 in. from the support and reached a maximum strain of 0.007182. FRP S10 was 55.75 in. from the support and reached a maximum strain of 0.007297.

Figure 5-48 below shows the strengthened beam set up before beginning the test. Figures 5-49 and 5-50 show the beam after testing. Figure 5-51 shows the load vs. deflection response of the beam and Figures 5-52 and 5-53 show the load vs. concrete strain and load vs. steel strain response respectively. Finally Figures 5-54 through 5-58 show the load vs. FRP strain response for the various strain gauges discussed above.



Figure 5-48: Beam T6 Setup before Test



Figure 5-49: Beam T6 after Test



Figure 5-50: Beam T6 Debonding of Glass FRP U-wrap with Exposed Rebar

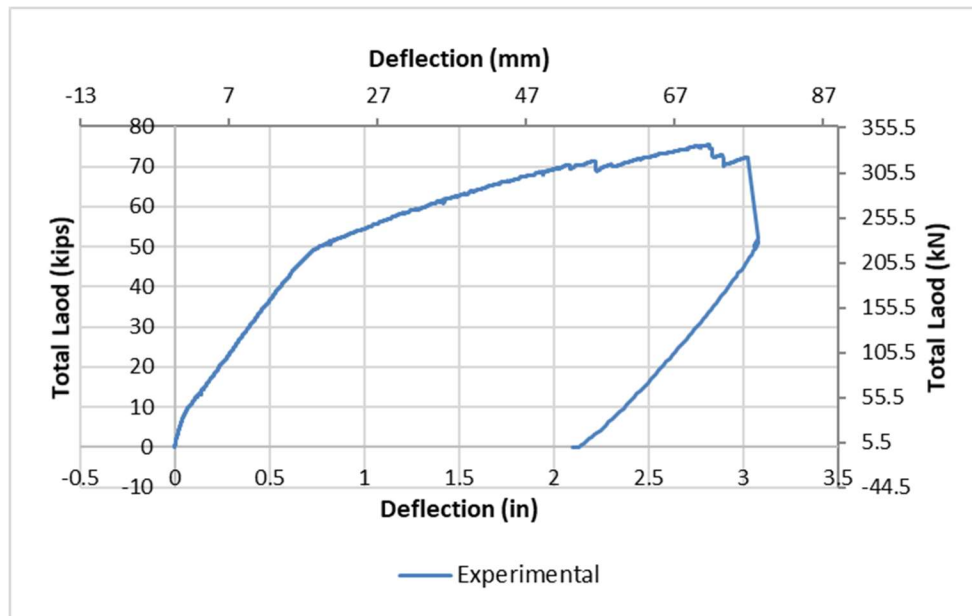


Figure 5-51: Beam T6 Load vs. Deflection Response

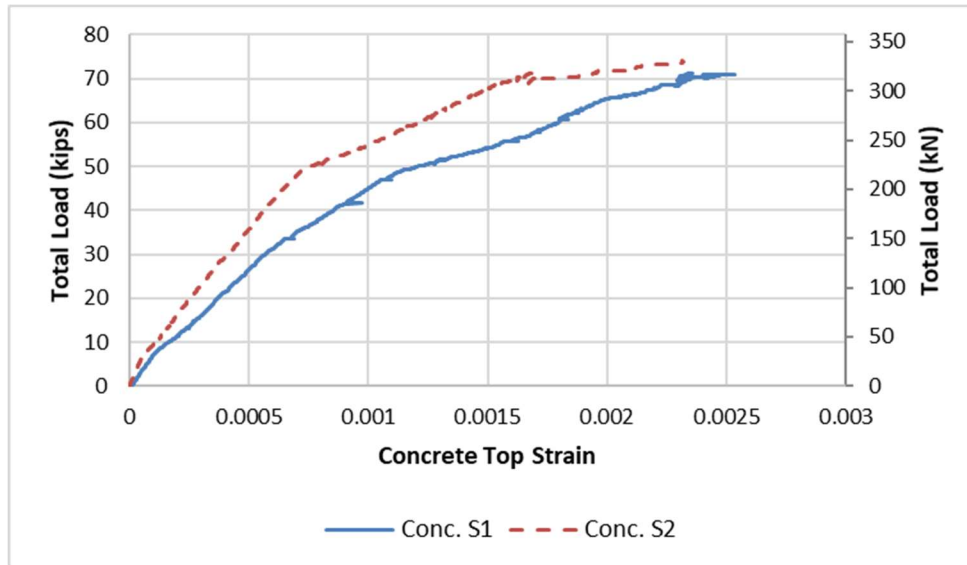


Figure 5-52: Beam T6 Load vs. Concrete Top Strain Response

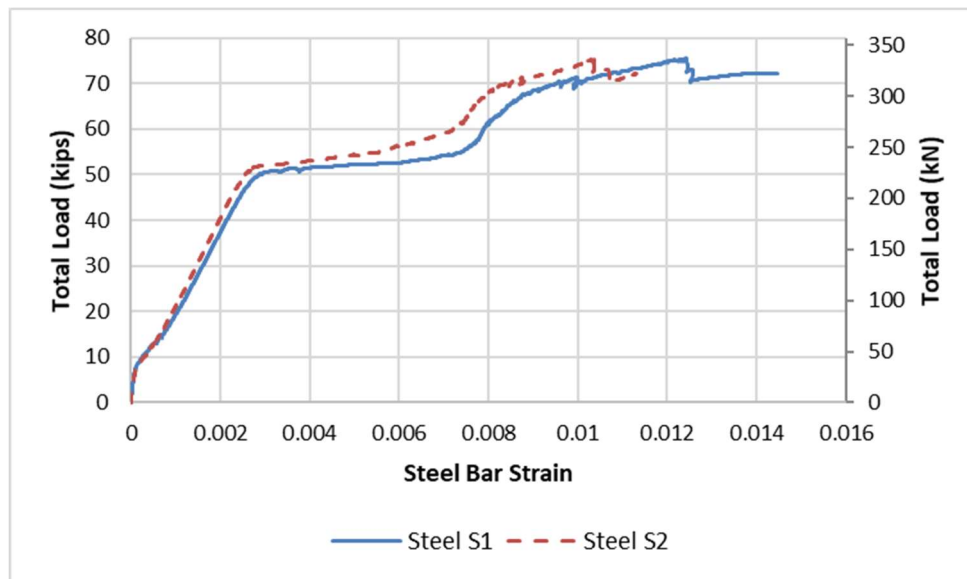


Figure 5-53: Beam T6 Load vs. Steel Bar Strain Response

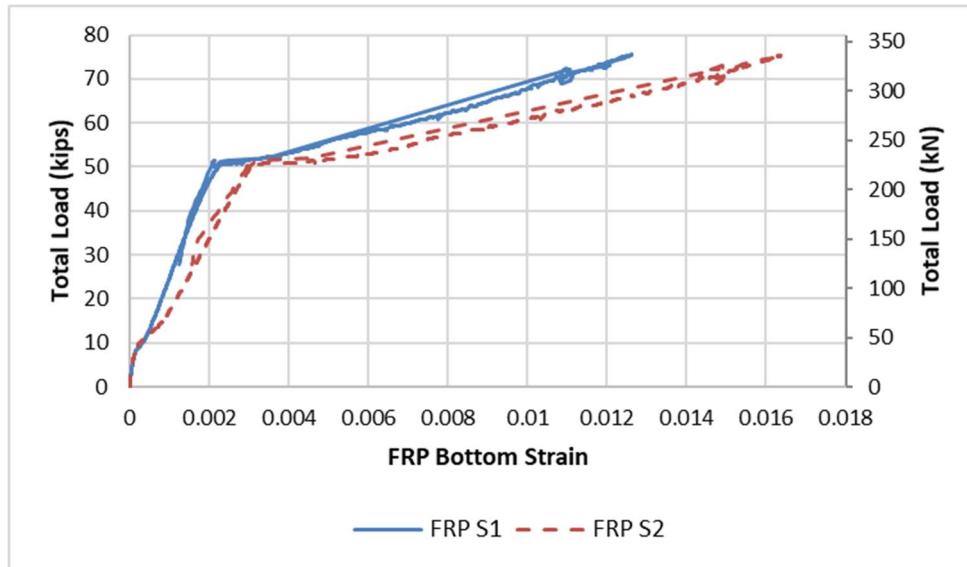


Figure 5-54: Beam T6 Load vs. FRP Strain Response at Mid-span

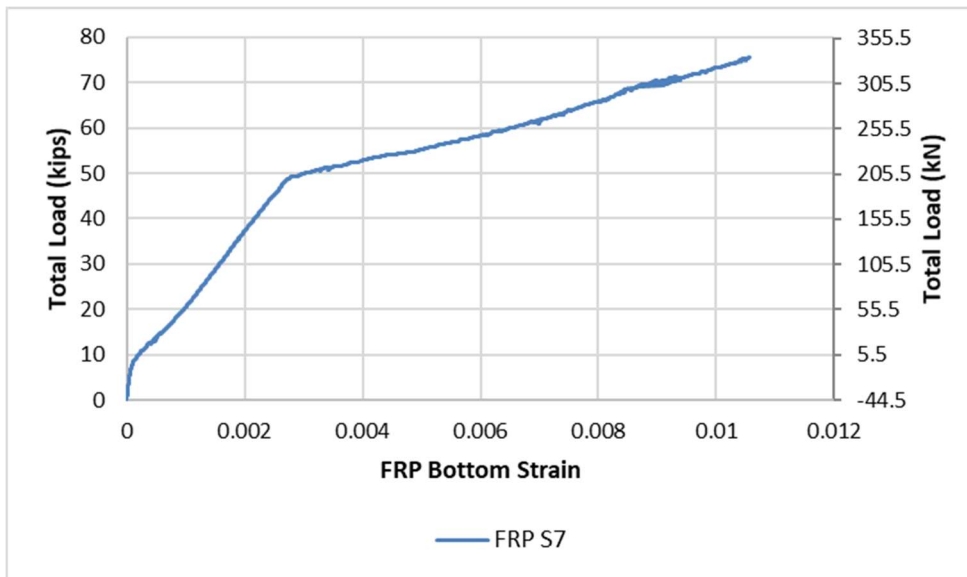


Figure 5-55: Beam T6 Load vs. FRP S7 Strain Response

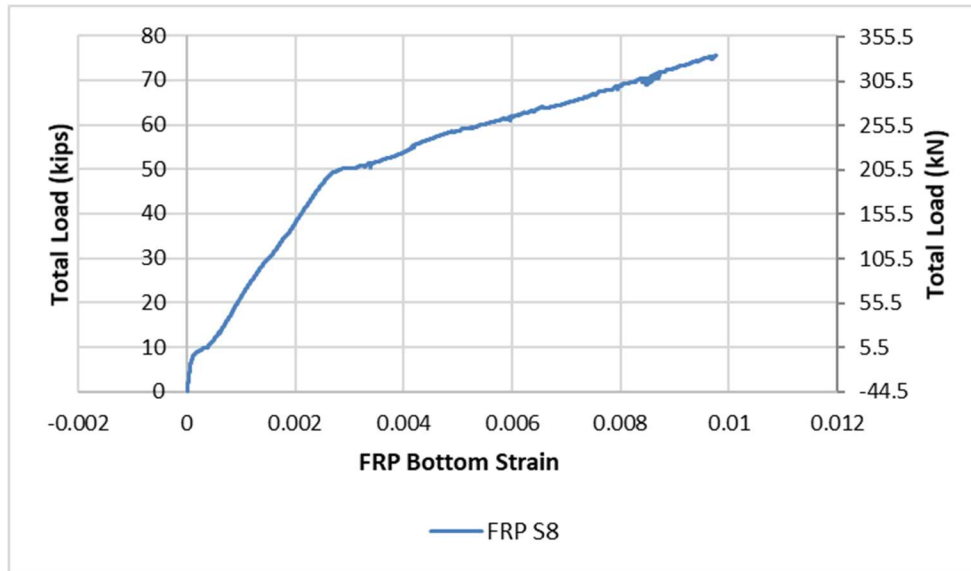


Figure 5-56: Beam T6 Load vs. FRP S8 Strain Response

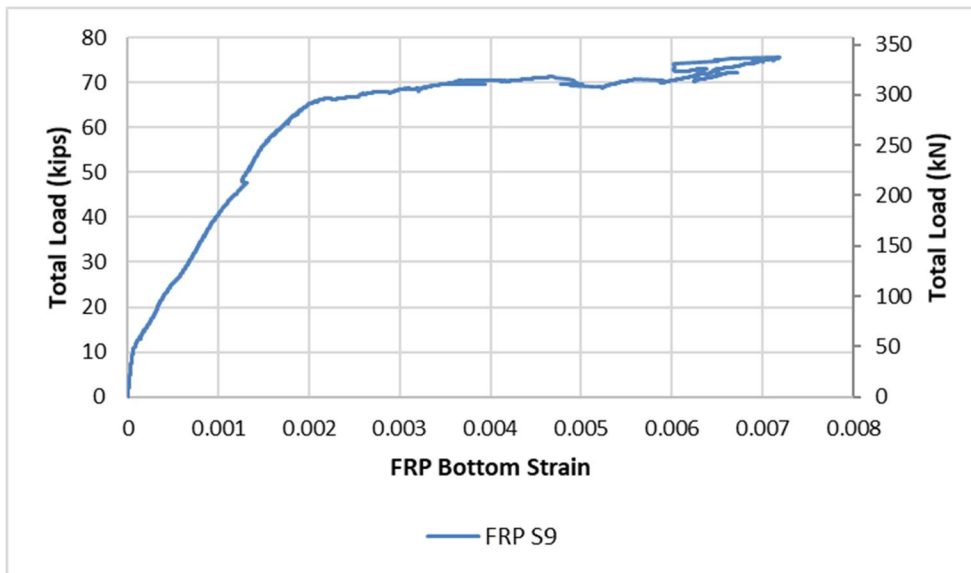


Figure 5-57: Beam T6 Load vs. FRP S9 Response

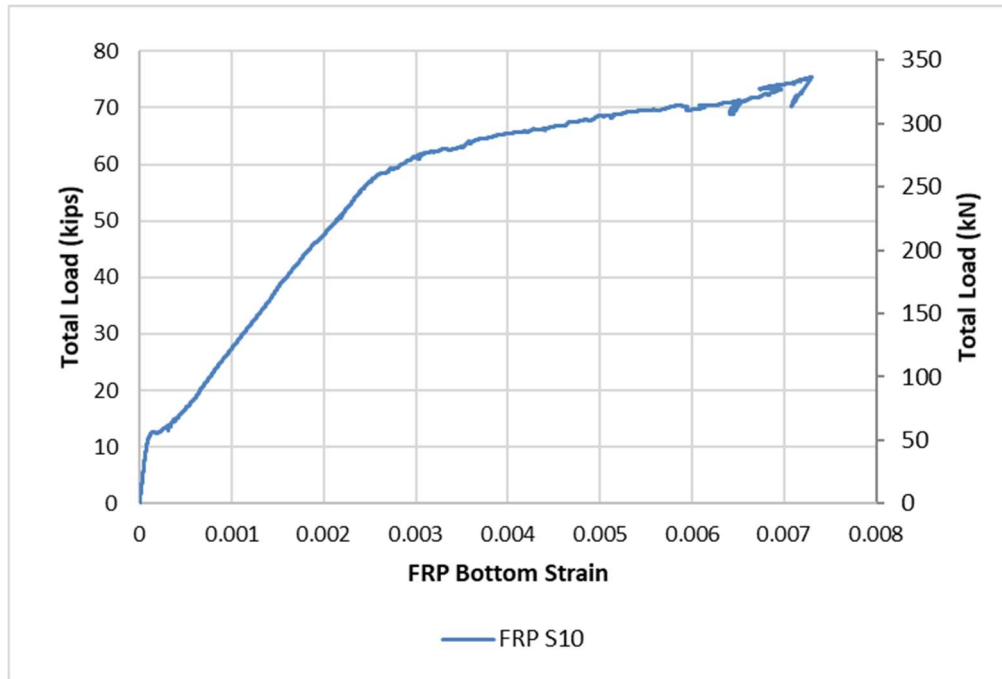


Figure 5-58: Beam T6 Load vs. FRP S10 Response

Comparison of Beam Results

Figure 5-59 below shows the comparison of the load vs. deflection behavior for the control beam, unanchored strengthened beam, and the three beams with $\pm 45^\circ$ bi-directional Glass FRP U-wraps.

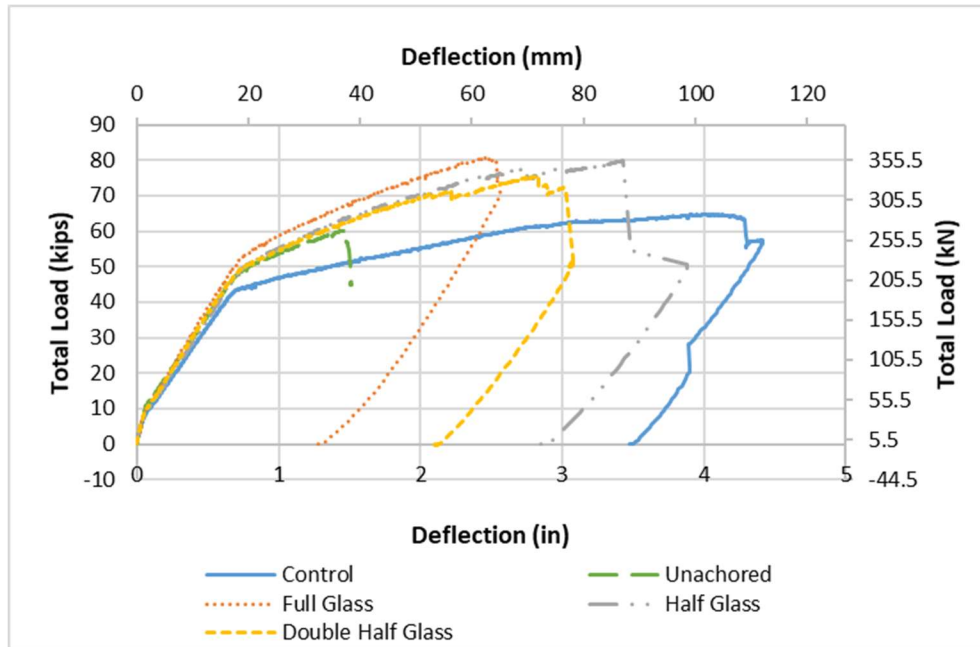


Figure 5-59: Comparison of Beams Load vs. Deflection Response

Even though not all of the strengthened beams reached an ultimate load that was higher than the control beam, all of them in this comparison reached the yielding point at a higher load. The beam strengthened with a full length U-wrap had the highest load at the yield point. The beams with one foot wide U-wraps and the unanchored beam all had similar loads at the yield point but the beams with U-wraps reached higher ultimate loads.

Chapter 6 - Analysis of Results

Analysis Program

The analysis program used to analyze the specimens was a Microsoft Excel based software. It was developed by Calvin Reed, a former graduate student at Kansas State University by assuming elastic-perfectly plastic steel behavior. The program allows for the user to input different information and run a flexural analysis to predict moment vs. curvature and load vs. deflection response. The first set of user input data is the specimen cross section. The program has the option to enter either a rectangular cross section or a T-beam cross section. The second set of input data is the reinforcement information. The reinforcement options in the program include prestressed, mild steel, glass bars, and FRP. The information that can be inserted for each of these is the layout and the specific material properties. For this study only mild steel and FRP were used. The third set of data required to insert into the spreadsheet is the concrete material properties. The final input information is the loading of the specimen. The spreadsheet allows for three-point bending, four-point bending, and a uniform live load. Once these inputs have all been entered then a flexural analysis is performed using strain compatibility and incremental deformation. The program first defines the moment vs. curvature response of the main section by calculating various bending moments for the beam and then determining the corresponding curvature based on the strain profile. After the moment vs. curvature response has been defined, then deflection is calculated using the moment area method. This allows for the load vs. deflection response of the beam to be calculated.

The original program was extended by Professor Hayder Rasheed to incorporate a bilinear response for the behavior of steel reinforcement. After testing the control beam and examining the strain outputs for the steel it was determined that the response of the steel used in

the beams, due to strain hardening, had a trilinear behavior with a flat plateau between the yield point and the beginning of strain hardening. In order to more accurately capture the behavior of the beams, the analysis program was updated to have a trilinear response for the steel reinforcement. After updating the program, it was calibrated so that the properties of the steel in the program matched the actual steel properties from the experimental results of the control beam. In order to accomplish this the steel strains vs. load from the program were plotted against the steel strains vs. load for the control beam, and the value for the strain hardening modulus was changed until the curves had the same slope after the flat plateau.

Specimen T1

From the flexural analysis program, the control beam was determined to have a moment capacity of 258.06 kip-ft. This moment capacity corresponds to 0.003 strain in the concrete extreme top fiber, which is the strain value for concrete crushing according to ACI 318 code. The analysis program assumes confinement in the beam and allows the strain value for concrete to exceed 0.003. Based on this and the fact that the experimental test of this specimen was halted prematurely, the capacity of the beam at 0.003 concrete compressive strain was considered to correspond to the failure load from the analysis. The failure load from analysis was 66.60 kips which resulted in a maximum deflection of 3.51 in. at the mid-span. The experimental test results for specimen T1 showed a maximum load of 64.58 kips and a deflection of 4.13 in. at the mid-span. The difference between the analytical and experimental results is 2.02 kips for the load and 0.62 in. for the deflection. The experimental beam had a lower maximum load but a higher maximum deflection when compared to the analysis. Based on the analysis program assumption of concrete crushing at 0.003, this matched the experimental failure mode of ductile concrete crushing. The experimental values are close to the analytical values which means that the

analysis program is a good representation of the actual beam behavior. The load vs. deflection curves from the experiment and the analysis program confirm this as well. Figure 6-1 below shows the load vs. deflection response of the beam from the experiment and the analysis. Figures 6-2 through 6-3 show the load vs. concrete strain and load vs. steel strain responses respectively for both the experiment and the analysis.

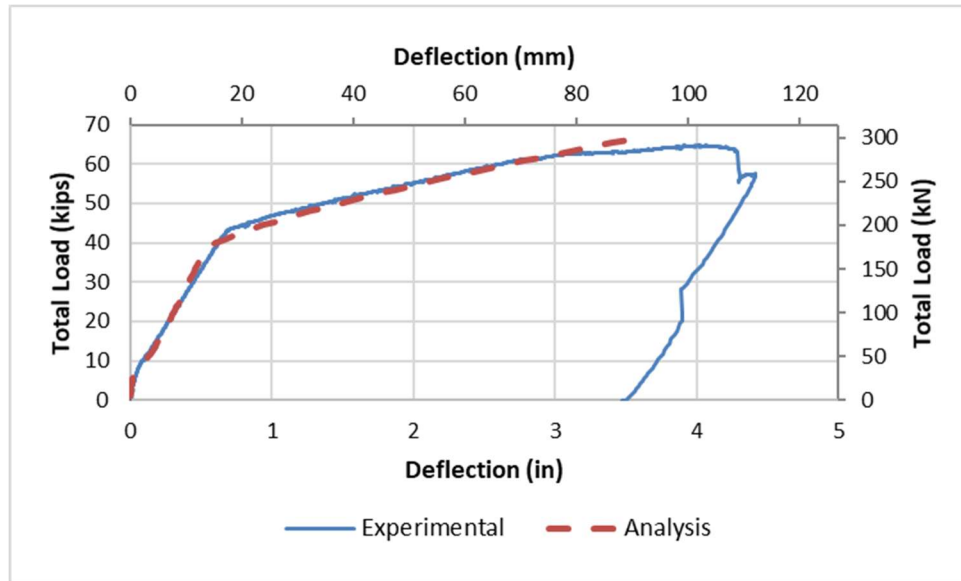


Figure 6-1: Beam T1 Experiment and Analytical Load vs. Deflection Response

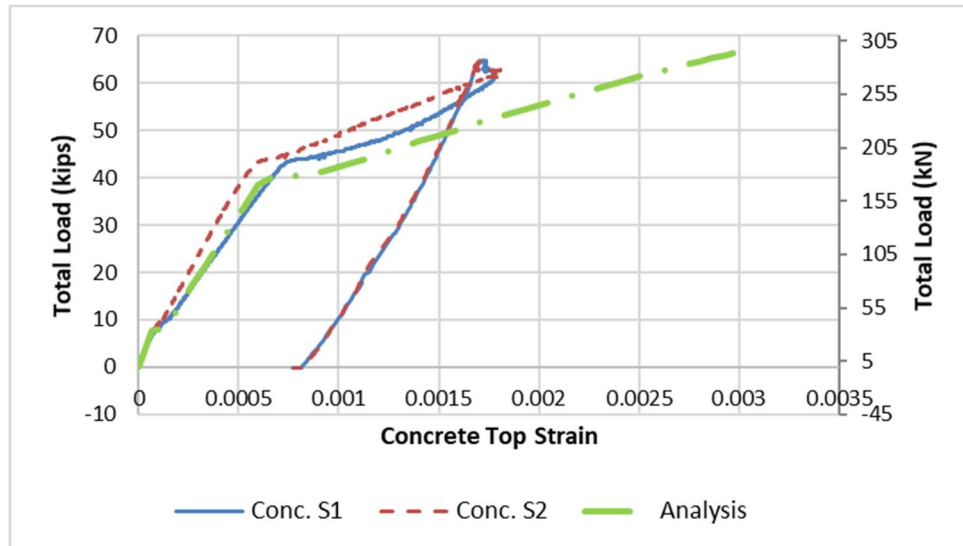


Figure 6-2: Beam T1 Experiment and Analytical Load vs. Concrete Top Strain Response

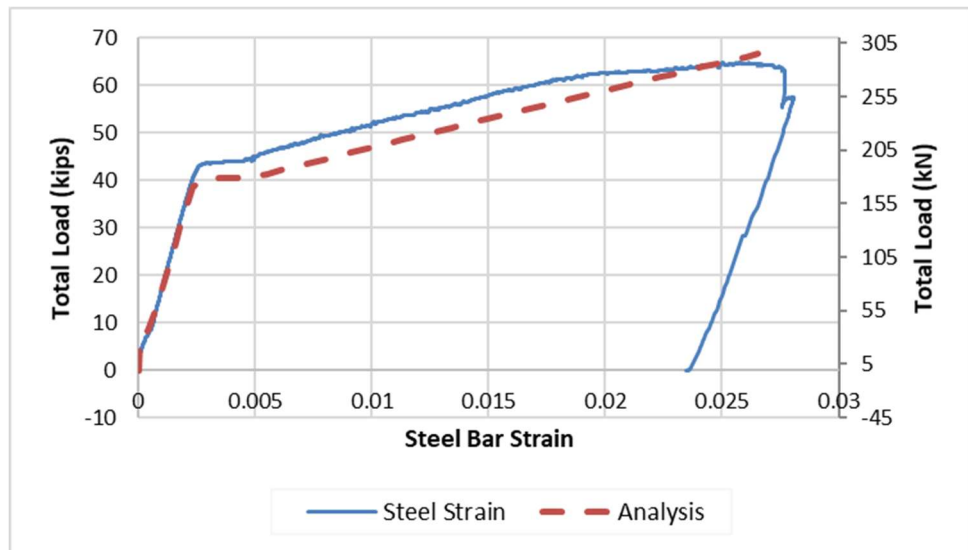


Figure 6-3: Beam T1 Experiment and Analytical Load vs. Steel Bar Strain Response

Specimen T2

The flexural analysis program predicted the beam strengthened with one layer of carbon FRP to have a moment capacity of 254.42 kip-ft. This maximum moment corresponded to a maximum load of 65.66 kips and a maximum deflection of 1.25 in. at the mid-span. The experimental test results showed a maximum load of 60.13 kips and a maximum deflection of 1.442 in. at the mid-span. The difference between the analysis and the experiment is 5.53 kips for the load and 0.192 in. for the mid-span deflection. The analysis showed a larger failure load with a smaller maximum deflection, but the analysis was close to the experimental. In addition, the behavior of the analytical concrete, steel, and FRP strains closely followed the experimental results. The reason for the difference between the analysis and the experimental results is because the analysis assumes that the Carbon FRP sheet remains perfectly bonded to the beam until it reaches the debonding failure strain. This is not how the beam behaved experimentally. The Carbon FRP sheet experiences localized debonding leading up to the failure, which causes the beam to experience more deflection than if the sheet was perfectly bonded. Figure 6-4 below shows the load vs. deflection of the beam from the experiment and from the analysis. Figures 6-5 to 6-7 show the load vs. strain response from the analysis and the experimental results for the concrete strain, steel strain, and FRP strain respectively.

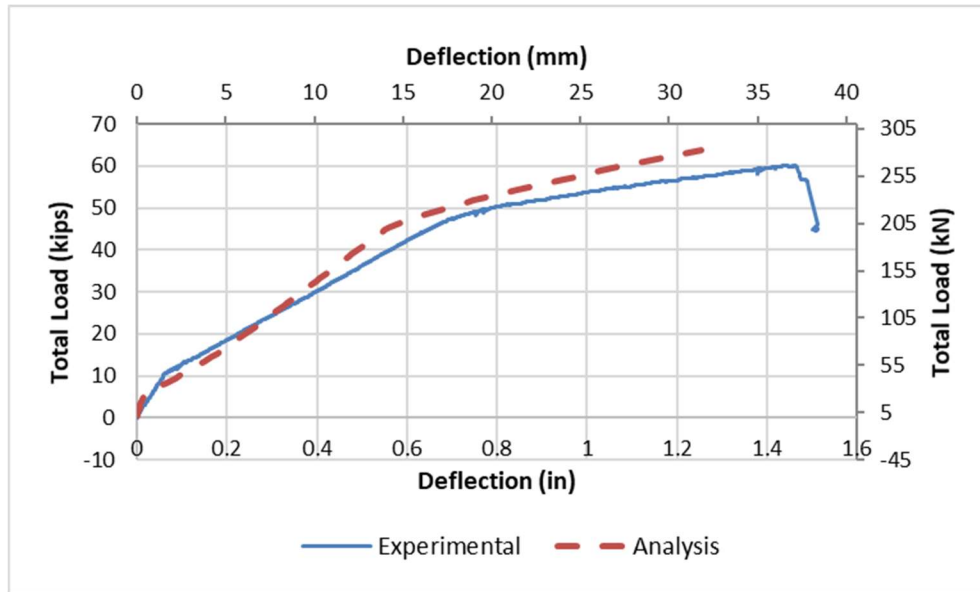


Figure 6-4: Beam T2 Experiment and Analytical Load vs. Deflection Response

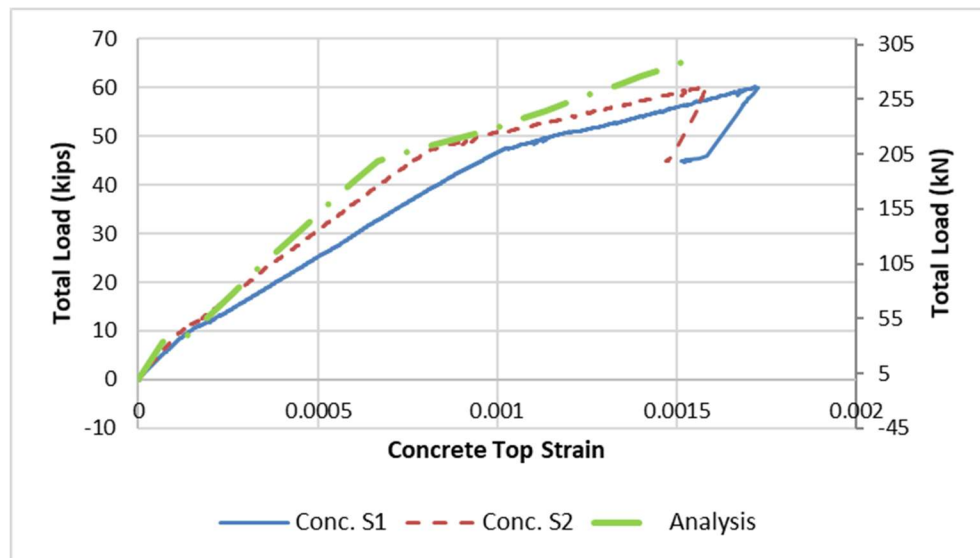


Figure 6-5: Beam T2 Experiment and Analytical Load vs. Concrete Top Strain Response

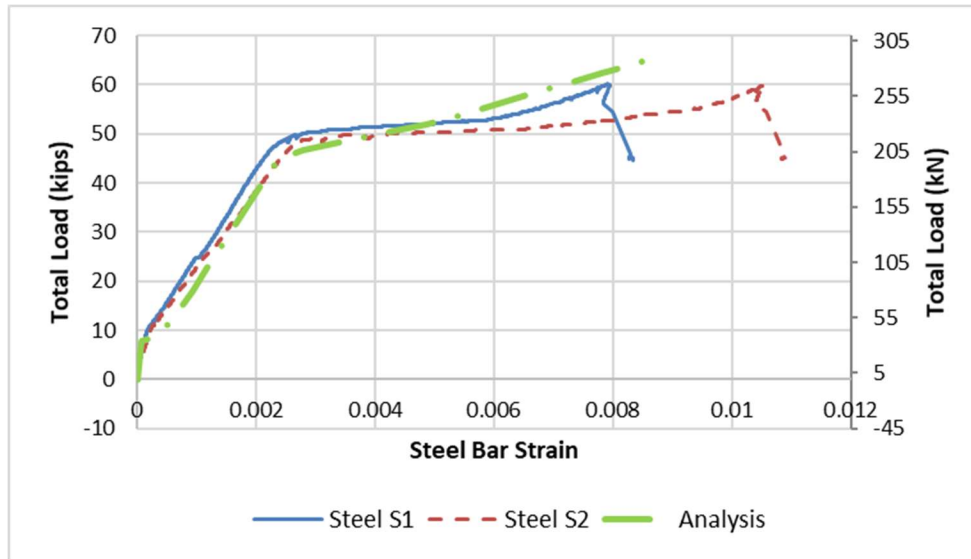


Figure 6-6: Beam T2 Experiment and Analytical Load vs. Steel Bar Strain Response

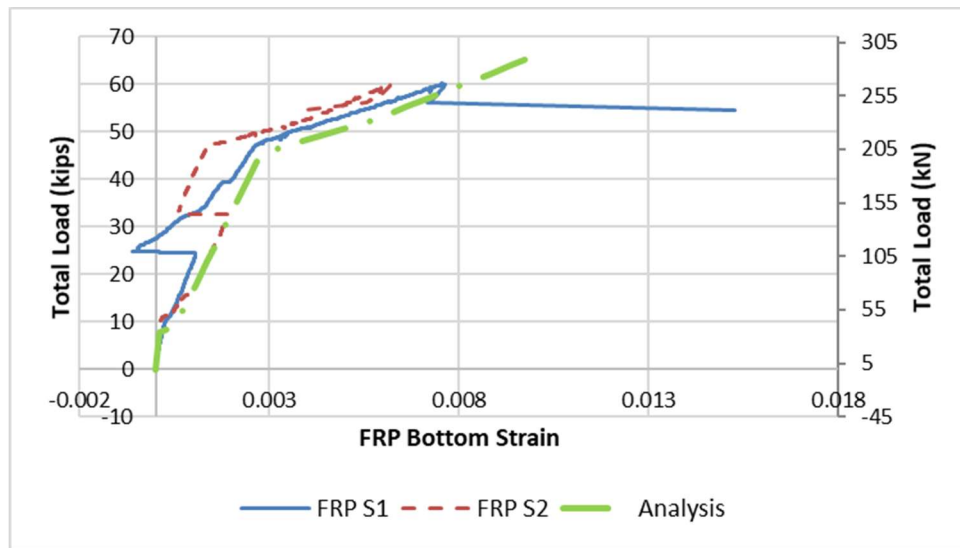


Figure 6-7: Beam T2 Experiment and Analytical Load vs. FRP Strain at Mid-span Response

Specimen T3

The flexural analysis program predicted the beam strengthened with one layer of Carbon FRP and anchored with five Carbon FRP splay anchors per shear span to have a moment capacity of 310.54 kip-ft. This maximum moment corresponded to a maximum load of 80.14 kips and a maximum deflection of 1.96 in. at the mid-span. The experimental test results showed a maximum load of 58.88 kips and a maximum deflection of 2.823 in. at the mid-span. The difference between the analysis and the experiment is 21.26 kips for the load and 0.862 in. for the mid-span deflection. The analysis showed a larger failure load with a smaller maximum deflection. The experiment and analysis both showed a failure mode of FRP rupture. The differences for this beam from the analysis to the experiment were the largest seen in this study. The main reason for this large difference is that the method used to install the CFRP on this beam may not have been sufficient to fully saturate the fiber which would alter the fiber properties from those used in the analysis program. Despite the differences in predicted maximum load and deflection versus the actual load-deflection curve, the general behavior of the load vs. strain curves for the steel, concrete, and FRP for the analysis followed the experimental results. Figure 6-8 shows the experimental and analytical load vs. deflection response for the beam. Figures 6-9 through 6-11 show the experimental and analytical load vs. strain response for the concrete, steel, and the FRP at the mid-span respectively. Figures 6-12 through 6-17 show the experimental and analytical load vs. FRP strain response for the additional locations where FRP strains were collected, see Table 5-1.

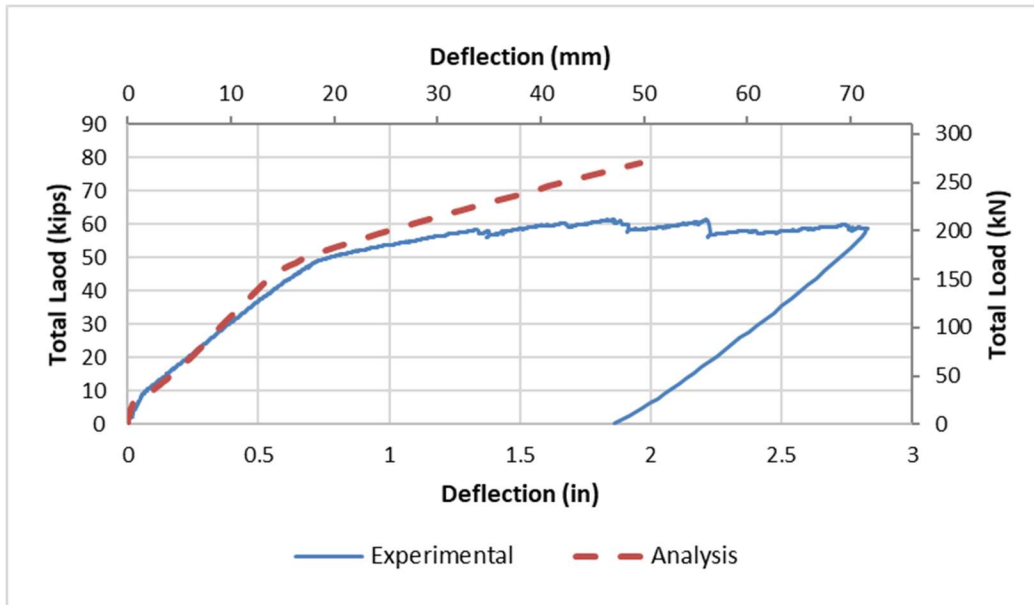


Figure 6-8: Beam T3 Experiment and Analytical Load vs. Deflection Response

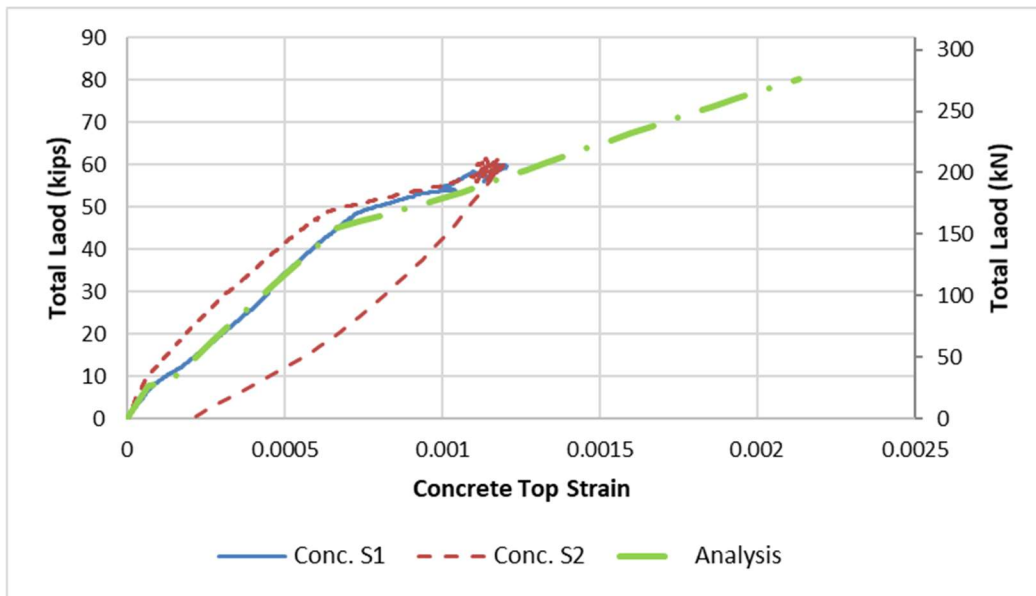


Figure 6-9: Beam T3 Experiment and Analytical Load vs. Concrete Top Strain Response

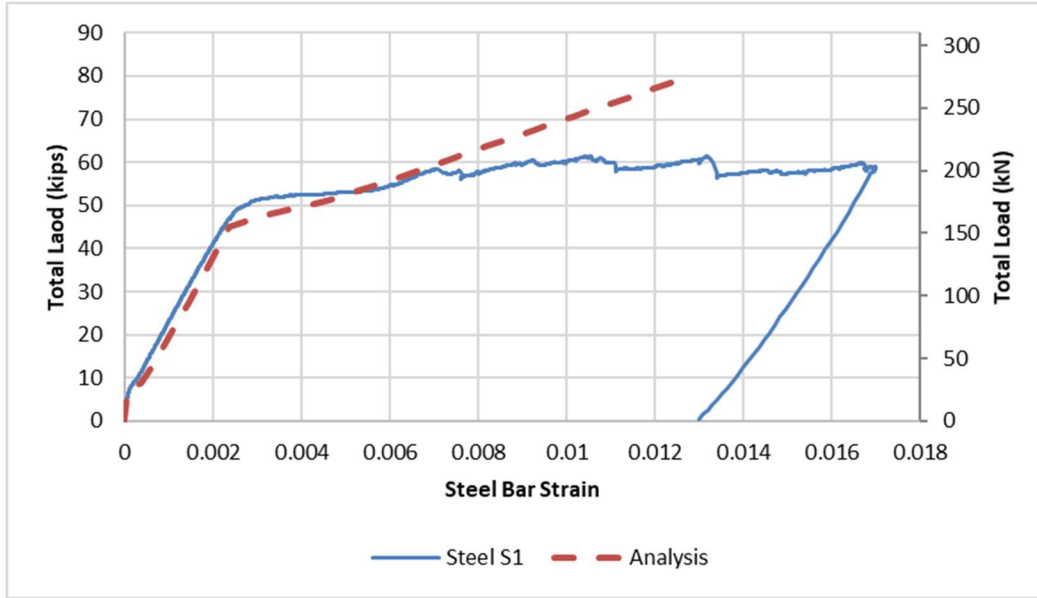


Figure 6-10: Beam T3 Experiment and Analytical Load vs. Steel Bar Strain Response

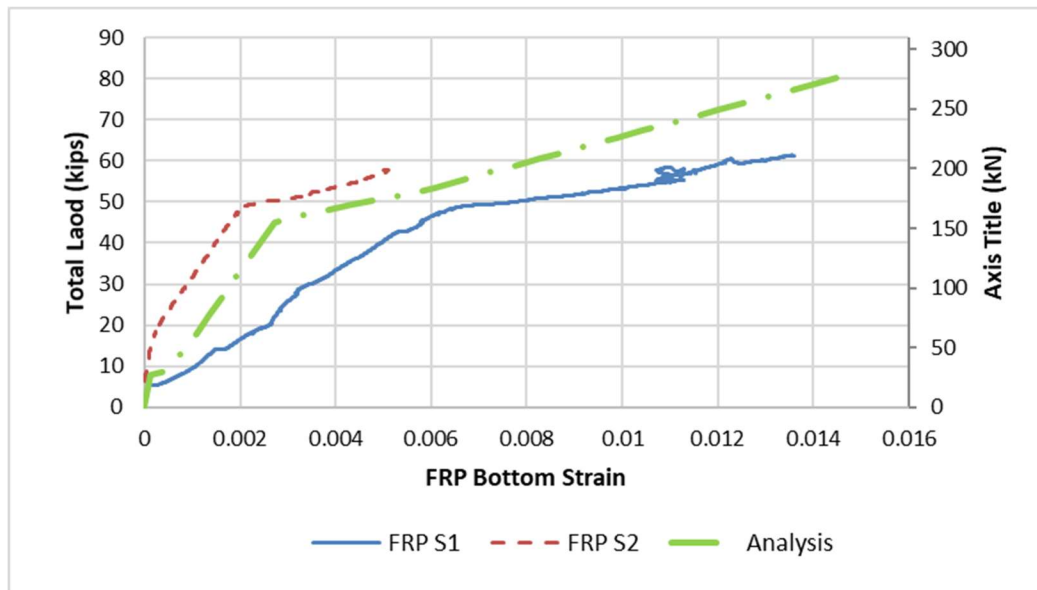


Figure 6-11: Beam T3 Experiment and Analytical Load vs. FRP Strain at Mid-span Response

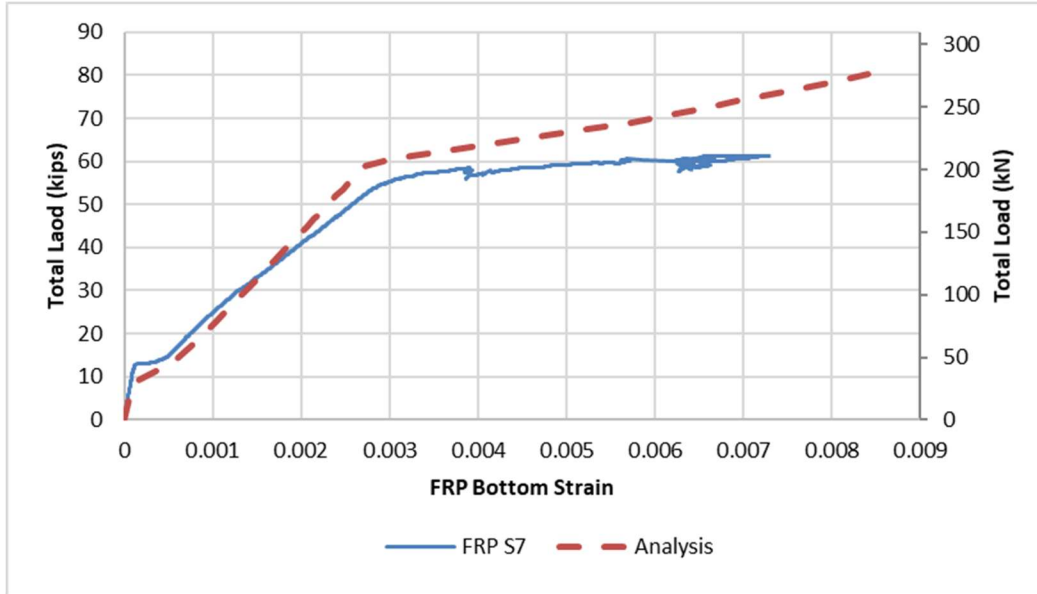


Figure 6-12: Beam T3 Experiment and Analytical Load vs. FRP S7 Strain Response

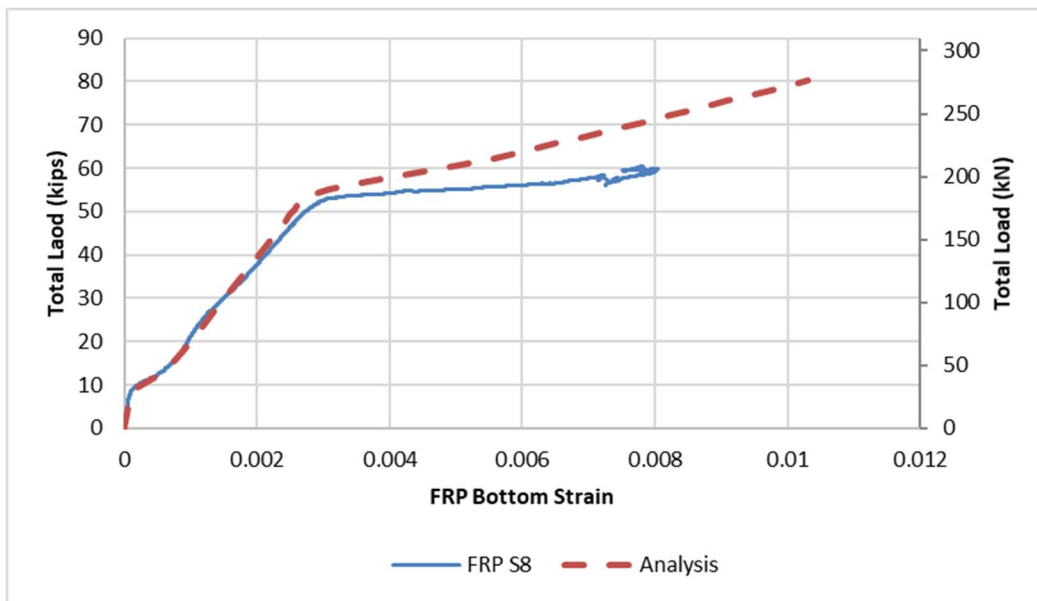


Figure 6-13: Beam T3 Experiment and Analytical Load vs. FRP S8 Strain Response

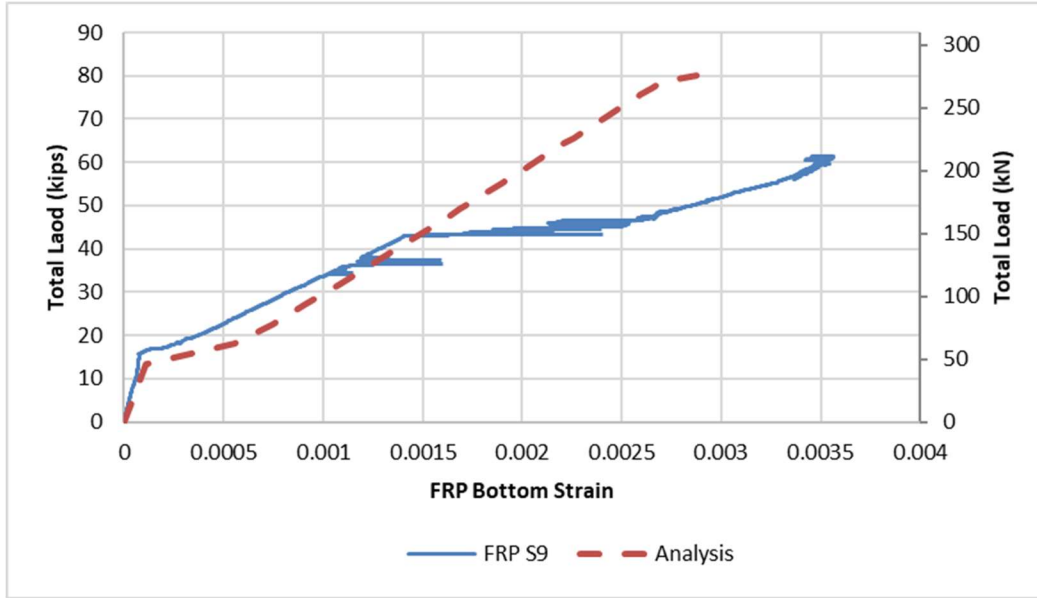


Figure 6-14: Beam T3 Experiment and Analytical Load vs. FRP S9 Strain Response

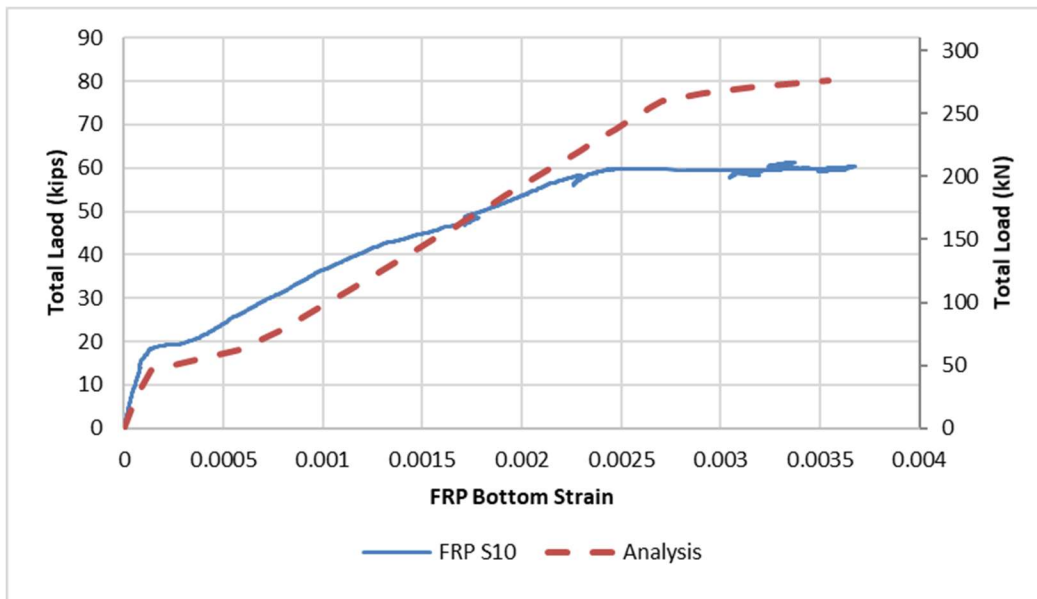


Figure 6-15: Beam T3 Experiment and Analytical Load vs. FRP S10 Strain Response

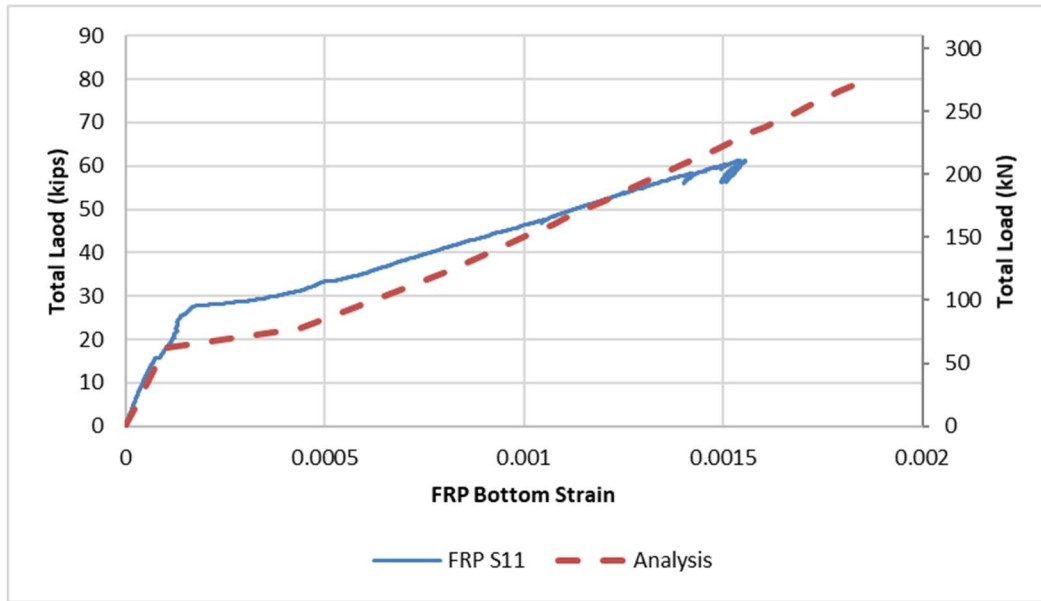


Figure 6-16: Beam T3 Experiment and Analytical Load vs. FRP S11 Strain Response

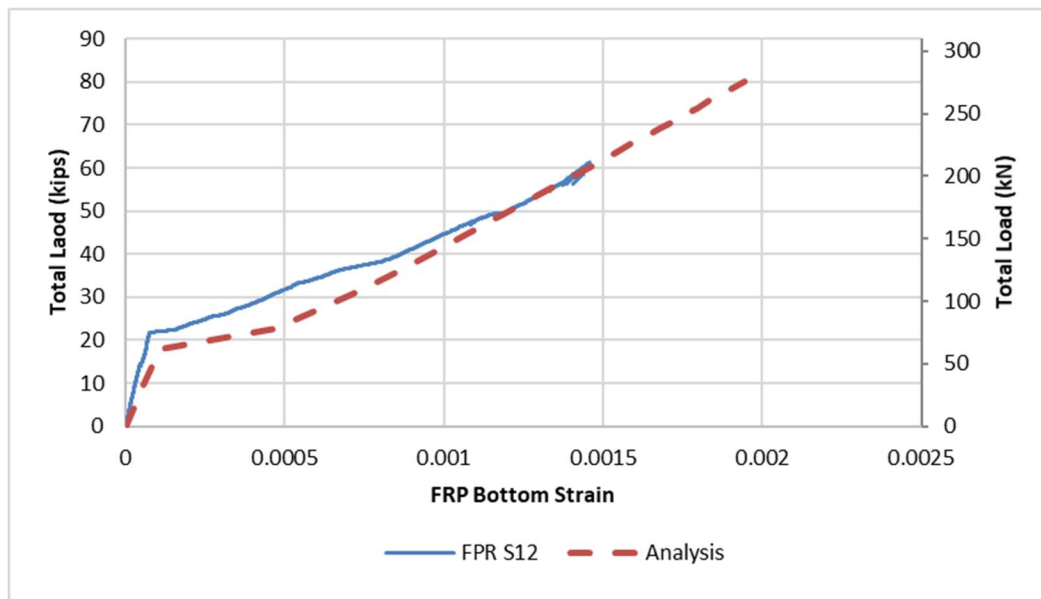


Figure 6-17: Beam T3 Experiment and Analytical Load vs. FRP S12 Strain Response

Specimen T4

The flexural analysis program predicted the beam strengthened with one layer of Carbon FRP and anchored with one layer of a full length $\pm 45^\circ$ bi-directional Glass FRP U-wrap to have a moment capacity of 304.69 kip-ft. This maximum moment corresponded to a maximum load of 78.63 kips and a maximum deflection of 1.90 in. at the mid-span. The experimental test results showed a maximum load of 80.02 kips and a maximum deflection of 2.52 in. at the mid-span. The difference between the analysis and the experiment is 1.39 kips for the load and 0.62 in. for the mid-span deflection. The analysis showed a smaller failure load with a smaller maximum deflection. The analysis program predicted an FRP rupture failure but the experiment had a GFRP debonding failure. One reason for the difference between the analysis and the experiment is the combination of the $\pm 45^\circ$ bi-directional Glass FRP with the Carbon FRP. In the analysis program the failure strain for the FRP was chosen to be the failure strain of the Carbon FRP alone when in reality, the $\pm 45^\circ$ bi-directional Glass has higher strain at failure than the carbon. Accordingly, the rupture strain for the combined FRP in this beam would be between the rupture strain values for the Carbon FRP and $\pm 45^\circ$ bi-directional Glass FRP. This can be seen in the experimental results from the FRP strains because one of the strain gauges reached a maximum value of 0.0175 which is above the ultimate strain value of 0.014 for the Carbon FRP. Figure 6-18 shows the experimental and analytical load vs. deflection response for the beam. Figures 6-19 through 6-21 show the experimental and analytical load vs. strain response for the concrete, steel, and the FRP at the mid-span respectively.

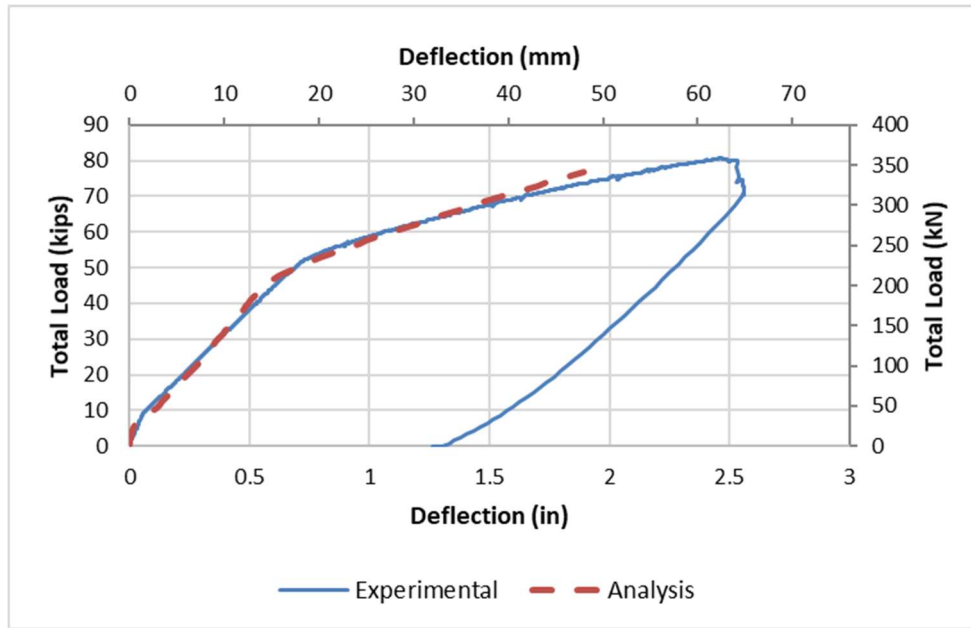


Figure 6-18: Beam T4 Experiment and Analytical Load vs. Deflection Response

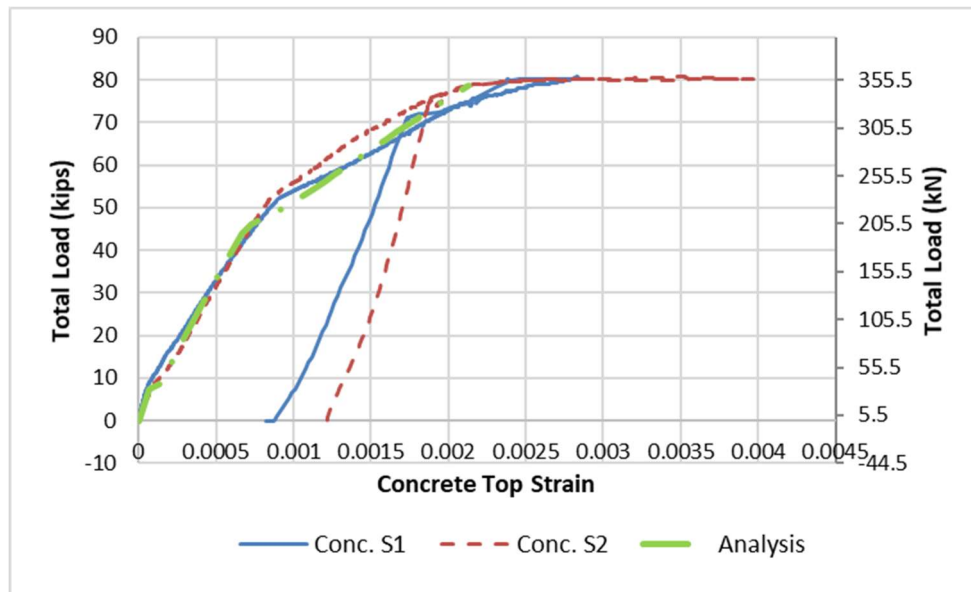


Figure 6-19: Beam T4 Experiment and Analytical Load vs. Concrete Top Strain Response

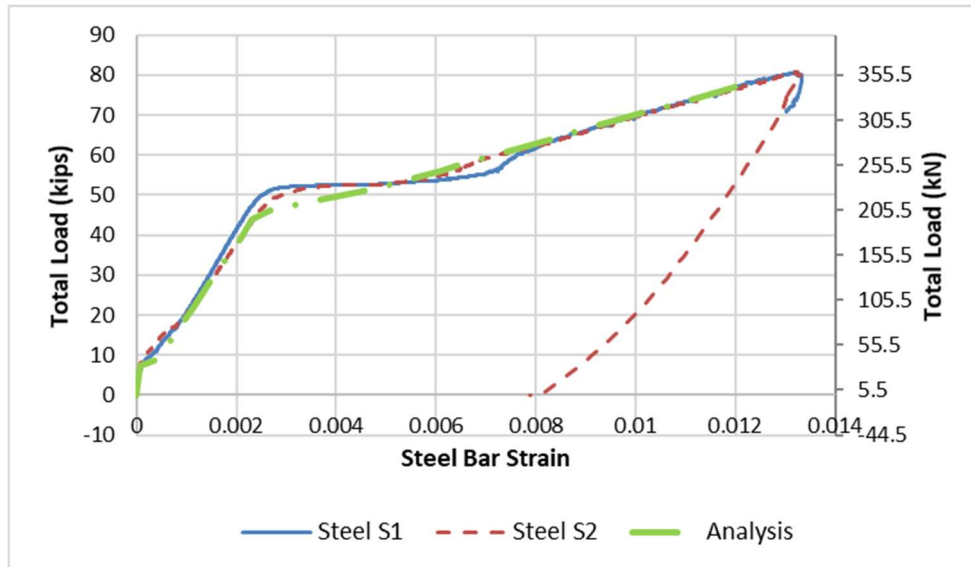


Figure 6-20: Beam T4 Experiment and Analytical Load vs. Steel Bar Strain Response

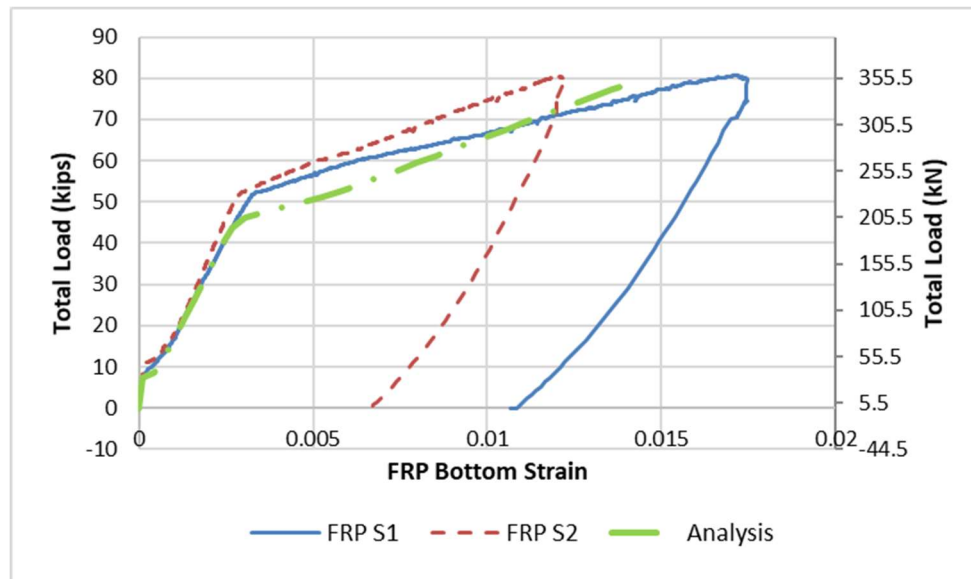


Figure 6-21: Beam T4 Experiment and Analytical Load vs. FRP Strain Response at Mid-span

Specimen T5

The flexural analysis program predicted the beam strengthened with one layer of Carbon FRP and anchored with one layer of one foot wide $\pm 45^\circ$ bi-directional Glass FRP U-wraps to have a moment capacity of 304.69 kip-ft. This maximum moment corresponded to a maximum load of 78.63 kips and a maximum deflection of 1.90 in. at the mid-span. The experimental test results showed a maximum load of 79.76 kips and a maximum deflection of 3.428 in. at the mid-span. The difference between the analysis and the experiment is 1.13 kips for the load and 1.528 in. for the mid-span deflection. The analysis showed a smaller failure load with a smaller maximum deflection. The analysis program predicted a CFRP rupture failure, but the experiment had a GFRP debonding failure from the U-wraps. The difference between the analysis program and the experimental results comes from the combination of the $\pm 45^\circ$ bi-directional Glass with the Carbon and the fact that the U-wraps do not provide perfect anchorage and allow the Carbon FRP sheet to slip. The critical section with U-wrap and carbon FRP will not rupture at the Carbon FRP ultimate strain but admits a higher composite rupture strain. In addition, the slippage that occurs with the Carbon FRP sheet allows the beam to experience more deflection because it is not as stiff that way. Figure 6-22 shows the experimental and analytical load vs. deflection response for this beam. Figures 6-23 through 6-25 show the experimental and analytical load vs. strain response for the concrete, steel, and the FRP at the mid-span respectively. Figures 6-26 through 6-29 show the analytical and experimental load vs. FRP strain response of the beam at various locations along the shear span.

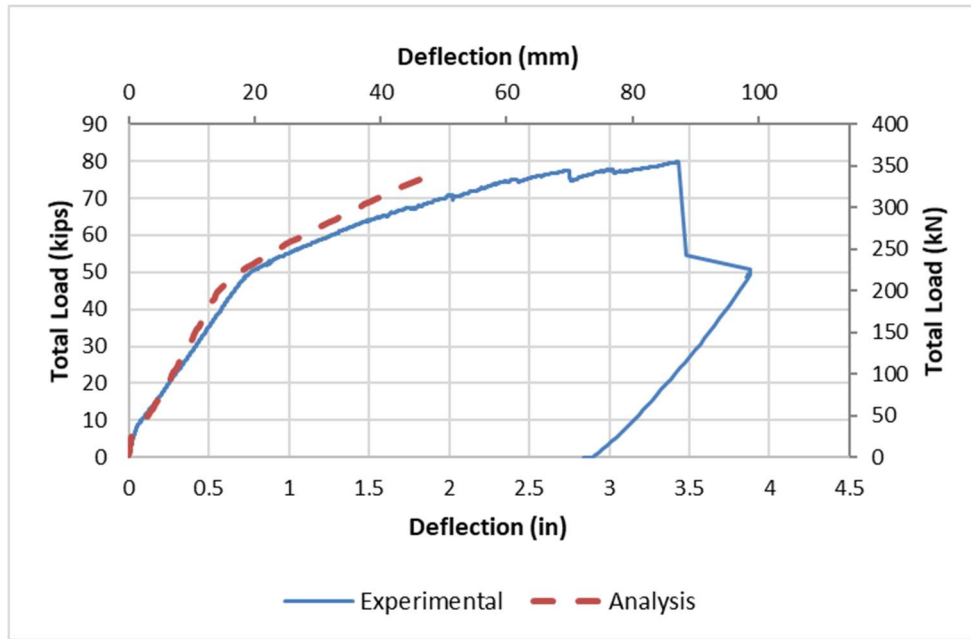


Figure 6-22: Beam T5 Experiment and Analytical Load vs. Deflection Response

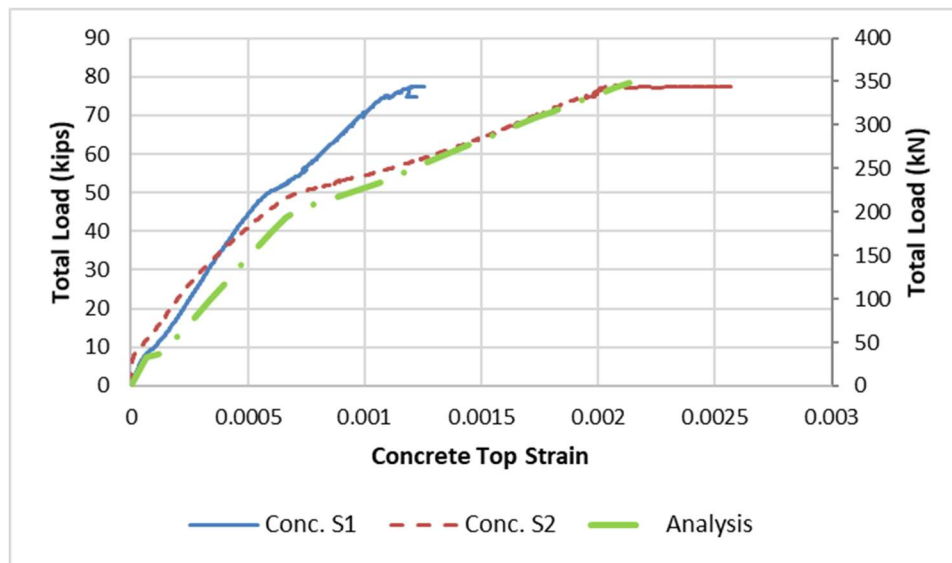


Figure 6-23: Beam T5 Experiment and Analytical Load vs. Concrete Top Strain Response

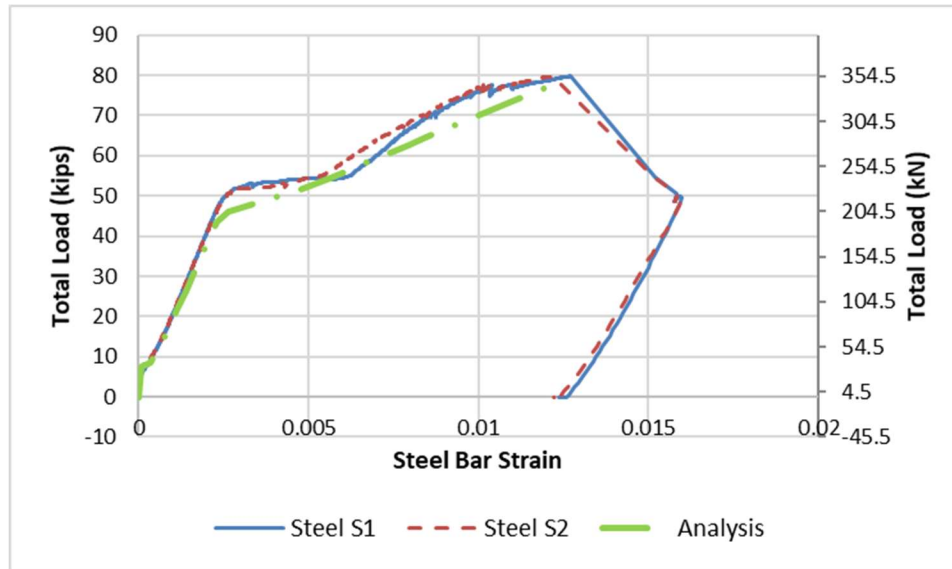


Figure 6-24: Beam T5 Experiment and Analytical Load vs. Steel Bar Strain Response

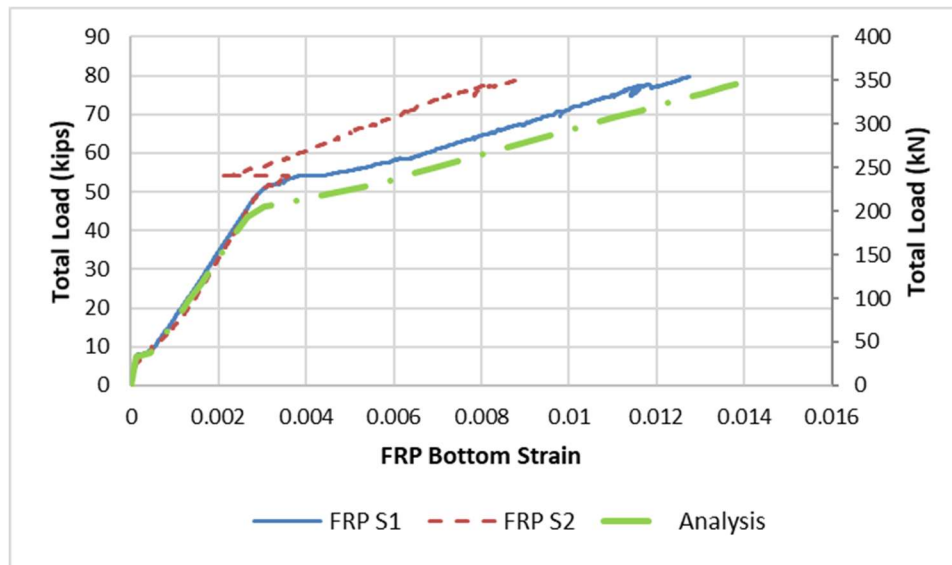


Figure 6-25: Beam T5 Experiment and Analytical Load vs. FRP Strain Response at Mid-span

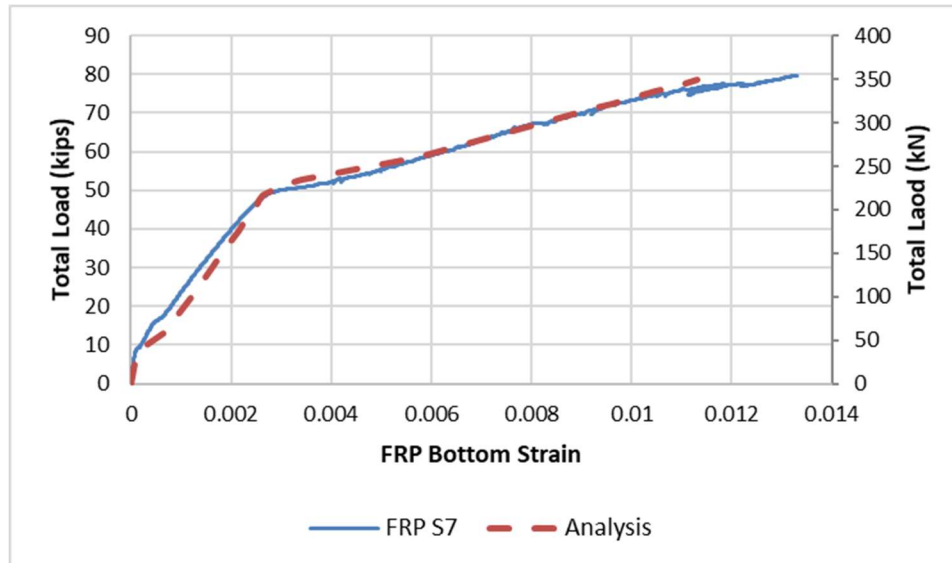


Figure 6-26: Beam T5 Experiment and Analytical Load vs. FRP S7 Strain Response

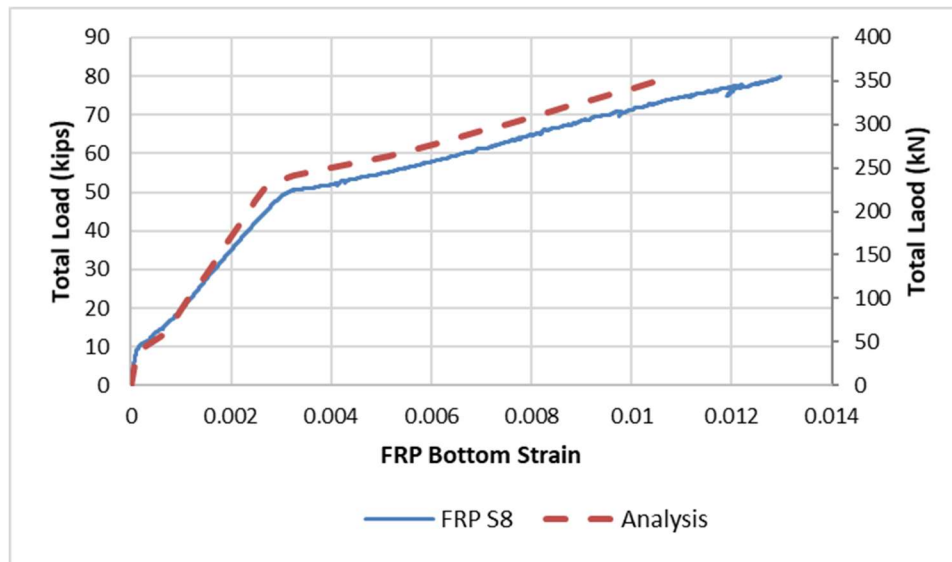


Figure 6-27: Beam T5 Experiment and Analytical Load vs. FRP Strain S8 Response

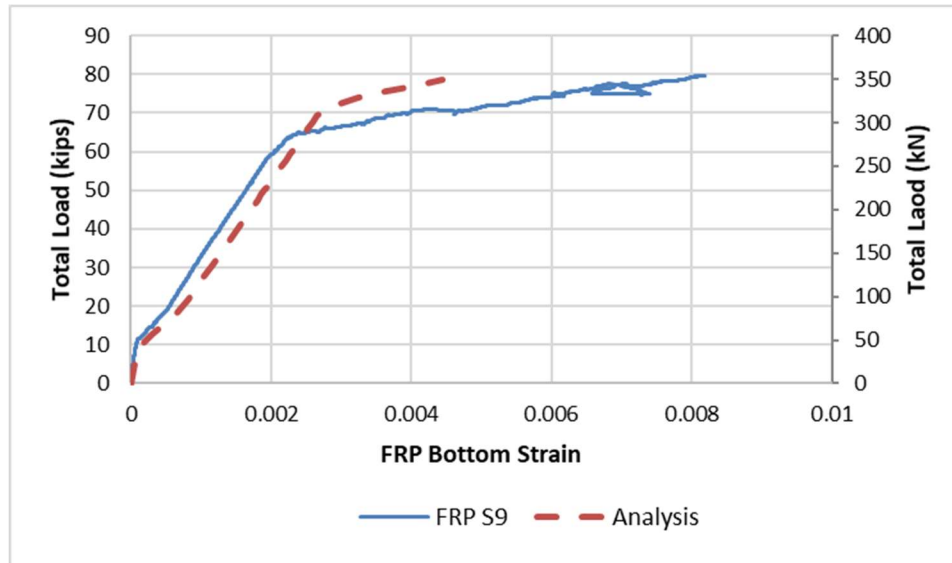


Figure 6-28: Beam T5 Experiment and Analytical Load vs. FRP S9 Strain Response

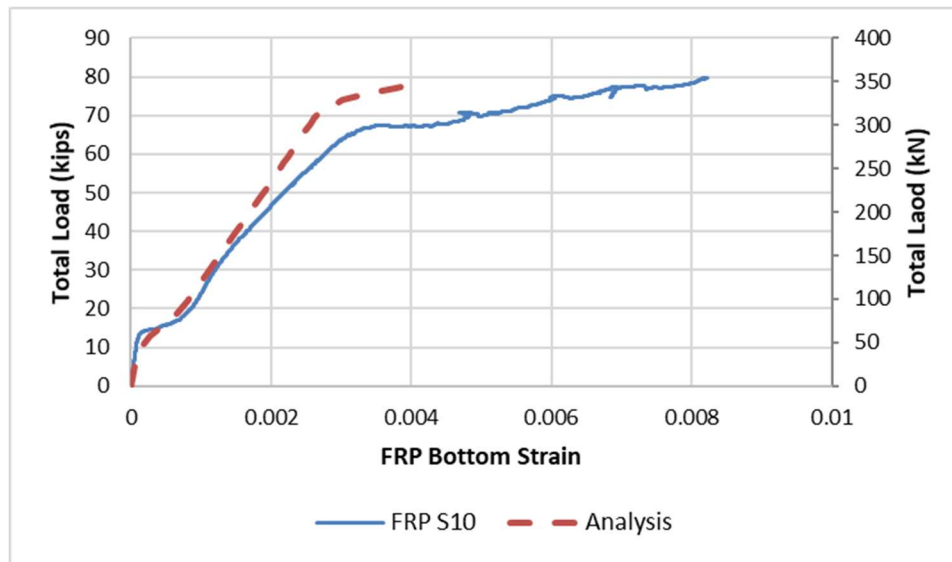


Figure 6-29: Beam T5 Experiment and Analytical Load vs. FRP S10 Strain Response

Specimen T6

The flexural analysis program predicted the beam strengthened with one layer of Carbon FRP and anchored with two layers of one foot wide $\pm 45^\circ$ bi-directional Glass FRP U-wraps to have a moment capacity of 304.69 kip-ft. This maximum moment corresponded to a maximum load of 78.63 kips and a maximum deflection of 1.90 in. at the mid-span. The experimental test results showed a maximum load of 72.17 kips and a maximum deflection of 3.025 in. at the mid-span. The difference between the analysis and the experiment is 6.46 kips for the load and 1.125 in. for the mid-span deflection. The analysis showed a larger failure load with a smaller maximum deflection than the experimental values. The analysis program predicted a CFRP rupture failure but the experiment had a GFRP debonding failure from the U-wraps. The difference between the analysis program and the experimental results comes from the combination of the $\pm 45^\circ$ bi-directional Glass with the carbon and the fact that the U-wraps do not provide perfect anchorage and allow the Carbon FRP sheet to slip. The locations with U-wrap and Carbon FRP will not rupture at the Carbon FRP ultimate strain, as assumed in the analysis program. In addition the slippage that occurs with the Carbon FRP sheet allows the beam to experience more deflection because it is not as stiff. Figure 6-22 shows the experimental and analytical load vs. deflection response for the beam. Figures 6-23 through 6-25 show the experimental and analytical load vs. strain response for the concrete, steel, and the FRP at the mid-span respectively. Figures 6-26 through 6-29 show the analytical and experimental load vs. FRP strain response of the beam at various locations along the shear span.

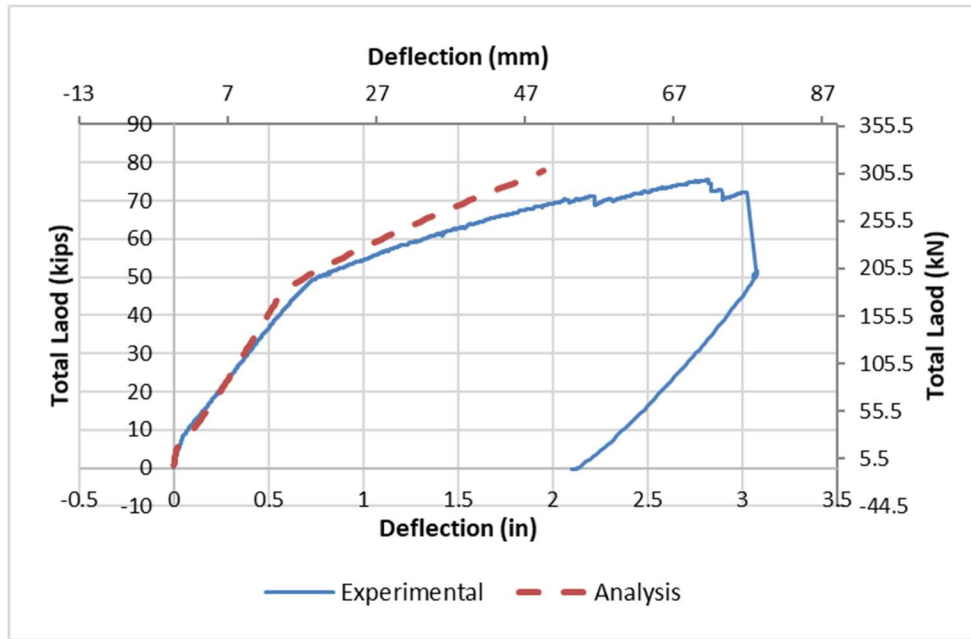


Figure 6-30: Beam T6 Experiment and Analytical Load vs. Deflection Response

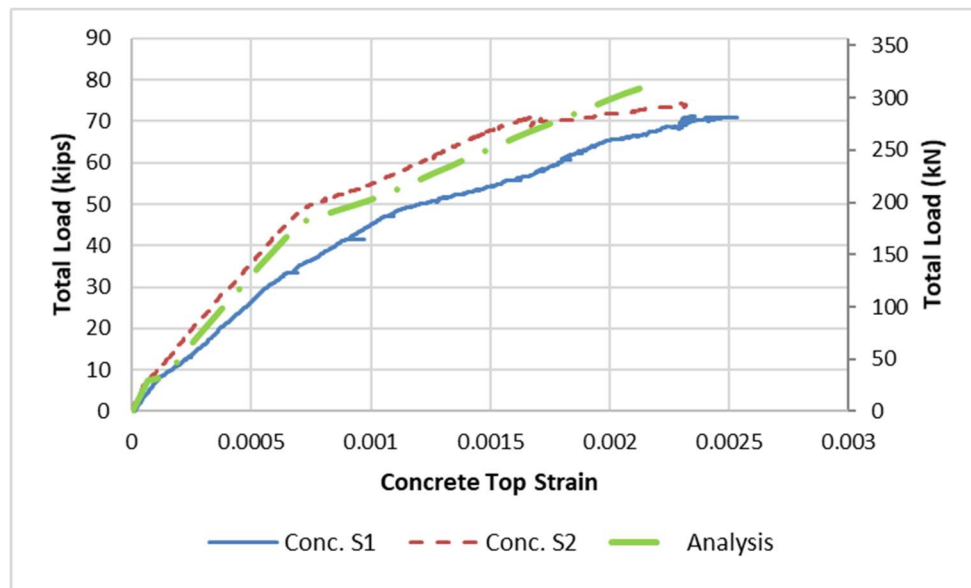


Figure 6-31: Beam T6 Experiment and Analytical Load vs. Concrete Top Strain Response

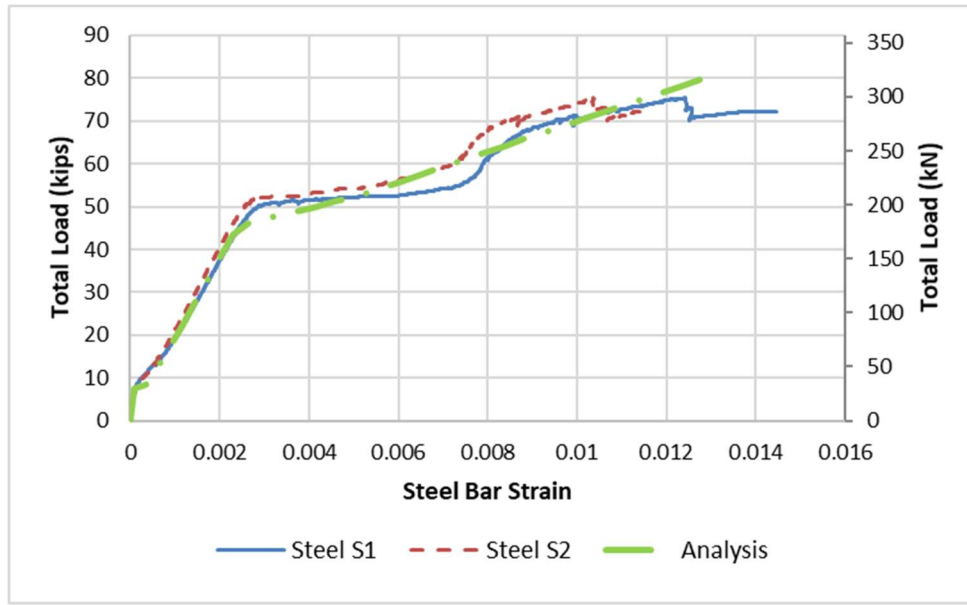


Figure 6-32: Beam T6 Experiment and Analytical Load vs. Steel Bar Strain Response

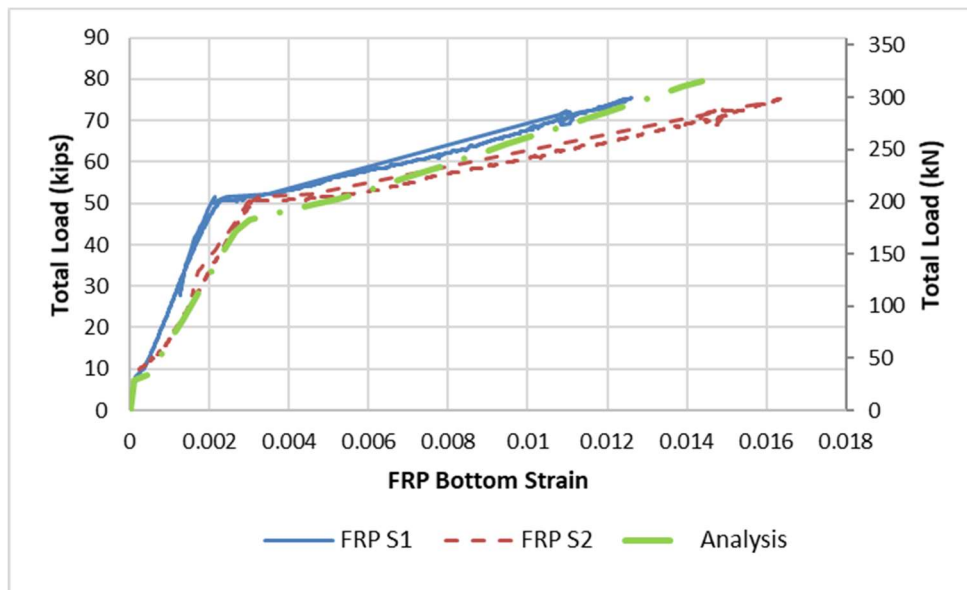


Figure 6-33: Beam T6 Experiment and Analytical Load vs. FRP Strain Response at Mid-span

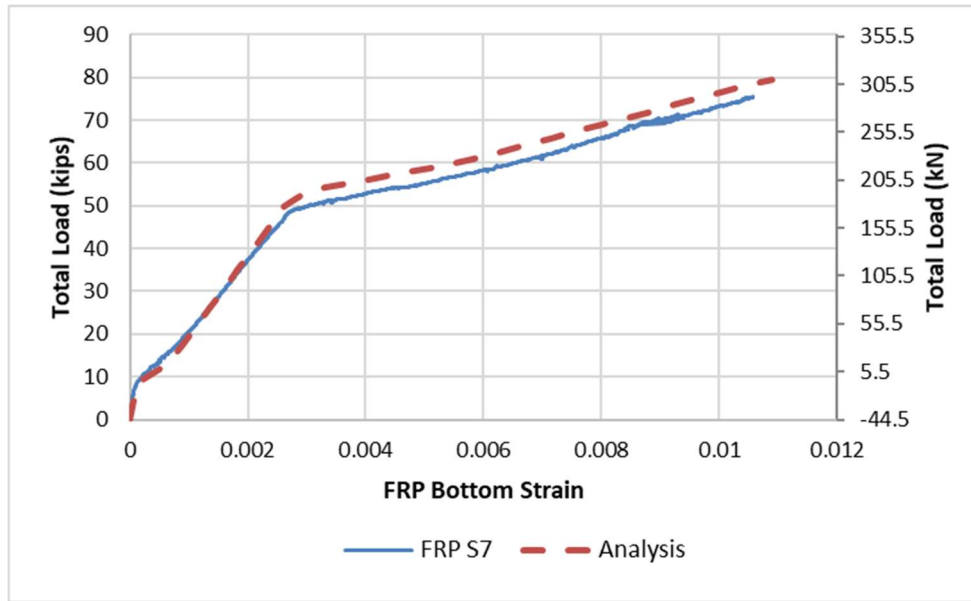


Figure 6-34: Beam T6 Experiment and Analytical Load vs. FRP S7 Strain Response

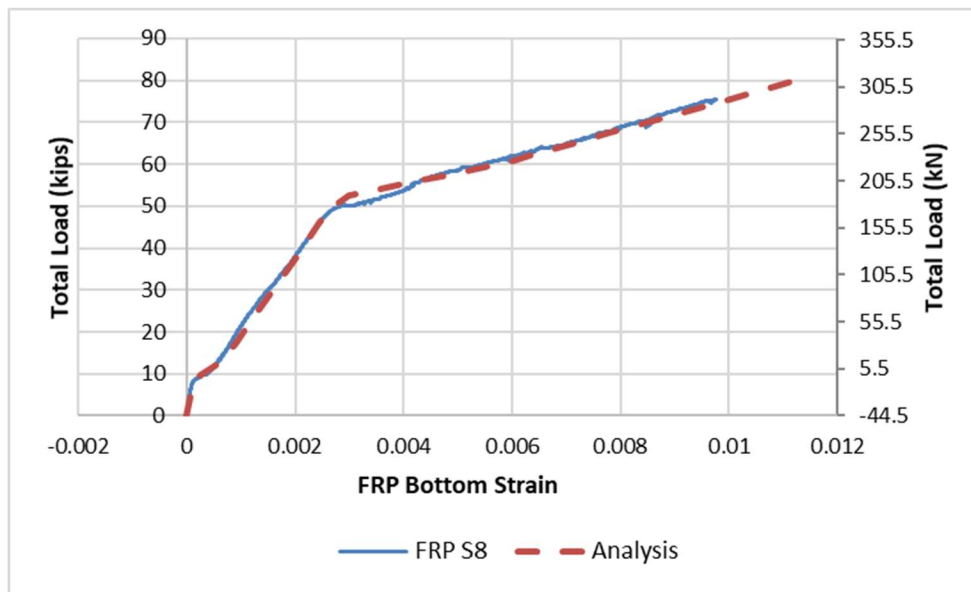


Figure 6-35: Beam T6 Experiment and Analytical Load vs. FRP S8 Strain Response

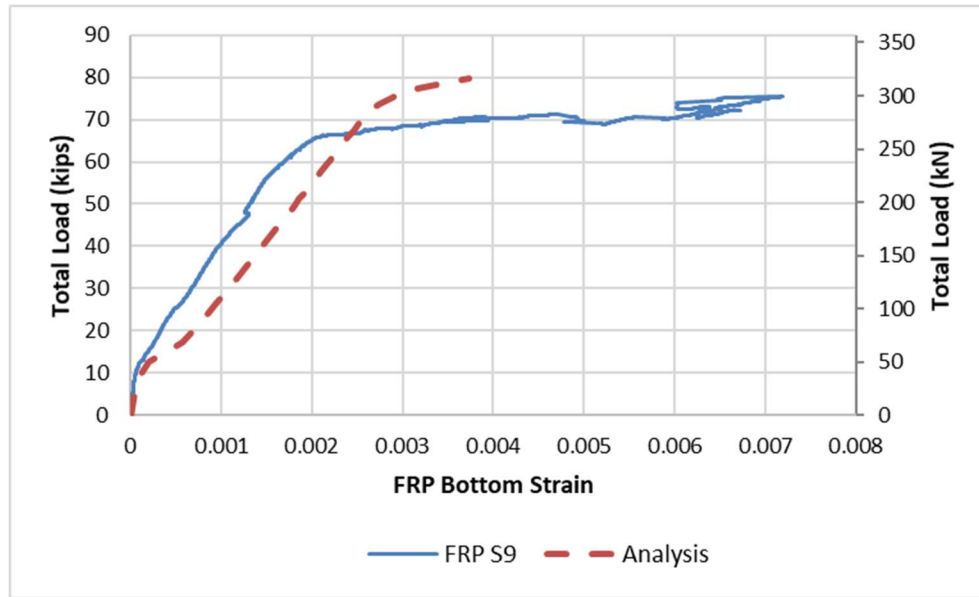


Figure 6-36: Beam T6 Experiment and Analytical Load vs. FRP S9 Strain Response

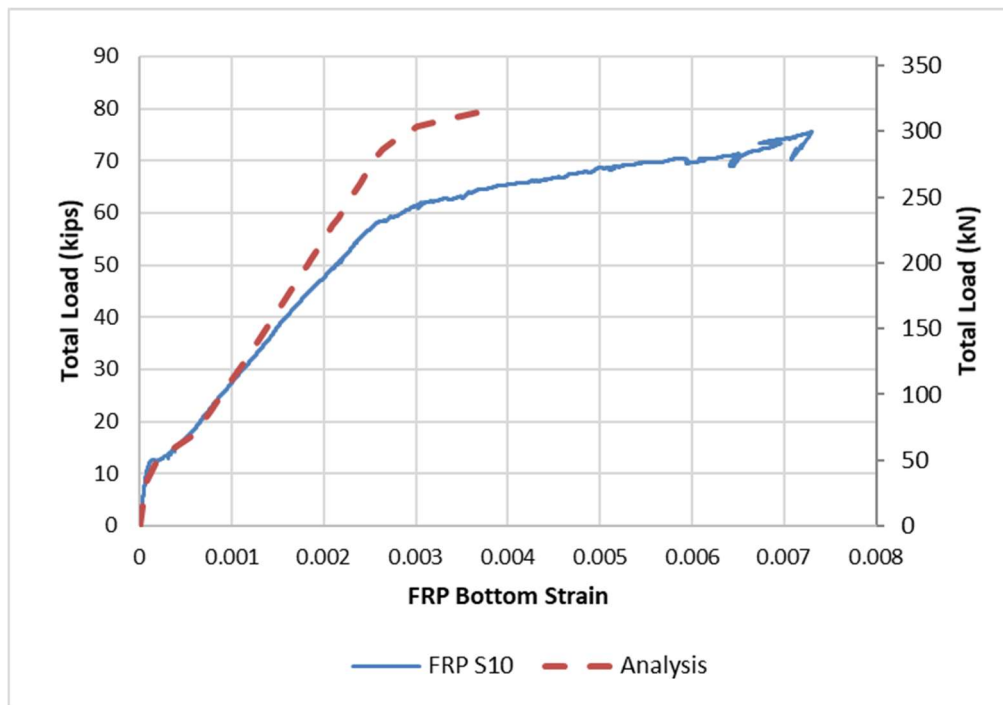


Figure 6-37: Beam T6 Experiment and Analytical Load vs. FRP S10 Strain Response

Improvement Strain Ratio of Strengthened Beams

Two different improvement strain ratios were calculated for the strengthened beams. The first ratio was K_ϵ . This ratio compares the experimental ultimate strain of the FRP based on strain compatibility of the anchored beams with the debonding strain of the FRP from ACI 440. The second ratio was \hat{K}_ϵ , which compares the experimental ultimate strain of the FRP based on strain compatibility of the anchored beams with the experimental debonding strain of the FRP based on strain compatibility for the unanchored beam. The equations below are for the two different improvement strain ratios used.

$$K_\epsilon = \frac{\epsilon_{fu} \text{ exp. failure} - \text{strain compatibility}}{\epsilon_{fd} - \text{ACI 440}} \quad (6-2)$$

$$\hat{K}_\epsilon = \frac{\epsilon_{fu} \text{ exp. failure} - \text{strain compatibility}}{\epsilon_{fd} \text{ experimental} - \text{strain compatibility}} \quad (6-2)$$

Table 6-1 below shows the results for the strain improvement ratios for all of the strengthened beams. The three beams with U-wrap anchorage systems show relatively similar strain improvements while the beam with splay anchors actually showed lower strains than debonding. These lower strains for beam T3 may have been caused by the Carbon FRP not being fully saturated as a result of the installation process.

Table 6-1: Improvement Strain Ratio of Strengthened Beams

Beam	Pu (kips)	ϵ_{fd} - ACI 440	ϵ_{fd} exp - strain compatability	ϵ_{fu} exp - strain compatability	K_ϵ	\hat{K}_ϵ
T2	60.13	0.0098	0.0085	-	0.867347	1
T3	58.88	0.0098	-	0.0082	0.836735	0.96471
T4	80.02	0.0094	-	0.0149	1.585106	1.75294
T5	79.76	0.0094	-	0.0147	1.56383	1.72941
T6	72.17	0.0094	-	0.0125	1.329787	1.47059

Chapter 7 - Summary, Conclusions and Recommendations

Summary

The results from this study lead to many different conclusions. Six T-beams, one being a control beam, were tested in three point bending in this study. Five of the beams were strengthened with a Carbon FRP sheet. Of those five beams, one was anchored with Carbon FRP splay anchors and three were anchored with $\pm 45^\circ$ bi-directional Glass FRP. The control beam failed at a load of 64.58 kips and a deflection of 4.13 in. at the mid-span. The second beam was strengthened with one layer of Carbon FRP. This beam failed at a load of 60.13 kips and a deflection of 1.442 in. at the mid-span. The third beam was strengthened with one layer of Carbon FRP and anchored with five Carbon FRP splay anchors per shear span. The beam failed at a load of 58.88 kips and a deflection of 2.823 in. at the mid-span. The fourth beam was strengthened with one layer of Carbon FRP and anchored with one layer of a full length $\pm 45^\circ$ bi-directional Glass FRP U-wrap. This beam failed at a load of 80.02 kips with a deflection of 2.52 in. at the mid-span. The fifth beam was strengthened with one layer of carbon FRP and one layer of one foot wide $\pm 45^\circ$ bi-directional Glass FRP U-wraps with one foot of space between them. The beam failed at a load of 79.76 kips and a deflection of 3.428 in. at the mid-span. The final beam was strengthened with one layer of Carbon FRP and two layers of one foot wide $\pm 45^\circ$ bi-directional Glass FRP U-wraps with one foot of space between them. This final beam failed at a load of 72.17 kips and a deflection of 3.025 in. at the mid-span.

Conclusions

From these results many different conclusions can be drawn. The first conclusion is that all three U-wrap systems were effective in strengthening the beams because all of the beams with these systems reached failure loads above the control beam. The U-wrap systems worked better

than the Carbon FRP splay anchors for anchoring the sheet, but this could also have been because of the improvement in FRP installation processes after the beam with splay anchors. The second conclusion is that the U-wrap layout that contained half the amount of $\pm 45^\circ$ bi-directional Glass FRP was just as effective as the systems that had twice as much. The main difference between the two amounts of $\pm 45^\circ$ bi-directional Glass used was the stiffness of the beam. The beam with half of the amount experienced more deflection because the system was not as stiff. As long as this additional deflection does not cause the beam to not meet deflection requirements it is better to use one layer of one foot wide $\pm 45^\circ$ bi-directional Glass FRP U-wraps to reach a similar maximum load with less fiber. The third conclusion is that all three U-wrap configurations showed similar strain improvement ratios. The three configurations used were all effective in anchoring the Carbon FRP sheet to the beam. Finally, the analysis program that was updated as a part of this study is a good predictor of flexural behavior of strengthened beams. The failure loads predicted by the analysis and the various load vs. strain and load vs. deflection responses of the beams were similar between the analysis and the experiment.

Recommendations for Future Work

This study suggests a couple of recommendations for future work and research related to this experiment. The first recommendation is to conduct additional tests using $\pm 45^\circ$ bi-directional Glass FRP as U-wraps. The idea to use this type of fiber for U-wraps is new, so there is no other work to compare the results of this study to. It would be helpful to have additional results in order to verify the results of this study. This study shows that $\pm 45^\circ$ bi-directional Glass FRP works well as a U-wrap so it would be beneficial to continue conducting tests using this material. The second recommendation from this study is to use the analysis program to evaluate additional beams so that the validity of the updated program can be checked. This can be accomplished by

either using previously tested beams or by creating new beams and comparing the results. The program produced good results and showed that it was a good predictor of the behavior of the beams, but it did not incorporate the contribution of the bidirectional Glass FRP to the flexural response of the beams anchored with that technique.

References

- ACI Committee 318 (2014). Building Code Requirements for Structural Concrete and Commentary (ACI 318-14). *American Concrete Institute*.
- ACI Committee 440 (2017), “Design and Construction of Externally Bonded FRP Systems for Strengthening Concrete Structures (ACI 440.2R-17).” *American Concrete Institute*.
- Ali, A., Abdalla, J., Hawileh, R. and Galal, K., 2014. CFRP mechanical anchorage for externally strengthened RC beams under flexure. *Physics Procedia*, 55, pp.10-16.
- Ali-Ahmad, M., Subramaniam, K. and Ghosn, M., 2006. Experimental investigation and fracture analysis of debonding between concrete and FRP sheets. *Journal of engineering mechanics*, 132(9), pp.914-923.
- Orton, S.L., Jirsa, J.O. and Bayrak, O., 2008. Design considerations of carbon fiber anchors. *Journal of Composites for Construction*, 12(6), pp.608-616.
- Pham, H.B. and Al-Mahaidi, R., 2006. Prediction models for debonding failure loads of carbon fiber reinforced polymer retrofitted reinforced concrete beams. *Journal of composites for construction*, 10(1), pp.48-59.
- Rasheed, H., Decker, B., Esmaily, A., Peterman, R. and Melhem, H., 2015. The influence of CFRP anchorage on achieving sectional flexural capacity of strengthened concrete beams. *Fibers*, 3(4), pp.539-559.
- Yalim, B., Kalayci, A.S. and Mirmiran, A., 2008. Performance of FRP-strengthened RC beams with different concrete surface profiles. *Journal of composites for construction*, 12(6), pp.626-634.
- Zaki, M. A., 2018. Behavior of reinforced concrete beams strengthened using CFRP sheets with superior anchorage devices, PhD Dissertation, Department of Civil Engineering, Kansas State University.